

3-10-2010

Low Dose Sarin Leads to Murine Cardiac Dysfunction

Michael W. Horezniak

Follow this and additional works at: <https://scholar.afit.edu/etd>

 Part of the [Toxicology Commons](#)

Recommended Citation

Horezniak, Michael W., "Low Dose Sarin Leads to Murine Cardiac Dysfunction" (2010). *Theses and Dissertations*. 2135.
<https://scholar.afit.edu/etd/2135>

This Thesis is brought to you for free and open access by the Student Graduate Works at AFIT Scholar. It has been accepted for inclusion in Theses and Dissertations by an authorized administrator of AFIT Scholar. For more information, please contact richard.mansfield@afit.edu.



LOW DOSE SARIN LEADS TO MURINE CARDIAC DYSFUNCTION

THESIS

Michael W. Horenziak, Captain, USAF, BSC

AFIT/GIH/ENV/10-M03

**DEPARTMENT OF THE AIR FORCE
AIR UNIVERSITY**

AIR FORCE INSTITUTE OF TECHNOLOGY

Wright-Patterson Air Force Base, Ohio

APPROVED FOR PUBLIC RELEASE; DISTRIBUTION UNLIMITED

The views expressed in this thesis are those of the author and do not reflect the official policy or position of the United States Air Force, the Department of Defense, or the United States Government.

AFIT/GIH/ENV/10-M03

LOW DOSE SARIN LEADS TO MURINE CARDIAC DYSFUNCTION

THESIS

Presented to the Faculty

Department of Systems and Engineering Management

Graduate School of Engineering and Management

Air Force Institute of Technology

Air University

Air Education and Training Command

In Partial Fulfillment of the Requirements for the

Degree of Master of Science in Industrial Hygiene

Michael W. Horenziak, MS

Captain, USAF, BSC

March 2010

APPROVED FOR PUBLIC RELEASE; DISTRIBUTION UNLIMITED

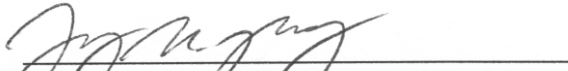
LOW DOSE SARIN LEADS TO MURINE CARDIAC DYSFUNCTION

Michael W. Horenziak, M.S.
Captain, USAF, BSC

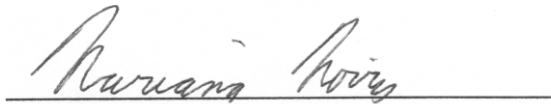
Approved:


Lt Col David A. Smith (Chairman)

3/4/2010
Date


Major Jeremy M. Slagley (Member)

4 March 2010 AD
Date


Mariana Morris, PhD (Member)
Wright State University

3/4/2010
Date

Abstract

It has been reported that low dose sarin is associated with long-term pathology in the brain and heart; however, the effects of sarin on the heart have yet to be determined. In addition, sarin has been implicated as an etiological agent in *Gulf War Illness*. Thus, the role of sarin in producing illness has important military consequences. This study used echocardiography, electrocardiography, and histology to determine sarin's effect on the murine cardiovascular system. C57BL/6J mice were injected with sarin at 0.4 LD₅₀, 0.5 LD₅₀, or saline on two consecutive days and studied for 10 weeks post exposure. The sarin animals had marked increases in heart weight to body weight ratios ($p = 0.026$), and the left ventricular lumen size was significantly decreased ($p = 0.0014$). In addition, cardiomyocytes were significantly larger in the sarin mice ($p = 0.025$) and atrial/brain natriuretic peptide levels were increased ($p = 0.028$ and 0.010 , respectively). Results of the electrocardiograms show significant ST/T-wave changes in the sarin groups ($p = 0.0015$ and 0.032 , respectively). Similarly, echocardiograms showed significantly decreased performance of the left ventricle in the sarin animals. This study indicates that sarin plays a role in cardiac remodeling and reducing cardiac performance.

Acknowledgments

This work directly supported a grant held by Wright State University, grant # GW060050, from the United States Army Medical Research Acquisition Activity, Congressionally Directed Medical Research Programs (CDMRP) – Gulf War Veterans’ Illnesses Research Program (GWVIRP). I would like to thank Lt. Col. Smith, who made innumerable contributions to the completion of this project, and Maj. Slagley, who has led me through this Masters Degree program. I would also like to extend a special thanks to Dr. Mariana Morris for the opportunity to join the project, and the students at Wright State University for their objective and knowledgeable assistance throughout the project. And to my wife and children, whose unquestioning love and devotion saw me through this academic rigor.

Michael Horezniak

Table of Contents

	Page
Abstract.....	v
Acknowledgments	vi
List of Figures	x
List of Tables	xiv
I. Introduction	1
A Brief Review on the Toxicology of Sarin	1
Historical Perspective on the Use and Implications of Sarin to the US Military.....	2
Sarin Health Effects and Gulf War Illness.....	4
Specific Effects of Sarin Relevant to the US Military and Civilian Populations.....	5
Problem Statement	6
Research Objective/Hypothesis	8
Proposed Experiment.....	8
Contributions.....	9
II. Literature Review.....	10
Introduction.....	10
Animal Considerations	10
Choice of Anesthesia and Expected Effects	10
Environmental Concerns.....	12
Dobutamine Stress Testing	13
Noninvasive In Vivo Measurements.....	14
Echocardiograms	14
Electrocardiograms (ECG).....	15
In Vitro/Histological Markers	17
Utility of ANP/BNP Measurements	17
Collagen and Picosirius Red Staining.....	18
Hematoxylin and Eosin (H&E) Staining.....	19

	Page
III. Methodology.....	20
Animal Experimental Protocol	20
Tissue Collection, Heart Sectioning, and Heart Size Measurement Methods	21
Heart Section Size Measurements	23
Echocardiogram Methods.....	24
Transthoracic Echocardiogram Method.....	24
Echocardiography Analysis Method	26
ECG Methods.....	29
Telemetry Collection Procedure.....	29
ECG Analysis Method.....	30
ANP and BNP Methods.....	34
Method of ANP and BNP Staining	34
ANP and BNP Quantification	35
Cell Size Quantification using an H&E Stain Method	38
H&E Method of Staining	38
Cell Size Quantification.....	38
Picosirius Red Staining Methods.....	41
Method of Picosirius Red Staining.	41
Picosirius Red Quantification	41
Statistical Methods.....	43
IV. Results and Analysis	45
Results of Body Weights, Tissue and Heart Sectioning Weights	45
Results of Body Weights, Tissue Weights, and Heart Sectioning.....	45
Results of Echocardiography Analysis.....	48
Results of the ECG Analysis	51
Results of ANP/BNP Stain Quantification.....	55
Results of Cardiomyocyte Size via H&E Analysis.....	57

	Page
Results of Collagen Quantification via Picosirius Red Staining.....	59
V. Discussion	60
Body Weights, Tissue and Heart Sectioning Weights	60
Signification of Histological Evidence.....	60
Electrocardiographs: Inference of Ventricular Performance and Hypertrophy	62
Echocardiograms and Implication to Left Ventricular Performance	64
Additional Observations of Sarin’s Effects on the Heart.....	68
Dobutamine Stress Testing.....	68
The ECG PR Interval	68
Limitations of this Study.....	69
Future Work	70
Conclusion	71
Appendix A: Tabulated Average Results of Controls, 0.4 LD ₅₀ , and 0.5 LD ₅₀ Groups.....	73
Tabulated Results of Weights and Heart Section Measurements	74
Tabulated Results of Echocardiograms.....	75
Tabulated Results of ECG Data Analysis.....	78
Tabulated Results of Histology: ANP/BNP Quantification	79
Tabulated Results of Cell Size Quantification from H&E Staining, Collagen Quantification from Picosirius Red Staining	80
Appendix B: Unpublished Heart Weight Data	81
Heart Weight Data (Unpublished Study)	82
Bibliography	84

List of Figures

Figure	Page
FIGURE 1 DEMOLITION OF BUNKERS AT KHAMISIYAH, 4 MARCH 1991.....	4
FIGURE 2 PLUME MODELS FOR THE DEMOLITION OF BUNKERS AT KHAMISIYAH, 12 MARCH 1991.....	4
FIGURE 3 TYPICAL HUMAN ECG	16
FIGURE 4 TYPICAL MOUSE ECG ILLUSTRATING THE DIFFERENCE IN THE T-WAVE WHEN COMPARED TO THE HUMAN ECG	16
FIGURE 5 BLOOD CHOLINESTERASE LEVELS 24 HOURS AFTER 2 CONSECUTIVE SARIN INJECTIONS.....	21
FIGURE 6 REPRESENTATIVE 3MM HEART SECTIONING	22
FIGURE 7 PICTURE OF ATRIAL SIDE OF A 3MM THICK HEART LV/RV SECTION	22
FIGURE 8 REPRESENTATION OF MANUAL CROPPING OF THE RV AND LV USING ADOBE® PHOTOSHOP TO OBTAIN LV/RV AREA	23
FIGURE 9 REPRESENTATION OF PHOTOSHOP® ENHANCED IMAGE TO OBTAIN TOTAL HEART AREA	23
FIGURE 10 MOUSE ANESTHESIA PROCEDURE	24
FIGURE 11 MOUSE BEING DE-HAIRED IN THE PRECORDIUM	24
FIGURE 12 REPRESENTATIVE ECHOCARDIOGRAM TECHNIQUE	25
FIGURE 13 METHOD OF DOBUTAMINE INJECTION	26
FIGURE 14 REPRESENTATIVE AREA MEASUREMENT METHOD FOR 2-D ECHOCARDIOGRAMS	27
FIGURE 15 REPRESENTATIVE MEASUREMENT METHODS FOR 2-D M-MODE ECHOCARDIOGRAMS	27
FIGURE 16 EXAMPLE PULSED WAVE DOPPLER IMAGE SHOWING EIGHT FULL SINUS RHYTHMS	27
FIGURE 17 PULSED WAVE DOPPLER METHOD OF QUANTIFICATION	27
FIGURE 18 ECG ELECTRODE PLACEMENTS AND TECHNIQUE OF ATTACHMENT	29
FIGURE 19 REPRESENTATIVE ECG TRACING	31
FIGURE 20 REPRESENTATIVE ECG TRACE WITH SOFTWARE MARKINGS.....	31

	PAGE
FIGURE 21 ECG TRACE SHOWING END OF T-WAVE ENCROACHMENT ON THE P-WAVE START.....	32
FIGURE 22 ECG TRACE WITH AN INDISCERNIBLE T-WAVE DUE TO A RESPIRATION	32
FIGURE 23 ECG TRACE DEMONSTRATING ST AND T CALCULATIONS	34
FIGURE 24 5X MAGNIFICATION PHOTOGRAPH OF A BNP STAINED HEART SECTION BEFORE BACKGROUND CORRECTION	36
FIGURE 25 5X MAGNIFICATION PHOTOGRAPH OF A BNP STAINED HEART SECTION AFTER BACKGROUND CORRECTION	36
FIGURE 26 REPRESENTATION OF BNP/ANP SELECTION VIA THRESHOLD SELECTION	37
FIGURE 27 WHOLE HEART SECTION COMPOSITE OF 5X MAGNIFICATION IMAGES WITH REPRESENTATIVE OF REGION PLACEMENT IN A BNP STAINED HEART	38
FIGURE 28 20X MAGNIFICATION PICTURE OF GRAY SCALE IMAGE SHOWING H&E STAINING OF CARDIOMYOCYTES IN THE SEPTUM.....	39
FIGURE 29 20X MAGNIFICATION H&E PICTURE W/MAGNIFIED CUT-OUT WITH NUCLEI SELECTED USING METAMORPH'S IMA TOOLKIT	40
FIGURE 30 20X MAGNIFICATION H&E PICTURE WITH TOTAL TISSUE SELECTED USING METAMORPH'S THRESHOLD TOOL	40
FIGURE 31 5X MAGNIFICATION PHOTOGRAPH OF A PICROSIRIUS RED STAINED HEART SECTION IN CROSSED POLARIZED LIGHT.	42
FIGURE 32 PHOTOSHOP® ENHANCED IMAGE OF A SIRIUS RED STAINED HEART IMAGE SHOWING THE TOTAL HEART AREA.	42
FIGURE 33 REPRESENTATION OF PHOTOSHOP® ENHANCED SIRIUS RED STAINED HEART IMAGE TO OBTAIN TOTAL HEART AREA.....	43
FIGURE 34 RESULTS OF MURINE BODY WEIGHTS.	45
FIGURE 35 RESULTS OF PERCENT CHANGE IN BODY WEIGHT.	45
FIGURE 36 RESULTS OF HEART WEIGHTS (CORRECTED BY BODY WEIGHT).	46
FIGURE 37 RESULTS OF CORRECTED HEART WEIGHTS WITH COMBINED SARIN GROUPS.....	46

	PAGE
FIGURE 38 REPRESENTATIVE 3MM SECTION OF CONTROL MOUSE SHOWING NORMAL VENTRICULAR SIZE	47
FIGURE 39 REPRESENTATIVE 3MM SECTION OF 0.4 LD ₅₀ GROUP SHOWING SEVERELY DEPRESSED VENTRICULAR AREAS	47
FIGURE 40 RESULTS OF VENTRICULAR SIZE.....	47
FIGURE 41 RESULTS OF ECHOCARDIOGRAM ESA.....	48
FIGURE 42 RESULTS OF ECHOCARDIOGRAM EDA.	48
FIGURE 43 RESULTS OF ECHOCARDIOGRAM AFS.	49
FIGURE 44 RESULTS DOPPLER DERIVED ET.	50
FIGURE 45 RESULTS DOPPLER DERIVED ICT + IVRT.	50
FIGURE 46 RESULTS ECHO/DOPPLER DERIVED AFS/MPI.	51
FIGURE 47 RESULTS ECHO/DOPPLER DERIVED VCF.	51
FIGURE 48 CONTROL MOUSE ECG TRACE BEFORE DOBUTAMINE INJECTION.....	52
FIGURE 49 CONTROL MOUSE ECG TRACE AFTER DOBUTAMINE INJECTION.....	52
FIGURE 50 SARIN MOUSE ECG TRACE BEFORE DOBUTAMINE INJECTION.....	52
FIGURE 51 SARIN MOUSE ECG TRACE AFTER DOBUTAMINE INJECTION SHOWING ST DEPRESSION.	52
FIGURE 52 SARIN MOUSE ECG TRACE BEFORE DOBUTAMINE INJECTION.....	53
FIGURE 53 SARIN MOUSE ECG TRACE AFTER DOBUTAMINE INJECTION SHOWING SEVERE ST DEPRESSION.	53
FIGURE 54 RESULTS OF ST SEGMENT MEASUREMENTS.	54
FIGURE 55 RESULTS OF T-PEAK TO T-END.	54
FIGURE 56 RESULTS OF PR INTERVAL.....	54
FIGURE 57 5X MAGNIFICATION IMAGES OF BNP STAINING IN THE CONTROL GROUP REPRESENTATIVE BNP (AND ANP) STAIN PATTERN FOR THE CONTROL MICE	55

	PAGE
FIGURE 58 5X MAGNIFICATION IMAGES OF BNP STAINING IN THE 0.4 LD ₅₀ SARIN GROUP AND REPRESENTATIVE OF THE BNP (AND ANP) STAIN PATTERN FOR BOTH SARIN GROUPS.....	55
FIGURE 59 UNITLESS REPRESENTATION OF ANP QUANTIFICATION.	56
FIGURE 60 ANP QUANTIFICATION WITH THE TWO SARIN GROUPS (0.4 LD ₅₀ AND 0.5 LD ₅₀) COMBINED.	56
FIGURE 61 UNITLESS REPRESENTATION OF BNP QUANTIFICATION.	57
FIGURE 62 BNP QUANTIFICATION WITH THE TWO SARIN GROUPS COMBINED (0.4 LD ₅₀ AND 0.5 LD ₅₀).	57
FIGURE 63 40X MAGNIFICATION IMAGE OF THE CARDIOMYOCYTES IN THE LV WALL OF AN H&E STAINED CONTROL MOUSE	57
FIGURE 64 40X MAGNIFICATION IMAGE OF THE CARDIOMYOCYTES IN THE LV WALL OF AN H&E STAINED SARIN MOUSE SHOWING MYOCYTE ENLARGEMENT AND EXPANSION INTO THE INTERCELLULAR SPACE	57
FIGURE 65 RESULTS OF H&E ANALYSIS.....	58
FIGURE 66 RESULTS OF COMBINED H&E ANALYSIS.	58
FIGURE 67 HISTOLOGY SHOWING LV HYPERTROPHY IN SARIN MICE.....	61
FIGURE 68 ECG SHOWING ST CHANGES IN SARIN MICE.....	63
FIGURE 69 ECHOCARDIOGRAPHY DATA SHOWING DECREASED LV PERFORMANCE IN SARIN MICE.....	65
FIGURE 70 UNPUBLISHED HEART WEIGHT TO BODY WEIGHT DATA.....	82
FIGURE 71 UNPUBLISHED HEART WEIGHT TO KIDNEY WEIGHT DATA	83

List of Tables

Table	Page
TABLE 1 TABULATED RESULTS OF AVERAGE PERCENT CHANGES IN BODY WEIGHT	74
TABLE 2 TABULATED RESULTS OF AVERAGE BODY WEIGHT	74
TABLE 3 TABULATED RESULTS OF WEEK 10 AVERAGE BODY WEIGHTS, HEART WEIGHTS, AND CORRECTED HEART WEIGHTS (HEART WEIGHT/BODY WEIGHT)	74
TABLE 4 TABULATED RESULTS OF THE HEART AREAS IN SQUARE MILLIMETERS.....	74
TABLE 5 TABULATED RESULTS OF 2-DIMENSIONAL ECHOCARDIOGRAPH DATA	75
TABLE 6 TABULATED RESULTS OF M-MODE ECHOCARDIOGRAPH DATA	76
TABLE 7 TABULATED RESULTS OF PULSED-WAVE DOPPLER DATA & DERIVED PARAMETERS	77
TABLE 8 TABULATED RESULTS OF ECG TELEMETRY	78
TABLE 9 TABULATED RESULTS OF THE AVERAGE ANP EXPRESSED AS THE NATURAL LOG OF THE AVERAGE PERCENT IN EACH AREA.....	79
TABLE 10 TABULATED RESULTS OF THE AVERAGE BNP EXPRESSED AS THE AVERAGE PERCENT OF BNP IN EACH AREA	79
TABLE 11 TABULATED RESULTS OF CELL SIZE IN THE LEFT VENTRICLE EXPRESSED AS PIXELS/NUCLEI.....	80
TABLE 12 TABULATED RESULTS OF COLLAGEN IN THE HEART EXPRESSED AS A RATIO OF PIXELS STAINED WITH SIRIUS RED TO TOTAL HEART AREA (PIXELS)	80

List of Acronyms

ACh – Acetylcholine

AChE – Acetylcholine Esterase

aFS – Area Fraction Shortening

ANOVA – Analysis of Variance

ANP – Atrial Natriuretic Peptide

Ao – Aorta/Aortic

AV – Atrioventricular

BNP – Brain Natriuretic Peptide

CNS – Central Nervous System

CVS – Cardiovascular System

ECG – Electrocardiogram

EDA – End Diastolic Area

EDD – End Diastolic Diameter

ESA – End Systolic Area

ESD – End Systolic Diameter

ET – Ejection time

FS – Fractional Shortening

GWII – *Gulf War Illness*

H&E – Hematoxylin and Eosin

ICT + IVRT – Isovolumetric Contraction Time plus Isovolumetric Relaxation Time

ISF – Isoflurane (anesthesia)

LD₅₀ – Lethal Dose to 50 Percent of the Population

LV – Left Ventricle

MPI – Myocardial performance index

NPRA – Natriuretic peptide receptor A

OP – Organophosphate

PWT – Posterior Wall Thickness

RV – Right Ventricle

SA – Sinoatrial

ST_C – Corrected ST Interval for a Mouse

SWT – Septal Wall Thickness

T_C – Corrected T-Peak to T-End Interval for a Mouse

VCF – Circumferential Fiber Shortening Velocity

VTI – Velocity Time Index

LOW DOSE SARIN LEADS TO MURINE CARDIAC DYSFUNCTION

I. Introduction

A Brief Review on the Toxicology of Sarin

Sarin belongs to the chemical class known as organophosphates (OP). OPs are a group of chemical toxins that inhibit acetylcholinesterase (AChE) and are widely used as pesticides and chemical warfare agents (CWA). Sarin, O-isopropyl methylphosphonofluoridate (military designation – GB), acts as an irreversible AChE inhibitor. Sarin reacts with the serine hydroxyl residue in the active site of AChE to form a phosphate or phosphonate ester; hence the AChE is inhibited (or deactivated). Deactivated AChE cannot hydrolyze the cholinergic neurotransmitter Acetylcholine (ACh) resulting in its accumulation and excessive stimulation of cholinergic receptors. Overstimulation of central and peripheral cholinergic sites occurs in smooth muscles, skeletal muscles, most exocrine glands, the central nervous system (CNS), and the cardiac system (central and ganglionic afferents).

Stimulation of muscarinic receptors at the smooth muscle level causes miosis, bronchoconstriction, vasodilation, increased peristalsis, and reduced heart rate at smooth muscle level; at exocrine glands, it causes secretions in the lung, nasal, oral, and sweat glands. Among clinical effects due to nicotinic receptor overstimulation at skeletal muscle are fasciculation, twitching, flaccid paralysis and stimulation of autonomic ganglia leading to tachycardia and hypertension. The CNS has both muscarinic and nicotinic receptors and overstimulation leads to seizures and can cause death; whereas,

a mild exposure leads to variety of symptoms which include forgetfulness, bad dreams, insomnia, and the ability to concentrate.

Sarin reacts with the cardiovascular system in a complex manner; effects are comprised of both ganglion and postganglionic consequences of accumulated ACh on the heart and blood vessels. The overall acute effect on the heart depends on the relative prevalence of sympathetic or parasympathetic effects. Cholinergic effects from ACh suppress vagal tone resulting in a decreased refractory period and conduction time at sinoatrial (SA) and atrioventricular (AV) nodes; whereas, excess ACh also affects the muscarinic ACh M2 receptors in the heart leading to negative chronotropic and ionotropic effects. Thus, ACh creates contradicting excitatory effects on parasympathetic ganglionic cells in the face of the inhibitory effects of the sympathetic ganglia. ACh elicits similar excitatory followed by inhibitory effects at the medullary vasomotor and cardiac centers. In severe ACh accumulation, hypoxia resulting from broncho-constriction also affects the cardiovascular system by reinforcing sympathetic tone, while ACh induced epinephrine released from adrenals leads to increased heart rate. As a result, sarin induces bradycardia, tachycardia, and arrhythmias in the heart that can lead to spontaneous cardiac failure (Taylor, 2001; Marrs, 2007).

Historical Perspective on the Use and Implications of Sarin to the US Military

The United States Air Force has become increasingly engaged with terrorist groups and other elusive enemies. As these activities increase, the potential for adversarial use of chemical weapons increases. Terrorist groups and other third world

countries have decisive conventional and technological disadvantages. As such, weapons of mass destruction proliferators could significantly ameliorate their tactical and strategic positions through the use of chemical weapons.

In the literature, there are several examples of the use of or potential use of sarin to gain an asymmetric advantage. During the 1980-1988 Iraq-Iran war both Iraq and Iran employed chemical weapons (including sarin) in an attempt to gain an advantage in a seemingly unending war (Ali, 2001). In addition to Iraq and Iran, the Japanese have experienced two separate terrorist attacks involving sarin. The first occurred in 1994 when nearly 600 Japanese citizens were exposed to sarin in an attack in a neighborhood of Matsumoto, Japan (Committee on Gulf War and Health: Updated Literature Review of Sarin, 2004). In 1995, the Aum Shinrikyo terrorist group deployed the chemical agent sarin against a civilian population as an attempt to divert police attempts to prostrate the organization. As a specific threat to the US, in 2001, Al Qaeda claimed acquisition of radiological, biological, and chemical weapons. The threat was deemed credible when videotapes aired in 2002 showing the ostensible killing of three dogs by a nerve agent (Robertson, 2002). These events demonstrate the intent and willingness of such organizations to employ chemical weapons.

Sarin became a particularly important topic in the US following the 1990 US-Iraq *Gulf War*. During the *Gulf War*, three sites were destroyed where munitions loaded with sarin and cyclosarin were stored. Of the three sites, plume models show that only the Khamisiyah site had the potential for US troop exposure (see Figure 1 and 2).



Figure 1 Demolition of bunkers at Khamisiyah, 4 March 1991
(Central Intelligence Agency; Department of Defense, 1997)

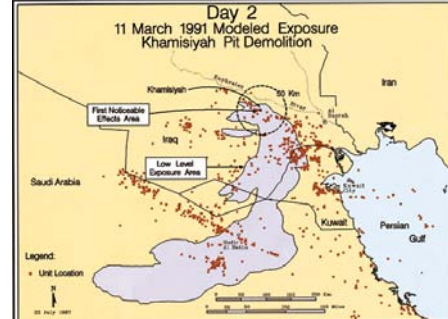


Figure 2 Plume Models for the Demolition of Bunkers at Khamisiyah, 12 March 1991
(Persian Gulf War Illnesses Task Force, 1997)

According to estimates, nearly 90,000 troops may have been exposed to sarin and cyclosarin as a result of the demolitions (Committee on Gulf War and Health: Updated Literature Review of Sarin, 2004). US troops performing demolitions were unaware of the presence of nerve agents because their detectors, being sensitive only to lethal or near-lethal concentrations of nerve agents, did not sound any alarms before demolition (CDC, 1999, p. 55). As a result, sarin and other organophosphate nerve agents were implicated as a possible etiological agent in *Gulf War Illness* (GWI) and subsequently investigated by the US Department of Veterans Affairs (Couzin, 2004).

Sarin Health Effects and Gulf War Illness

Gulf War veterans show a variety of poorly defined neurological, muscular and autonomic symptoms including poorer cognitive function, tiredness, muscle and joint pain, loss of balance, bladder dysfunction, and diarrhea (Jamal, 1998; Jamal, Hansen, Apartopoulos, & Peden, 1996). Studies of *Gulf War* veterans show altered diurnal patterns of HR and HR variability correlated to reduced parasympathetic drive to the heart possibly resulting from damage to the CNS (Haley, Fleckenstein, Marshall,

McDonald, Kramer, & Petty, 2000; Haley, et al., 2004; Menon, Nasrallah, Reeves, & Ali, 2004), and autonomic imbalance is a common symptom in sarin poisoning (Yokoyama, et al., 1998, pp. 317 - 323). Previous reports have shown comparable delayed autonomic effects of low dose sarin exposure in mice and rats (Morris, Key, & Farah, 2007; Grauer, et al., 2008). Recently, some human data from the Aum Shinrikyo-Tokyo subway attacks has indicated that sarin could produce neurological and autonomic changes (Murata, et al., 1997; Yokoyama, et al., 1998, pp. 249 - 256; Yokoyama, et al., 1998, pp. 317 - 323). Similarly, Haley *et al.* have shown similar symptoms in veterans exhibiting GWI (Haley, Kurt, & Hom, 1997). Nonetheless, although the latter proposes a link between nerve agents and GWI, there are almost no records on the source or level of exposure; the evidence is inconclusive and more data is needed (Committee on Gulf War and Health: Updated Literature Review of Sarin, 2004).

Specific Effects of Sarin Relevant to the US Military and Civilian Populations

While it is expected that potent, cholinergic poisoning would cause pathological changes, it is more likely that the majority of survivors following a sarin release would have been exposed to a much lower or even asymptomatic dose. There is evidence that even an exposure to a non-symptomatic dose causes long-term changes. Unfortunately, toxicological data for late onset low dose organophosphate exposure effects is sparse. Studies of cardiotoxicity due to OP poisoning have demonstrated long-term QT prolongation, arrhythmias, various conduction problems, cardiomyopathy, and sudden death (Alaoui, Mossadeq, Faroudy, & Sbihi, 2009; Bar-Meir, et al., 2007; Gohel, Oza,

Panjwani, & Gajjar, 1996; Marosi, Ivan, Vass, Gajdacs, & Ugocsai, 1989; Kiss & Fazekas, 1979).

Studies involving sarin in rodents report susceptibility to epinephrine induced arrhythmia and long QT syndrome for initial period of four weeks from the single whole body exposure to sarin in rats (Allon, Rabinovitz, Manistersky, Weissman, & Grauer, 2005). Another study in rats shows QT prolongation and cardiac lesions for up to 12 weeks following a slightly higher dose sarin dose (Abraham, Oz, Sahar, & Kadar, 2001). Other low dose long-term changes have been reported in rats to include DNA synthesis, and brain cholinergic receptors and genetic expression (Kassa, et al., 2004; Damodaran, Jones, Patel, & Abou-Donia, 2003; Jones, Dechkovskaia, Herrick, Abdel-Rahman, Khan, & Abou-Donia, 2000). Recently, Morris *et al.* and Joaquim *et al.* have linked autonomic changes with the heart; showing an increase in heart rate variability (HRV) following an AChE inhibition (Morris, Key, & Farah, 2007; Joaquim, Farah, Bernatova, Rubens Jr., Grubbs, & Morris, 2004). As with the GWI data, the literature lacks sufficient toxicological background to pinpoint the risk to the heart following a low/asymptomatic dose of nerve agent.

Problem Statement

The current literature lacks sufficient background on low dose and late-onset effects resulting from exposures to sarin or other OPs. Understanding these effects has significant interest to the military – from both a GWI perspective as well as performing military operations in a chemical agent environment. Current Air Force doctrine allows for selective chemical protection (known as split-MOPP (Mission Oriented Protective

Posture)) following a chemical warfare agent attack (United States Air Force, 2007). At present, the literature is vague as to the long-term risk split-MOPP may pose to military forces that might receive an asymptomatic dose of nerve agent when not wearing their chemical protection equipment. Additionally, as seen in the *Gulf War*, munitions demolition poses a risk to US military personnel (CDC, 1999).

The Japanese terrorists' attacks of 1994 and 1995 demonstrate that civilians are at risk as well. In addition, nearly all the known living humans with sarin exposures were victims of Japanese terrorists' attacks, and these attacks are the source of the bulk of the literature on human exposures. Unfortunately, there is little documentation on the extent of exposure in these cases (Committee on Gulf War and Health: Updated Literature Review of Sarin, 2004). Thus researchers must rely on animal studies to investigate long-term sarin effects.

The literature, however, has few descriptive and long-term cardio-toxicological studies following a low dose sarin exposure. Recent high dose studies have shown a link between sarin and long-term electrocardiogram (ECG) changes in rats. Similarly, OP poisonings (high-dose) have shown long-term cardiovascular changes to include ECG abnormalities (e.g. QT prolongation), cardiomyopathy, and arrhythmias. No study (to the author's knowledge), however, has combined echocardiography and histology/morphology evidence with ECG.

In summary, data is scarce concerning low dose sarin, long-term effects on the cardio-vascular system (CVS), and relating to molecular/morphological changes in the heart. In addition, the conduction abnormalities observed at high doses of sarin need to

be critically analyzed at low doses to help provide early diagnosis. Similarly, functional and structural changes in the heart have not been evaluated. Finally, CVS studies thus far have analyzed the heart under basal conditions; assessment of CVS under stressed conditions is known to provide invaluable information regarding response of CVS under load (i.e. stress of running).

Research Objective/Hypothesis

Subclinical doses (0.4 LD₅₀ and 0.5 LD₅₀ on two consecutive days) of sarin cause cardiac remodeling/performance degradation over a period of time.

Specific Aims:

- 1) To test the hypothesis that low dose Sarin causes delayed cardiac remodeling.
- 2) To test the hypothesis that low dose Sarin has a negative effect on cardiac performance over a period of time.
- 3) To test the hypothesis that subtle effects from low dose Sarin will become apparent as a result of stressing.

Proposed Experiment

C57BL/6J strain mice will be injected on two consecutive days with saline (controls), 0.4, or 0.5 times the LD₅₀ for sarin, and will be studied for cardiac pathology. Mice cholinesterase levels will be measured 24 hours post exposure to confirm the effect of the sarin injection levels. The mice will be studied for 10 weeks after exposure, sacrificed, and relevant tissues and organs collected. A short-acting β 1 specific agonist, dobutamine, will be used to create stress in the heart. 2-D and 2-D M-mode echocardiography will be used to measure left ventricular structure and performance

before and after a dobutamine stress test at two, four, and 10 wks. Additionally, electrocardiogram tracings will be obtained at the 10-week point, baseline and after dobutamine. Finally, histological methods, such as atrial natriuretic peptide (ANP), brain natriuretic peptide (BNP), and collagen staining will be used to determine additional measures of pathology.

Contributions

The contribution of this research is to close the gap between the current literature and the effects of low dose sarin. Where the current literature suggests that sarin causes cardiac dysfunction, more analysis is required to link low dose sarin to long-term cardiac impairment. This research will focus on cardiac pathology with an in-depth temporal evaluation of murine cardiac performance; combining, toxicological techniques to include histology, echocardiography, and ECGs. As such, this study will provide important parameters to the medical community in the diagnosis following a sarin exposure, and allow the military to develop post deployment health assessments with late-onset pathology in mind.

II. Literature Review

Introduction

Studies have expressed ECG changes in rodents and humans following acute exposures to sarin and OPs indicating cardiovascular changes. Yet, the literature is lacking with regard to cardiac morphology and other fundamental changes. As such, this study presents a first look at cardiac performance and morphological parameters under a variety of conditions. The following discussion communicates the importance of these parameters and conditions as described in the current literature.

Animal Considerations

Unlike humans, mice have high levels of carboxylesterase which rapidly degrades sarin and modifies the dose-response curve (Li, et al., 2005; Jokanovic, Kosanovic, & Maksimovic, 1996). In order to reduce the effect of carboxylesterase, the animal's susceptibility to sarin can be enhanced by dosing on consecutive days. The first dose consumes serum carboxylesterase so that the second dose has greater effect on the cholinergic receptors; thus making the toxicity curve more similar to that seen in humans. In order to ensure this effect, serum cholinesterase (ChE) assays are used to ensure adequate depression of ChE levels (Sidell & Borak, 1992).

Choice of Anesthesia and Expected Effects

The use of anesthesia has been shown to have a significant effect on echocardiograms and ECGs when compared to conscious mice. In echocardiograms, the studies have shown decreased cardiac performance such as heart rate variability,

fraction shortening, and ejection fraction. (Tan, et al., 2003; Stein, et al., 2005; Roth, Swaney, Dalton, Gilpin, & Ross Jr, 2002). Similarly, ECG tracings have shown significant decreases in heart rate, and increases in QT and PR intervals (Chavesa, Dech, Nakayama, Hamlin, Bauera, & Carnes, 2003).

Nevertheless, Tan *et al.* have shown that the use of sedatives may help to reduce stress and significantly reduce the variability seen in echocardiograms using conscious mice; this is apparently due to stress differences created because of restraints or the amount of training the mice received (Tan, et al., 2003). Additionally, Roth *et al.* quote several sources in the literature that have been unable to record images in conscious mice due to extremely high heart rates (stress induced despite training) and the difficulty of transducer placement in conscious animals (due to small movements). Therefore, the difficulty of transducer placement and training, variations in sympathetic and parasympathetic tone during restraint, and relatively high HR make measurements in conscious mice less than ideal for all applications of echocardiography (Roth, Swaney, Dalton, Gilpin, & Ross Jr, 2002; Tan, et al., 2003). Furthermore, the use of restraints in mice has been shown to increase body temperature, heart rate, blood pressure, plasma epinephrine/nor-epinephrine levels, and change responses to pharmaceuticals (Kramer, Kinter, Brockway, Voss, Remie, & Van Zutphen, 2001). Similar findings have been found in ECG recordings; movement artifacts, animal acclimation, and the ability to only capture very short ECG recordings have been listed as some of the drawbacks of using conscious animals (Chavesa, Dech, Nakayama, Hamlin, Bauera, & Carnes, 2003). Finally,

the use of conscious animals requires implantation of the ECG probes or restraint, and implantation is a costly alternative to the use of anesthesia.

Of the anesthesia widely used in the literature, isoflurane (ISF) has been shown to affect the heart less than other anesthesia in echocardiograms and ECGs (Tan, et al., 2003; Stein, et al., 2005; Roth, Swaney, Dalton, Gilpin, & Ross Jr, 2002; Chavesa, Dech, Nakayama, Hamlin, Bauera, & Carnes, 2003). Additionally, Stein *et al.* have cited that ISF is easier to use, produces reproducible results, has short-lived action, and is ideal for multiple short lived experiments (Stein, et al., 2005). Given the drawbacks of using conscious animals and the advantages of ISF, ISF was chosen for use in this experiment. Because all of the animals will be anesthetized in the same manner, the use of anesthesia is thought to have minimal (if any) impact on the experimental outcomes.

Environmental Concerns

Temperature has been shown to significantly influence murine cardiac performance. Hartley *et al.* have shown fluctuation of body temperature during surgical and monitoring procedures under anesthesia. As mice are unable to maintain body temperature under ISF, significant alterations occur in heart rate and cardiac function with changes in body temperature (Hartley, Michael, & Entman, 1995; Hartley, Taffet, Reddy, Entman, & Michael, 2002). Likewise, Swoap *et al.* have shown that variations in room temperature (as small as 4°C) can significantly affect heart rate and blood pressure in a mouse (Swoap, Overton, & Garber, 2004). For these reasons, all procedures are carried out in a temperature controlled room (22°C ± 1°C), and a heating

blanket will be used to ensure body temperature is maintained throughout all procedures. Finally, as with the anesthesia, all of the animals will be maintained in the same manner, and temperature effects are thought to have minimal (if any) impact on the experimental outcomes.

Dobutamine Stress Testing

In order to test stimulated heart function in mice, a low dose (1 mg/kg) of dobutamine will be injected. Dobutamine, a short-acting and preferential β_1 adrenergic agonist (Anderson, Moore, & Larson, 2008; Daly, Linares, Smith, Starling, & Supiano, 1997), is widely used in the analysis and stratification of cardiac function under stress (Mertes, et al., 1993; Shaheen, Luria, Klutstein, Rosenmann, & Tzivoni, 1998).

Dobutamine increases heart rate, contractility, and cardiac output (Wiesmann, et al., 2001; Weissman, Levangie, Guerrero, Weyman, & Picard, 1996), and its effects last for approximately 25 minutes (Wiesmann, et al., 2001). By creating positive inotropic and chronotropic effects, the β -agonist increases myocardial oxygen demands, producing abnormalities (otherwise not apparent) that appear in ECG and echocardiography as the result of the supply-demand mismatch (Weissman, Levangie, Guerrero, Weyman, & Picard, 1996). Additionally, because dobutamine preferentially binds β_1 -adrenoreceptors, the stress test can offer information on the overall health of the receptor cascade (Anderson, Moore, & Larson, 2008).

In general, dobutamine has not been shown to have any long lasting effects, however Anderson *et al.* have shown that large doses (40 μg /mouse/day for seven days)

can increase fibrosis and lead to hypertrophy (Anderson, Moore, & Larson, 2008). This experiment will use low doses (1 mg/kg body weight, or approx. 30 µg/mouse), and each mouse will only be injected 3 times (at the 2, 4, and 10 week points); thus the mice should not be subject to any long-term effects. Therefore, dobutamine offers a readily reproduced method of measuring cardiac performance under stressful conditions.

Noninvasive In Vivo Measurements

Echocardiograms

Echocardiography is a commonly used technique to give important geometric and temporal information about the heart. Imaging techniques have been adapted from human systems (and imaging systems designed for larger animals) and usually have less than ideal temporal resolutions (frame rates) when used with mice (human rate is near 60 beats per minute whereas murine heart rate is as high as 600).

Nonetheless, echocardiography is one of the most widely used noninvasive techniques for testing murine cardiac function (Hartley, Taffet, Reddy, Entman, & Michael, 2002).

Long axis views of 2-Dimensional (2-D) and guided M-mode are frequently acquired parameters to give area and diameter measurements of the left ventricle (LV) and LV walls in systole and diastole (Schiller & Foster, 1996; Morgan, et al., 2004). Other important derived parameters (e.g. area fractional shortening (aFS)) can be calculated from the long axis end systolic and diastolic areas (ESA and EDA) and diameters (ESD and EDD). Such derived parameters are well documented and reproducible indicators of LV and cardiac function (Morgan, et al., 2004). Pulse wave Doppler imaging of trans-mitral flow provides time profiling, and is useful for calculating a variety of parameters

related to ventricular dysfunction such as myocardial performance index or MPI (Tei, Nishimura, Seward, & Tajik, 1997; Syed, Diwan, & Hahn, 2005). Combinations of the above parameters (2 D, M-mode and Doppler) can be used to obtain a pressure-independent measure of LV contractile function such as velocity of circumferential fiber shortening (Vcf) and aFS/MPI. These combined parameters serve as superior indicators of overall LV function since these values take into account both geometric and temporal measures of LV function (Broberg, et al., 2003; Syed, Diwan, & Hahn, 2005).

Electrocardiograms (ECG)

Electrocardiograms are used in humans to detect a multitude of cardiac problems to include bradycardia, tachycardia, atrioventricular (AV) block, ischemia, Torsades de Pointes (also known as long QT syndrome), and other arrhythmic dysfunctions (Roden, 2001). In general, ECGs measure the impulse propagation through the conduction system. Cardiac impulses originate in the sinus node and depolarizing currents ($\text{Na}^+ - \text{K}^+$ exchange) spread anisotropically from the sinus node. Upon leaving the sinus node, the impulse rapidly propagates throughout the atria, resulting in the P-wave (atrial systole) seen on the ECG (see Figure 3). Propagation is then markedly slowed through the AV node where inward Ca^+ channels are much smaller than the Na^+ current in the atria. This delay, corresponding to the PR interval on the ECG, allows the atrial contraction sufficient time to fill the ventricle. As the impulse leaves the AV node, the propagation rate is substantially increased (through large Na^+ channels) and ventricular contraction ensues (forming the QRS complex on the ECG) as impulses race through the *Bundle of His* to the *Purkinje Fibers*. Finally, the ventricle relaxes (ST

segment in the ECG) and then undergoes repolarization, forming the T-wave on the ECG; after which the impulses diffuse from the endocardium to the epicardium forming the iso-volumetric relaxation time (inactivity on the ECG from T-end to start of the P-wave). Thus, the PR interval on the ECG corresponds to the AV nodal conduction time, the QRS complex represents the ventricular conduction time, and the QT interval describes the complete ventricular action potential (Roden, 2001). As such, the ECG is an excellent measure of the overall health of a cardiac system.

The first ECGs in mice were reported nearly 70 years ago (Hartley, Taffet, Reddy, Entman, & Michael, 2002), and the progress of ECG studies in mice has been summarized by Wehrens *et al.* (Wehrens, Kirchhoff, & Doevendans, 2000). With the exception of the T-wave, mice ECGs are similar to the human ECG (see Figure 4).

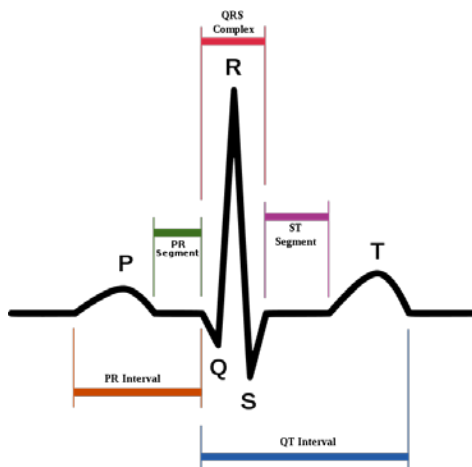


Figure 3 Typical Human ECG
(This image is licensed for unrestricted redistribution (Atkielski, 2007)).

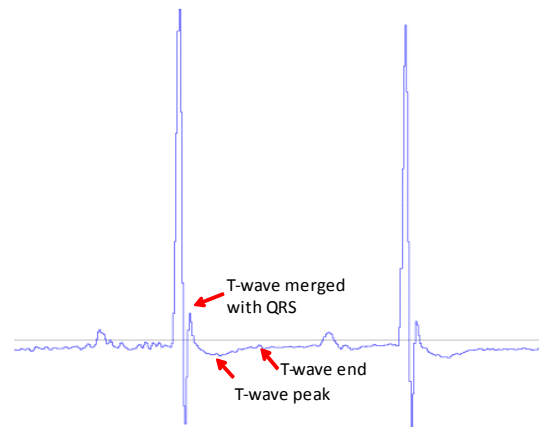


Figure 4 Typical Mouse ECG Illustrating the Difference in the T-wave when Compared to the Human ECG

In mice, the T-wave merges with the end of the QRS complex and the ST segment is not discernable (Wehrens, Kirchhoff, & Doevendans, 2000; Mitchell, Jeron, & Koren, 1998; London, 2001). This merged T-wave rises above the iso-electric line and has a long tail that falls below the iso-electric line before returning to mark the iso-volumetric relaxation time (Mitchell, Jeron, & Koren, 1998). Despite these differences, the ECG represents a valuable diagnostic tool for overall health of the murine cardiovascular system and has widely been used in literature to detect dysfunctions in mice analogous to those seen in humans, i.e. ischemia, Torsades de Pointes, etc. (Kramer, van Acker, Voss, Grimbergen, van der Vijgh, & Blast, 1993; Hartley, Taffet, Reddy, Entman, & Michael, 2002; Mitchell, Jeron, & Koren, 1998; Wehrens, Kirchhoff, & Doevendans, 2000).

In Vitro/Histological Markers

Utility of ANP/BNP Measurements

Atrial natriuretic peptide and Brain natriuretic peptide (ANP and BNP) are hormones synthesized and secreted exclusively by the heart as a response to activation of hormonal or mechanical stimuli that occur during heart failure and ventricular dysfunction (Yasuno, et al., 2009). ANP/BNP function as cardiac contractile genes up-regulated during cardiac remodeling and are indicative of various pathologies such as cardiomyopathy, hypertrophy and heart failure, etc. ANP is synthesized in atrial myocytes, whereas, BNP is synthesized in ventricular myocytes; ANP/BNP increase as a response to wall stretch and cardiac stress (Goetze, Georg, Jorgensen, & Fahrenkrug, 2009; Mair, 2008).

ANP and BNP regulate blood pressure by vasodilatation and increasing the permeability of vasculature. Both ANP and BNP exert their natriuretic, diuretic, and vasorelaxant effects through activation of their common receptor Natriuretic Peptide Receptor A (NPRA) (Kawakami, et al., 2010). Studies in mice have shown protective role of ANP and BNP in models of dilated cardiomyopathy and of sudden death in guanylyl cyclase-A knockout (GC-A $-/-$) mice (Yasuno, et al., 2009). In addition, ANP is also shown to have growth inhibitory response in cardiac myocytes and fibroblasts upon stimulation by nor-epinephrin (Knowles, et al., 2001; Tamura, et al., 2000). Similarly, a NPRA knockout study (NPR $-/-$) shows development of hypertrophy independent of pressure overload (presumably solely due to the missing ANP/BNP receptor) (Scott, et al., 2009). Furthermore, ANP/BNP, also known as a subset of *fetal cardiac genes*, are expressed in fetal ventricles during development but are quiescent in adult ventricles (Scott, et al., 2009). Therefore, increased ANP/BNP levels in adult mice serve as excellent biomarkers of overall cardiac health, and are a likely indicator of cardiac detriment because of sarin exposure.

Collagen and Picrosirius Red Staining

Fibroblasts are widely recognized as a critical cell type involved in wound healing and tissue repair. During repair functions, quiescent fibroblasts are transformed into active myofibroblasts (smooth muscle-like fibroblasts) (Long & Brown, 2002; Powell, Mifflin, Valentich, Crowe, Saada, & West, 1999). In the heart, myofibroblasts produce collagen in response to an insult or infraction (Kerckhove, Kalkmana, Saxena, & Schoemaker, 2000; Lutgens, Daemen, Muinck, Debets, Leenders, & Smits, 1999). As

such, cardiac fibrosis is characterized predominantly by over expression of collagen types I, II, and III, into the interstitial and perivascular space (Diez, Lopez, Gonzadlez, & Querejeta, 2001). Excessive collagen deposition leads to myocardial stiffening, impaired cardiac relaxation and filling (diastolic dysfunction), and overload of the heart (Swaney, Roth, Olson, Naugle, Meszaros, & Insel, 2005). Therefore, increased collagen levels serve as a good indicator of cardiac insult.

Finally, Picrosirius Red is a highly specific dye for collagen fibers. Under cross-polarized light thicker strands of collagen appear yellow to orange, thinner fibers green, and the background is black. This birefringence is largely due to type I collagen. (Junqueira, Bignolas, & Brentani, 1979; Puchtler, Waldrop, & Valentine, 1973).

Hematoxylin and Eosin (H&E) Staining

H&E is a prevalent stain used in preparation of histology slides. H&E stains nuclei blue and the rest of the cell (cytoplasm, collagen, muscle fibers) is stained pink (Eroschenko, 2008). As such, the H&E stain provides important information about the nuclei and muscle fiber arrangement and cell size when heart sections are examined under a microscope.

III. Methodology

Animal Experimental Protocol

Thirty-six male C57BL/6J mice were housed individually at 22°C with a 12:12-hour dark-light cycle. Mice had free access to a standard diet and tap water. Mice were injected with sarin: 64µg/kg (0.4 LD₅₀ – lethal dose to 50 percent of the population) and 80 µg/kg (0.5 LD₅₀), respectively, or saline (control group) on two consecutive days. Each group (controls, 0.4 LD₅₀, and 0.5 LD₅₀) originally consisted of twelve mice. Mice body weights were collected 24 hours, four weeks, seven weeks, and 10 weeks following the sarin injections.

In order to ensure that the sarin dose affected the mice, blood cholinesterase levels were measured 24 hours after the second sarin injection using a modified version of the assay developed by Ellman *et al.* (Ellman, Courtney, Andres, & Feather-Stone, 1961). Blood was obtained by cheek puncture, mixed with tetraisopropylpyrophosphoramide (iso-OMPA), and diluted with a sodium phosphate buffer solution. This mixture was incubated and then dithionitrotoluene (DTNB) and acetylthiocholine (ATCh) were added. Total ChE was measured in the same manner with the exception that sodium phosphate was added in lieu of iso-OMPA. These samples were measured using a Fusion™ Microplate Analyzer (Packard Bioscience Company, Meriden, CT). Butyryl ChE was determined as total ChE less the AChE. Figure 5 demonstrates that average ChE levels were approximately 50 percent of the original level in both sarin affected populations.

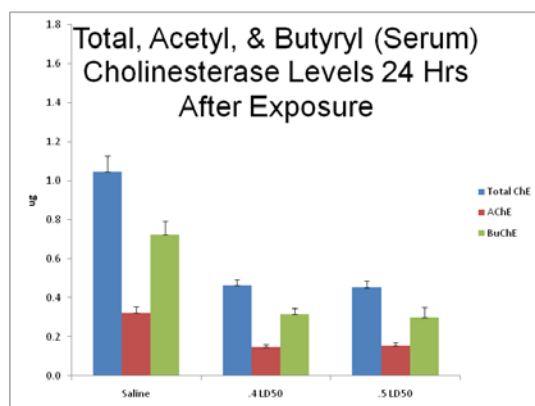


Figure 5 Blood Cholinesterase Levels 24 Hours after 2 Consecutive Sarin Injections

Following the second sarin injection, a total of six of the 12 0.5 LD₅₀ group seized and died; no mice from the 0.4 LD₅₀ group died, but three seized following the second injection. Throughout the 10 weeks one control mouse died, two of the 0.4 LD₅₀ group, and one more from the 0.5 LD₅₀ group died.

Tissue Collection, Heart Sectioning, and Heart Size Measurement Methods

In the 10th week after sarin infusion, the mice were sacrificed (following ECG and echocardiogram recordings) by decapitation. Immediately following decapitation, the heart was collected, weighed, and relaxed in a phosphate buffered saline (PBS) solution. The apex was removed using a straight razor and the heart (sans apex) was placed in a 4% paraformaldehyde (PFA) solution. This solution was stored at 4 °C for 48 hours. Following the 48 hour adsorption time, the hearts were removed from the PFA and fixed in a 20% sucrose/4% PFA solution. Hearts were stored for an additional 24 hours at 4 degrees Celsius, and then transferred to a -80 degree Celsius freezer where they were stored until they were shipped to AML Laboratories, Inc for cryostat sectioning.

Prior to shipment, a random selection of the fixed mouse hearts (7 control; 8, 0.4 LD₅₀; and 5, 0.5 LD₅₀) was selected for cryostat sectioning. Three-millimeter sections of the left and right ventricle were created using a 1 mm heart block (Zivic Laboratories, Inc., Pittsburg, PA.). The hearts were held in place using a razor blade and forceps while sectioning (Figure 6).



Figure 6 Representative 3mm Heart Sectioning

Photographs were taken of the atrial side (larger side nearest the atriums) from each section. A Nikon D50 camera (Chiyoda-ku, Tokyo) with an AF-Micro Nikkor® 60mm lens was used to take each photograph. A ruler (with 1 mm sections) was included in the photograph to provide a reference for size measurements (see Figure 7).



Figure 7 Picture of Atrial Side of a 3mm Thick Heart LV/RV section

All pictures were taken the same day, with the same light settings and camera settings. The camera was mounted and sections were placed on the same reference point to

ensure that the camera perspective remained the same. These three-millimeter sections were sent to AML Laboratories, Inc. (Rosedale, MD) where five-micron paraffin slides of the sections were created from the atrial side of the ventricles.

Heart Section Size Measurements

Total heart, LV, and RV area were calculated using the Adobe® (San Jose, CA) Photoshop® CS3 software package (version 10.0.1). A single, blinded observer performed all the analysis on a single day. The RV and LV were manually cropped from the heart sections using the *quick selection* and *magic wand* tool sets (see Figure 8). Cropped sections were pasted into a new blank image with *transparent pixels*, and the total area (in pixels) was obtained via the programs *histogram* tool. After the ventricles were cropped, the heart section was selected (using the *quick selection/magic wand* tools as described above) and pasted into a blank image with transparent pixels; the histogram tool was used to calculate the total heart area.



Figure 8 Representation of manual Cropping of the RV and LV using Adobe® Photoshop to Obtain LV/RV Area



Figure 9 Representation of Photoshop® Enhanced Image to Obtain Total Heart Area

LV, RV and Total heart size were acquired for each image by creating a pixel to mm conversion factor (CF) using Microsoft® Paint, version 5.1 (Redmond, WA). A straight line was drawn from the center of a millimeter marking on the ruler to the adjacent

marking and the length in pixels was recorded. Finally, areas in mm² [for each LV, RV, and total heart area) were calculated by dividing each section area (in pixels) by CF squared.

Echocardiogram Methods

Transthoracic Echocardiogram Method

Two-dimensional echocardiography was used to measure the left ventricular structure and function two, four, and 10 weeks after the sarin injections. Mice were anesthetized with 2% isoflurane in pure oxygen (five liters per minute) in an anesthesia chamber and maintained with 1% isoflurane by nose cone. A Surgivet Anesco® Isotec 4™ (Waukesha, WI) anesthesia machine was used to administer the isoflurane and oxygen. Mice were then weighed using a Denver Instruments® XP-500 electronic scale (Denver, CO). Once weighed, the mice were transferred to a heating pad and placed in a supine position. The precordium was de-haired using the commercial product Nair® and an isopropyl alcohol pad (see Figure 10 and Figure 11).

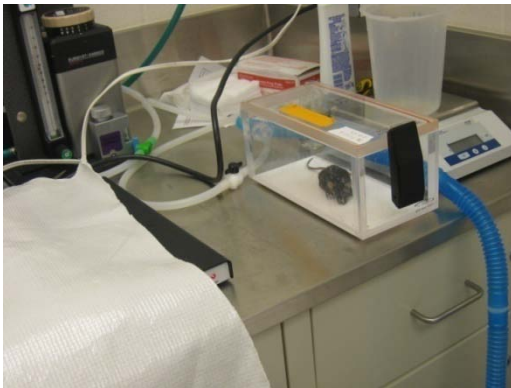


Figure 10 Mouse Anesthesia Procedure

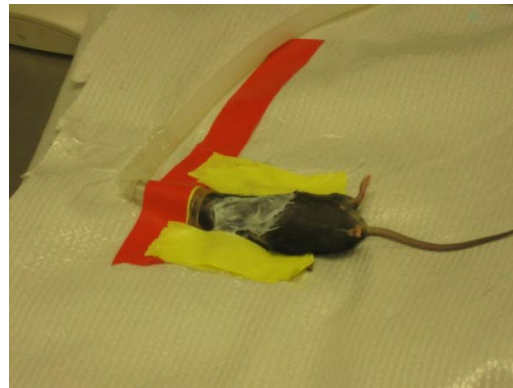


Figure 11 Mouse Being De-haired in the Precordium

Echocardiograms were recorded using a Seimens® ACUSON Sequoia 512 ultrasound system (New York, NY) with an ACUSON 15 megahertz transducer (model

15L8). The transducer was coated with pre-warmed ultrasound transmission gel (Aquasonic™ 100 from Parker Laboratories, Inc., Fairfield, NJ). Transthoracic two-dimensional guided M-mode (2-D M-mode) and two-dimensional images were obtained via the parasternal apical windows (see Figure 12).



Figure 12 Representative Echocardiogram Technique

Three-second axis *cine* loops of the left ventricle (LV) were obtained in 2-D mode using the *clip store* function on the machine. In addition, guided M-mode long axis LV, and pulsed wave Doppler images of the left ventricle were collected. In weeks two and four, the mice were injected with dobutamine and the above procedure was repeated five minutes following the dobutamine injection. (Five minutes was chosen to ensure that dobutamine had reached its onset of action; changes from the dobutamine were visually and acoustically obvious in the Doppler after one to two minutes, and Plante *et al.* have shown significant changes in a rat as soon as four minutes following a dobutamine injection (Plante, Lachance, Drolet, Roussel, Couet, & Arsenault, 2005)). In week 10, ECG analysis (see the ECG Methods section) took place before the post dobutamine echocardiogram images were obtained from the mouse. The mice were

injected with one milligram of dobutamine (in a saline solution) per kilogram of body weight (1 mg/kg). This injection was made intraperitoneally (see Figure 13).

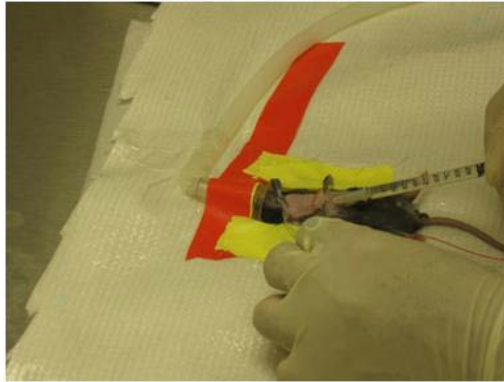


Figure 13 Method of Dobutamine Injection

Echocardiography Analysis Method

Analysis was performed by a single observer using the Siemens® ACUSON Sequoia machine's off-line analysis module. (A separate observer (inter-observer) also analyzed a random sampling of the controls and sarin groups at varying weeks to ensure data quality; inter-observer results did not vary significantly from the single observer). Diastolic and systolic areas were measured via frame-by-frame analysis of the 2-D *cine* loops. The inner edge of the ventricular endocardial border including the papillary muscle was measured for three consecutive sinus beats. These values were recorded and averaged. End diastolic area (EDA) measurements were made at the time of the perceptible maximal LV diastolic breadth, and end-systole (for end systolic area (ESA) measurements) was measured in the frame before ventricular expansion (see Figure 14). Ventricular septal wall thickness (SWT), posterior wall thickness (PWT), end diastolic diameter (EDD), and end systolic diameter (ESD) were made in accordance with the leading edge method from the 2-D M-mode images of the LV in both systole and

diastole as presented by the American Society of Echocardiography (Sahn, DeMaria, Kisslo, & Weyman, 1978) (see Figure 15). Three separate measurements were made for each (SWT, PWT, etc.) and the values were recorded and averaged.



Figure 14 Representative Area Measurement Method for 2-D Echocardiograms

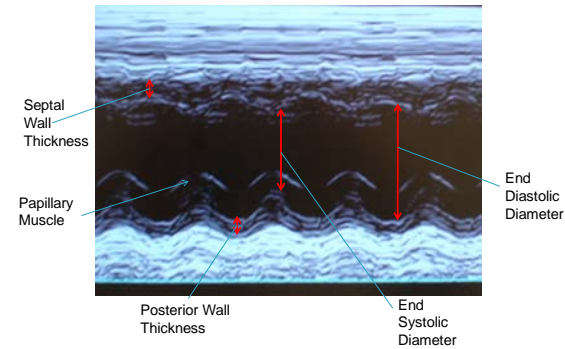


Figure 15 Representative Measurement Methods for 2-D M-mode Echocardiograms

Pulsed wave Doppler (see Figure 16) was used to measure B (iso-volumetric contraction time (ICT) plus iso-volumetric relaxation time (IVRT)), A (Ejection Time (ET)), aortic output velocity/time index (Ao VTI), and aortic output maximum velocity (Ao V_{max}) (see Figure 17) in accordance with the previously described methods in the literature (Tei, Nishimura, Seward, & Tajik, 1997; Morgan, et al., 2004). Three separate measurements (using a single observer) for each image were recorded and averaged.

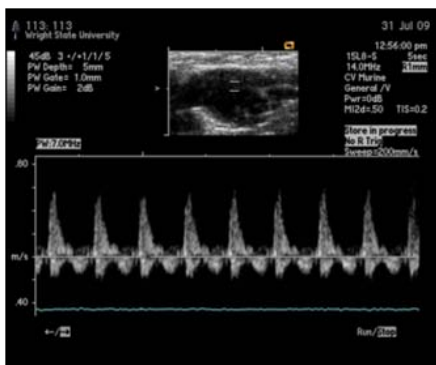


Figure 16 Example Pulsed Wave Doppler Image Showing Eight Full Sinus Rhythms

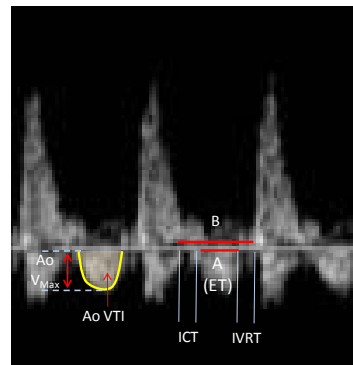


Figure 17 Pulsed Wave Doppler Method of Quantification

Fractional shortening (FS), relative wall thickness (RWT), area fraction shortening (aFS), and the myocardial performance index were calculated using Equation 1, Equation 2, Equation 3, and Equation 4 (Morgan, et al., 2004; Syed, Diwan, & Hahn, 2005).

Equation 1 Fractional Shortening Derived from M-mode Echocardiogram Images

$$FS = (EDD - ESD)/EDD \quad (1)$$

Equation 2 Relative Wall Thickness Derived from M-mode Echocardiogram Images

$$RWT = (PWT + SWT)/EDD \quad (2)$$

Equation 3 Area Fractional Shortening Derived from 2-D Echocardiogram Images

$$aFS = (EDA - ESA)/EDA \quad (3)$$

Equation 4 MPI Derived from Pulse Wave Doppler

$$MPI = (B - A)/A \quad (4)$$

(Where A and B are derived as per Figure 17).

Finally, the derived parameters from the 2-D geometric and Doppler temporal data aFS/MPI and the mean circumferential fiber shortening velocity (V_{cf}) were calculated. V_{cf} was calculated using modified formulas presented by Broberg *et al.* (Broberg, et al., 2003).

Equation 5 V_{cf} derived from 2-D mode and Pulse Wave Doppler Echocardiograms

$$V_{cf} = aFS/B \quad (5)$$

(Where B is derived as per Figure 17)

ECG Methods

Telemetry Collection Procedure

ECG tracings were collected on the mice in conjunction with the 10 week echocardiograms. The shaved area of the anesthetized mice was cleaned with an isopropyl alcohol pad and a two-lead telemetry probe, Data Sciences International (DSI) (St. Paul, MN) radiotelemetry probe model # TA11ETA-F10 (manufactured 15 May 2009), was externally attached to the shaved precordium. The upper right electrode was clipped just below the neck line in the dorsal thoracic region (near the front right limb); the lower left electrode was placed within the muscle tissue in the lower left abdominal wall, cranial to the groin area (see Figure 18).

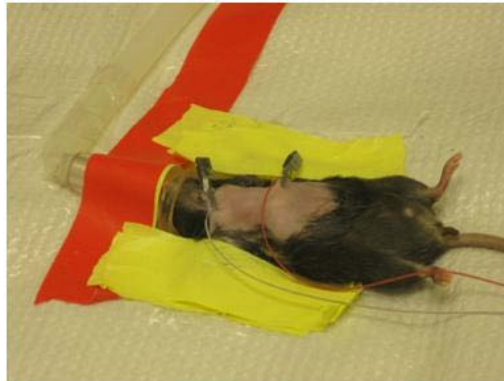


Figure 18 ECG Electrode Placements and Technique of Attachment

The electrodes were clipped using a Schwartz micro-serrefine clip, and the transmitting end of the probe was placed over a DSI PhysioTel® receiver. The heating pad had to be turned off during the ECG recordings (approximately 15 minutes) because the radio frequency generated by the induction coils interfered with the probe's communication to the PhysioTel® receiver.

Telemetry was recorded using DSI's Dataquest A.R.T.[™] (version 4.0) acquisition software. The manufacture's probe calibration information was entered into the program and the program was set to record in ECG mode with a sampling frequency of 5,000 hertz. Tracings were recorded for approximately five minutes. The mice were then injected with 1 mg/kg of dobutamine as described in the Echocardiogram Methods of this report. Using the Dataquest[®] software, a mark was added to the ECG trace to indicate that the drug had been administered at that time. The ECG tracings were recorded for an additional seven minutes after the dobutamine injection; this was done to ensure that ECG recordings were captured after the dobutamine took effect. This effect was visually obvious from the real time ECG trace and usually took between two and three minutes.

ECG Analysis Method

The ECG tracings were analyzed using DSI's Ponemah[™] software (version 4.90). The A.R.T.[™] files were imported into the Ponemah[™] Physiological Platform and the software was set to record all available derived parameters under the channel input tab. Thirty seconds of the ECG tracings from before the dobutamine injection and 30 seconds from after the dobutamine injection were analyzed for each mouse. The Ponemah[™] software's analysis tool was used to automatically detect and mark the P, Q, R, S and T-waves. The software was set to display all marks and all values in the *std. attributes* tab were set to the software's predetermined values for a mouse (with the exception of the QT interval which was set to 70 milliseconds (ms) rather than 100 ms

because at 100 ms the QT interval overlapped the PR interval and the software would not recognize the P-wave if the intervals overlap). Because the software had limited ability to detect all the P and T-waves, the software's template analysis toolkit was also used. One representative beat (P-start to T-end) was chosen and added to the template and the software was set to match all waves that matched the beat within 80% of the representative beat. The peak of the T-wave was defined as the lowest point on the T-wave after the end of the S-wave, and the end of the T-wave was placed where the T-wave crossed the apparent iso-electric line (where the ECG became parallel to the x-axis). A representative ECG trace is depicted in Figure 19 and wave placement marks are depicted in Figure 20.

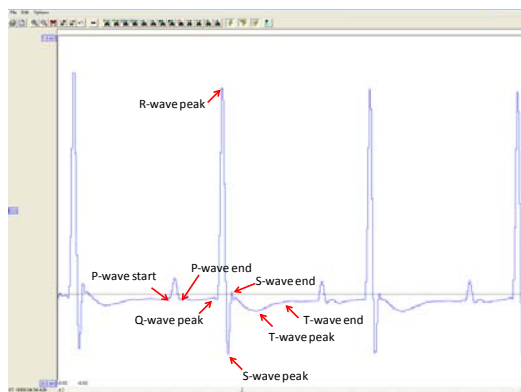


Figure 19 Representative ECG Tracing

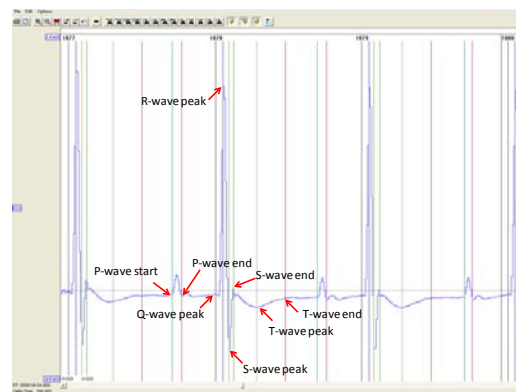


Figure 20 Representative ECG Trace with Software Markings

If the end of the T-wave encroached on the beginning of the P-wave (i.e. the T-wave does not return to the iso-electric level before the start of the P-wave), the end of the T-wave was defined as the point just before the start of the P-wave (Figure 21). Finally, the ECG trace was analyzed beat by beat by a single observer on separate days for each 30 second interval; if the ECG trace showed an aberration (e.g. due to a respiration), the

marks for the entire beat were excluded (see Figure 22); any missing marks from beats without aberration were added.

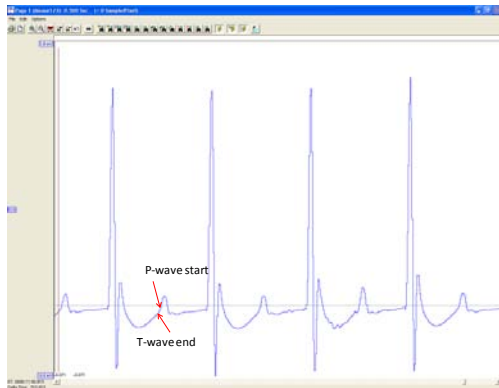


Figure 21 ECG Trace Showing End of T-wave Encroachment on the P-wave Start

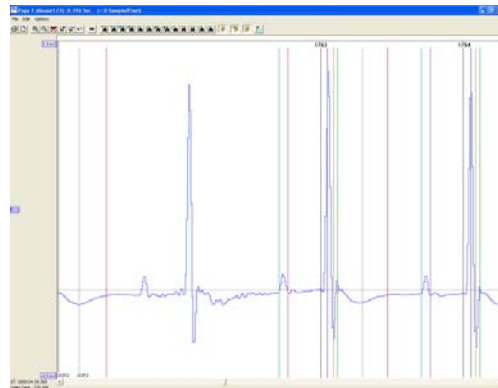


Figure 22 ECG Trace with an Indiscernible T-wave Due to a Respiration

The *Derived data* from the Ponemah™ program was then saved as a Microsoft® Excel™ file. The Ponemah™ derived RR intervals (giving heart rate) were corrected to compensate for the deleted beats (indiscernible beats described previously); for example, intervals that had one deleted beat (Ponemah™ calculates RR as the interval from one marked R-wave to the next marked R-wave; the software is unaware if an intervening mark has been deleted) were divided by two. In addition, a new QT corrected (QT_c) interval was calculated using modified Bazett's method (Bazett, 1920) from the corrected RR interval and the Ponemah™ derived QT interval. Mitchell *et al.* have shown that the high resting heart rate of the mouse requires normalization of the RR interval to 100 beats per minute (Mitchell, Jeron, & Koren, 1998)

Equation 6 Bazett/Mitchell QT Correction

$$QT_c = QT / \sqrt{RR/100} \quad (6)$$

To check for ST-T abnormalities using the Ponemah™ software, a novel method was developed. Mitchell *et al.* and others (Mitchell, Jeron, & Koren, 1998; Kramer, van Acker, Voss, Grimbergen, van der Vijgh, & Blast, 1993; London, 2001), have shown that with respect to the QT segment the electrocardiogram of an adult mouse differs considerably from that of humans; notably the absence of an identifiable ST segment. Mitchell *et al.* note that there is an early-peaking, upright T-wave (with a broad inverted tale) that is merged with the end QRS. In order to measure the ST segments and/or depressions/elevations van Acker *et al.* and others have used the interval from end of S to the T-peak (Nossuli, Lakshminarayanan, Baumgarten, G. E. Taffet, Michael, & Entman, 2000; van Acker, Kramer, Grimbergen, van der Vijgh, & Blast, 1996). (The Ponemah™ program's ST-I parameter measures the ST interval from the S-peak to the T-end; not from the S-end, the parameter of interest to show ST elevation/depression). Accordingly, the following formulae were developed to define ST-T deviations:

Equation 7 Corrected ST Segment Length

$$ST_C = \frac{QATN-QRS}{\sqrt{RR/100}} \quad (7)$$

Equation 8 Corrected Length of T-peak to End of T

$$T_C = \frac{QT-QATN}{\sqrt{RR/100}} \quad (\text{See Figure 23}) \quad (8)$$

QATN is defined as the distance from Q (in milliseconds) to the maximal deviation from the iso-electric line between the end of S and end of T. QATN was used in place of Tpe-I because QATN is defined by the Ponemah™ software and less subject to human error (Tpe-I is placed by the observer where they believe the maximum deflection occurs).

Finally, the data from the 30-second analysis was averaged (QRS, QT, T-peak to T-end interval (Tpe-I), QATN interval, T_c , and ST_c) for statistical analysis.

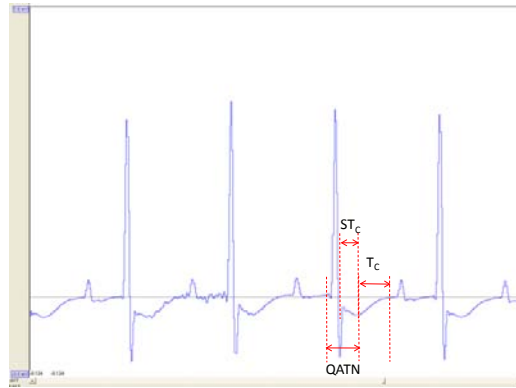


Figure 23 ECG Trace Demonstrating ST and T Calculations

Note that peak heights (such as T-peak measured as the deviation from the iso-electric line) may seem to be a viable way of measuring ST depression, peak height (commonly used in 12-lead ECG) is dependent on electrode placement and QRS right/left axis shift and is not normally used in 2-lead telemetric ECGs. (Kramer, Kinter, Brockway, Voss, Remie, & Van Zutphen, 2001; Conover, 2003).

ANP and BNP Methods

Method of ANP and BNP Staining

Slides containing five-micron sections of the fixed heart tissue were deparaffined. The sections were washed in a phosphate buffered saline (PBS) solution, subjected to 0.15% hydrogen peroxide for 15 minutes, and rewashed. Sections were then blocked (with a normal goat serum (NSG) blocking solution) for one hour. After blocking, the sections were rewashed and the primary antibody with dilution ratio was 1/500 for BNP and 1/1000 for ANP antibody. The primary ANP antibody was rabbit/anti-mouse and the primary BNP antibody was rabbit/anti-rat; both antibodies

were obtained from Bachem AG (Torrance, CA). The sections were allowed to incubate for 24 hours prior to addition of secondary antibody. The secondary ANP and BNP antibody was goat/anti-rabbit, and the dilution ratio for the BNP antibody was 1/400, and a 1/1000 dilution ratio was used for the ANP antibody. After a one hour incubation the sections were stained with an Elite® Vectastain™ ABC stain kit (rabbit Immoglobulin (IgG), catalogue number EK6101) in conjunction with 3-3'-Diaminobenzidine tetrahydrochloride (DAB) tablets. Finally, the slides were dehydrated and cleaned (with ethanol and xylene, respectively) and permount was used to bind a cover slip.

ANP and BNP Quantification

Both BNP and ANP were quantified using the same method. Pictures were taken at 5X magnification of the heart sections using a Leica Microsystems® (Bannockburn, IL) DMR microscope (type: 020-526-731) with a Optronics® (Goletta, CA) QuantFIRE® XI /MacroFIRE® 2.3A camera attached. Optronics® PictureFrame™ imaging software was used to acquire the images. A control group heart section was used to calibrate the light intensity, microscope settings, and camera settings. The white balance was adjusted using the software's *ROI white balancing* tool. Once the light intensity, microscope, and camera settings were selected, they remained unchanged. A single observer collected all the BNP photographs, and all images were collected using the same lighting and settings (ANP images were collected on a different day using the same procedures). Approximately five to six images were collected for each heart section. These images were taken around the heart section in a manner that consummated the whole section when the images are merged (see Figure 24, Figure 25, and Figure 27).

A single observer used Molecular Devices® (Sunnydale, CA) software package Metamorph® (version 7.6) to perform the analysis of the images. Uneven intensity of the 5X images was corrected using the software's *Background and Shading Correction* function. A blank slide was used to create two standard backgrounds (one background with the microscope's light turned off and one background with the light at the same intensity that was used to photograph the sections) that were used to correct each photograph prior to analysis. Figure 24 and Figure 25 show the difference of before and after the background correction. (This step ensured that software's color/intensity threshold selection tool would evenly select the staining regardless of its location on the slide).

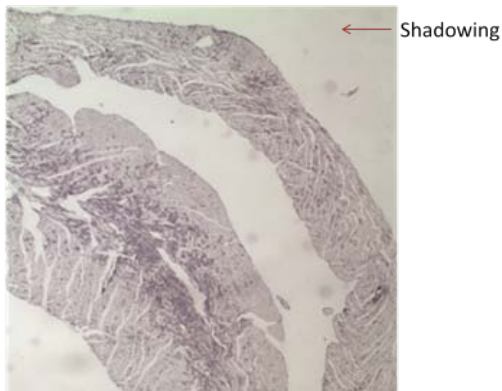


Figure 24 5X Magnification Photograph of a BNP Stained Heart Section before Background Correction

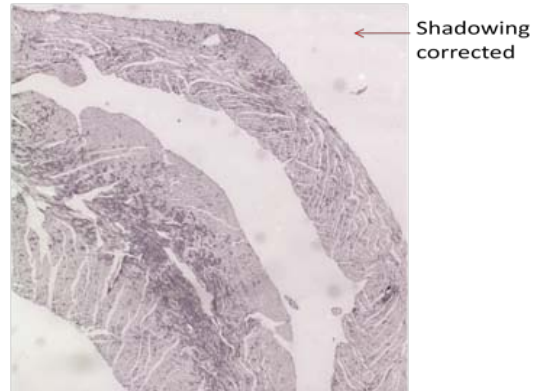


Figure 25 5X Magnification Photograph of a BNP Stained Heart Section after Background Correction

Using the control mice and the software's *Color/intensity threshold selection* tool, a threshold was chosen (a priori of the sarin mice) for the BNP/ANP stain. Figure 26 demonstrates the selectivity of BNP/ANP using the threshold tool.

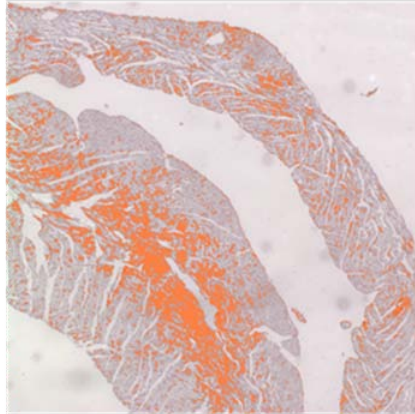


Figure 26 Representation of BNP/ANP Selection via Threshold Selection

Because the threshold selection tool could not distinguish between unstained heart tissue and the slide background, it was impossible to measure the unstained tissue directly. (Selecting the slide background would bias the results and artificially show increased BNP/ANP in the sarin mice since the ventricle space would be selected and the control mice showed significantly larger LV and RV space than the sarin mice; see section IV. Results and Analysis of this report). Therefore, representative regions of a known pixel area were used. Circular regions were selected to ensure that the heart section's orientation on the slide did not affect the results. Using the Metamorph[®] software all 5X images of a single heart were analyzed simultaneously such that five regions could be placed equidistantly in the left ventricle wall, and three regions in the septal wall and right ventricle wall. Figure 27 (a composite of the 5X images to show the whole) is representative of the regions placement.



Figure 27 Whole Heart Section Composite of 5X Magnification Images with Representative of Region Placement in a BNP Stained Heart

Finally, the *Show Regional Statistics* tool set was set to the *Active Region* setting and the data was logged to a Microsoft® Excel™ spreadsheet for each heart section. LV, RV, and septum measurements were averaged, total ventricular ANP/BNP percentage was calculated as an average of the LV and septum measurements, and total percentage was calculated as a composite average of all three areas.

Cell Size Quantification using an H&E Stain Method

H&E Method of Staining

Paraffin was removed from the slides containing 5 micron thick sections of the fixed heart tissue. The sections were washed, and then submerged in a Gill II hematoxylin solution for 30 seconds. Finally, they were rinsed with water for 5 to 10 minutes. Ensuing hematoxylin, the sections were dehydrated (with xylene) and cover slipped with permount.

Cell Size Quantification

Pictures were taken at 20X magnification of the heart sections using the Leica Microsystems® DMR microscope (see ANP and BNP Quantification section of this

report). The light intensity, microscope settings, and camera settings were setup as previously described and a single observer collected same day images using the same lighting and settings. Three (separate and random locations) images of the cardiomyocytes were taken in the LV wall and one image was taken in the septum (The H&E images were taken in *gray scale*; a posteriori analysis revealed that the software program could better distinguish the nucleus from the cell tissue, see Figure 28).

Figure 28 20X Magnification Picture of Gray Scale Image Showing H&E Staining of Cardiomyocytes in the Septum

As with the BNP/ANP quantification, a single observer used Metamorph® to perform the analysis of the H&E images and the background shading was corrected as previously described (see ANP and BNP Quantification). Two thresholds were created (same procedure as ANP/BNP): one threshold calibrated to select the nucleus and the second was calibrated to select the cell tissue. The nuclei were counted using the *Threshold* selection tool in combination with the *Integrated Morphometry Analysis* (IMA) toolkit. In the IMA toolkit, the *Area* filter was selected (to only select objects 30 to 300 pixels; size selected by measuring several nuclei in the control mice), and the *Shape* filter was selected to only capture objects with circularity between 0.5 – 1. Then

the total number of objects selected (as opposed to pixel count) was exported to Excel™ using the *Object* tab in the IMA toolkit. Total cell area was selected using the *Threshold* selection tool and the total number of pixels selected was exported to Excel™. As with the ANP/BNP, quantification settings (threshold, IMA, etc) were not changed throughout the analysis. Figure 29 demonstrates the software's ability to select nuclei (in green) and Figure 30 demonstrates the total tissue selection.

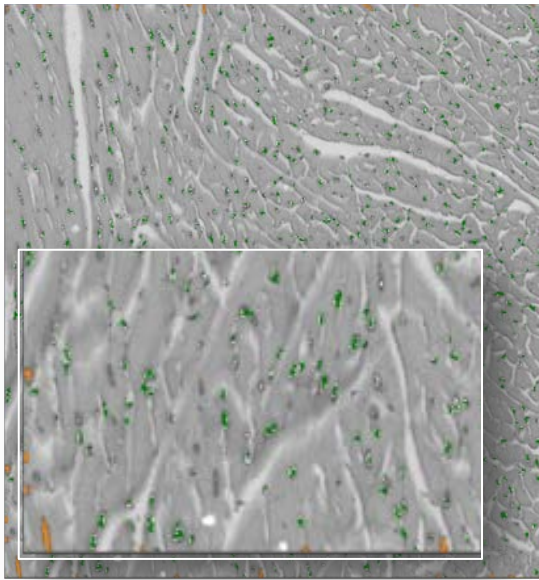


Figure 29 20X Magnification H&E Picture w/Magnified Cut-out with Nuclei Selected using Metamorph's IMA toolkit



Figure 30 20X Magnification H&E Picture with Total Tissue Selected using Metamorph's Threshold Tool

Cell size was computed as total tissue area (pixels) per nucleus (number of objects selected using the IMA toolkit). LV measurements were averaged and total average cell size was computed as an average of the LV measurements and the Septum measurement.

Picrosirius Red Staining Methods

Method of Picrosirius Red Staining

Slides containing five-micron sections of the fixed heart tissue were deparaffined and washed in PBS. The slides were then soaked in a Weigert's iron hematoxylin stain kit (ENG Scientific, Inc., East Clifton, N.J) for eight minutes. The slides were washed again. Following the second wash, the slides were stained in a picrosirius red solution containing five grams of *Direct Red 80* (Sigma-Aldrich Manufacturing, LLC, Lanexa, KA) and 500 ml of picric acid for 1 hour. Then the slides were washed with acidified water and dehydrated with ethanol. Finally, the slides were cleaned with xylene and covered with a permount bound cover-slip.

Picrosirius Red Quantification

Pictures were taken at 5X magnification of the heart sections using an Olympus® FluoView™ FV300 Tissue Culture Microscope (Waltham, MA). The FluoView™ application software was used to acquire the images. An external polarizing light transmitter was used via the instrument's external port. A section of a control group heart was used to calibrate the light intensity and plane of polarization (crossed polarized at ~90 degrees), microscope settings, and camera settings. Once the polarization, light intensity, microscope, and camera settings were selected, they were not changed. A single observer collected all the photographs, and all images were collected using the same lighting and settings. Approximately five to six images were collected for each heart section. These images were taken around the heart section in a

manner that consummated the whole section when the images are merged (see Figure 31 and Figure 32).

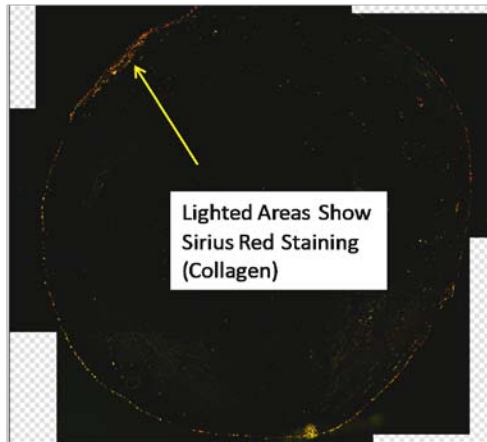


Figure 31 5X Magnification Photograph of a Picrosirius Red Stained Heart Section in Crossed Polarized Light. The collagen transmits red light while the picric acid stained tissue appears black.

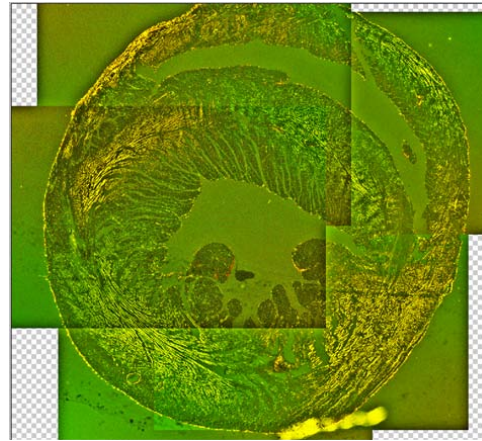


Figure 32 Photoshop® Enhanced Image of a Sirius Red Stained Heart Image Showing the Total Heart Area.

A single blinded observer used Adobe® Photoshop® CS3 (version 10.0.1), to perform the analysis of the images. The 5X images were copied on to a *transparent* background and merged using Photoshop's® *Auto-Align Layers* tool. The images were checked to ensure quality, and a preselected color range was used to quantify the sirius red staining from the dark image. This was accomplished using the *Color Range* toolset under the *Select* menu in Photoshop®. The preselected color range was not changed during the analysis and the same color range was used for all the images. The *Histogram* tool was used to record the total number of pixels selected for the sirius red stain.

Total heart section size (in pixels) was calculated in a similar manner as was used in the heart size quantification explained above (see the Tissue Collection, Heart

Sectioning, and Heart Size Measurement Methods/Heart Section Size Measurements section of this report). The image was enhanced using the software's *Adjustments* toolset to increase the brightness of the image (all images were increased by the same brightness level) (see Figure 32). The RV and LV were manually cropped from the heart sections using the *Quick selection* and *Magic wand* tool sets (see Figure 33). After the ventricles were cropped, the heart section was selected (using the *Quick selection/Magic wand* tools as described above) and pasted into a blank image with transparent pixels; the histogram tool was used to calculate the total heart area.

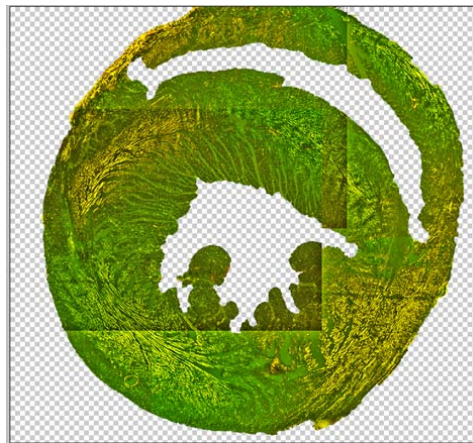


Figure 33 Representation of Photoshop® Enhanced Sirius Red Stained Heart Image to Obtain Total Heart Area

Finally, collagen levels were expressed as the ratio of the Sirius red stained pixels to the number of pixels in the total heart area.

Statistical Methods

Statistical analysis of the mice was performed using Prism 5® for Windows® (GraphPAD Software, Inc., La Jolla CA; version 5.01). In general, one-way Analysis of Variance (ANOVA) with *Nueman-Keuls* post-hoc test was used to compare the controls

to the 0.4 LD₅₀ and 0.5 LD₅₀ groups. Any significant results were checked for equal variances and normality; *Batlett's* test for equal variances ($p < 0.05$), and D'Agostino-*Pearson's* omnibus test ($p < 0.5$) or the *Shapiro-Wilks'* ($p < 0.5$) normality test (if the sample size was small, i.e. $n = 5$ for the 0.5 LD₅₀ group) were used, respectively. (Corrective methods used to compensate for failure of either test are given below). Any data that failed the normality tests were analyzed using *Kruskal-Wallis'* test with *Dunn's* post-hoc test.

In the case where data collection was repeated on multiple different weeks (body weights, echocardiography, etc), the mice were time-matched. One-way ANOVA was performed with the controls versus each sarin group (0.4 LD₅₀ and 0.5 LD₅₀) for each time-matched group (week 2 results, week 4 results, etc) with *Nueman-Keuls* post-hoc test. Additionally, two-way ANOVA (time-matched group x dobutamine) with a *Bonferonni* post-hoc test was performed on the time-matched data on any significant results (from the one-way ANOVA) in the ECG and echocardiograms where dobutamine was used.

Finally, when only two groups were analyzed (the sarin groups were combined and pitted against the controls) a Student's t-test was used. Results were checked for normality (*D'Agostino-Pearson*, $p < 0.5$), and equal variances (*Bartlett's* test). *Kruskal-Wallis* with a *Dunn's* post-hoc test was used if the data did pass the normality tests. *Welch's* correction for unequal variances was used if variances were not equal or could not be assumed ($p < 0.25$).

IV. Results and Analysis

Results of Body Weights, Tissue and Heart Sectioning Weights

Time-matched, one-way ANOVA on body weight shows a significant decrease in body weight of the sarin mice versus the control group after the sarin injections. By week 10 the differences in weights were no longer significant. ANOVA on weight gain percentages shows a significant decrease in body weight for the 0.5 LD₅₀ group. By week four, weight gains leveled and no significant weight loss/gains were observed for the duration of the experiment (see Figure 35). See Appendix A: Tabulated Average Results of Controls, 0.4 LD₅₀, and 0.5 LD₅₀ Groups/Tabulated Results of Weights and Heart Section Measurements for a complete list of body weights at the given time-intervals.

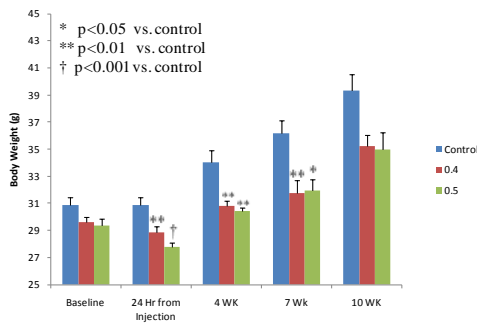


Figure 34 Results of Murine Body Weights.

Body Weight shows a significant decline in weight 24 hours post exposure and remains Low for the remainder of the experiment; although, not significantly lower in week 10.

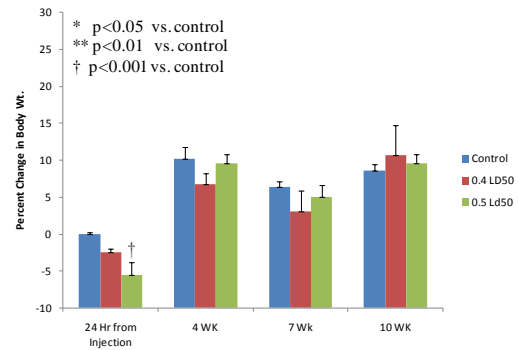


Figure 35 Results of Percent Change in Body Weight.

Percent change in body weight shows a significant decline in weight 24 hours post exposure for the 0.5 LD₅₀ group. By the 4th week change in body weights leveled, and by experiment end weight changes were nearly identical for each group.

Results of Body Weights, Tissue Weights, and Heart Sectioning

ANOVA of the corrected heart weights (time-matched heart weight/body weight) did not show a significant difference between the two sarin groups and the

control group (see Figure 36). The data, however, showed a trend for increased heart weights in both sarin groups (f-statistic = 2.9, $p = 0.07$). In order to gain statistical power (and reduce the error associated with the 0.5 group, $n = 5$), the two sarin groups were combined, and compared against the controls using *Student's* t-test with *Welch's* correction for unequal variances. Results indicate that corrected heart weights were increased ($p = 0.026$) in the mice subjected to sarin (see Figure 37).

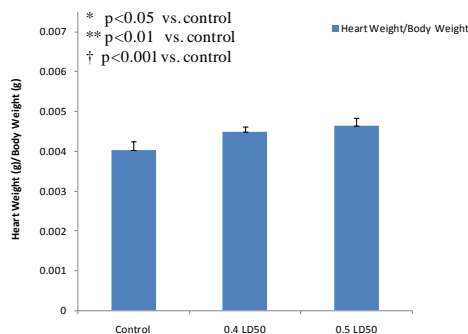


Figure 36 Results of Heart Weights (Corrected by Body Weight).

Results lack statistical power to show a significant difference ($p = 0.07$). Corrected heart weights for both sarin groups show an increasing trend in weights.

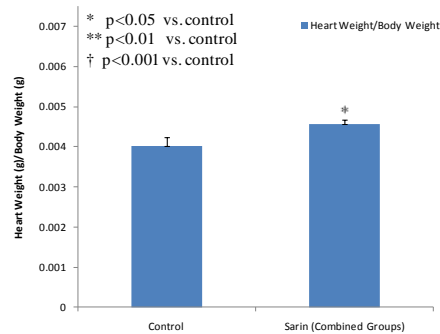


Figure 37 Results of Corrected Heart Weights with Combined Sarin Groups.

With the two sarin groups (0.4 LD₅₀ and 0.5 LD₅₀) combined, results of heart weights (corrected by body weight) show a significant difference ($p = 0.026$). Corrected heart weights for the sarin groups show increased corrected heart weight.

Similarly, an unpublished study by this lab showed significant increased corrected heart weight values (Morris, Lucot, & Shewale, 2009) eight weeks after exposure (see

Appendix B: Unpublished Heart Weight Data

The three-millimeter heart sections showed a significant decrease in LV lumen area for both sarin groups. Figure 38 shows a normal heart section of a control mouse and Figure 39 demonstrates decreased ventricular area in the sarin subjected mice.



Figure 38 Representative 3mm Section of Control Mouse Showing Normal Ventricular Size



Figure 39 Representative 3mm Section of 0.4 LD₅₀ Group Showing Severely Depressed Ventricular Areas

ANOVA on the three-millimeter heart section pictures show a significant decrease ($p = 0.0014$) in LV area for both the 0.4 LD₅₀ and 0.5 LD₅₀ sarin groups. Although not significantly, the RV area also appeared depressed and the total heart area increased.

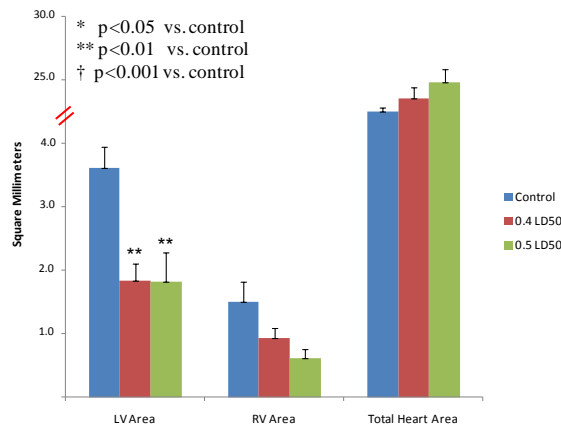


Figure 40 Results of Ventricular Size.
Results show a significant decrease ($p = 0.0014$) in LV area for both groups of sarin mice.

Tabulated results showing average values (\pm standard error) for the controls and sarin groups for the body weights, heart weights, and heart sizes are listed in Appendix A:

Tabulated Average Results of Controls, 0.4 LD₅₀, and 0.5 LD₅₀ Groups/Tabulated Results of Weights and Heart Section Measurements.

Results of Echocardiography Analysis

2-D echocardiograms show significant size increases in the ESA and EDA of both sarin groups versus the controls (time-matched one-way ANOVA). Both groups showed a significant increase in ESA by week 4, and the 0.5 LD₅₀ group also had a significantly increased EDA in week 4; the 0.4 LD₅₀ did not show significant results in EDA until week 10. By week 10, size differences in the 0.5 LD₅₀ group seemed to have reverted and differences were no longer apparent. Dobutamine significantly increased cardiac output and seemed to mute the differences between groups. After dobutamine administration, only the ESA in the week 4 of the 0.5 LD₅₀ group showed variation from the controls (see Figure 41 and Figure 42).

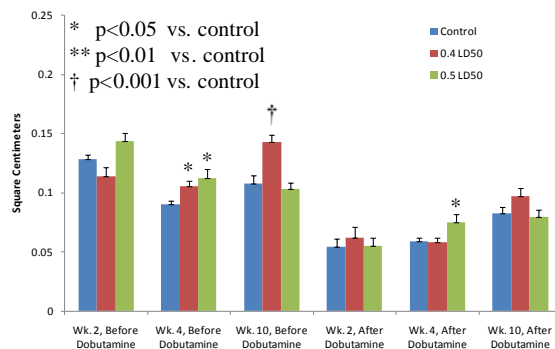


Figure 41 Results of Echocardiogram ESA.

Week 4 ESA (cm²) was significantly increased in the sarin groups before dobutamine, and in the 0.5 LD₅₀ group after dobutamine. Week 10 results show further increase in area in the 0.4 LD₅₀ group, While the 0.5 LD₅₀ group matched the controls. Two-way ANOVA (controls x 0.4 x 0.5 LD₅₀ groups) did not show a significant difference in the interaction (dobutamine had the same effect on each group).

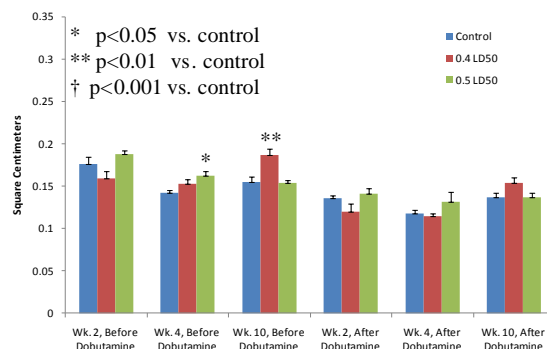


Figure 42 Results of Echocardiogram EDA.

Week 4 EDA (cm²) was significantly increased in the 0.5 LD₅₀ group before dobutamine. Week 10 results show an increased EDA in the 0.4 LD₅₀ group, While the 0.5 LD₅₀ group matched the controls. Two-way ANOVA (controls x 0.4 x 0.5 LD₅₀ groups) did not show a significant difference in the interaction.

Two-way ANOVA of the week 4 ESA showed significant differences between the controls and sarin ($p = 0.0005$) and for all groups before and after dobutamine ($p < 0.0001$), but did not give a significant interaction ($p = 0.24$) – dobutamine affected each

group equally. Week 10 two-way ANOVA of the ESA gave similar results to the week 4 data; significant differences between groups ($p = 0.014$) and pre/post dobutamine effect ($p < 0.0001$), but not a significant interaction ($p = 0.20$). Two-way ANOVA on EDA in both week 4 and week 10 gave similar results to that of the ESA analysis (significant difference between groups and pre/post dobutamine, and no significance in the interaction).

Area fractional shortening (aFS) is a dependent of ESA and EDA ($aFS = [EDA - ESA]/EDA$) and showed a similar pattern of results as the latter parameters. Both the 0.4 and 0.5 LD₅₀ groups showed decreased aFS in week 4 before dobutamine, but the results were not significant (f-statistic = 3.039, $p = 0.065$). By week 10, the 0.4 LD₅₀ group demonstrated a significant decrease in aFS (see Figure 43). As with the ESA and EDA parameters, dobutamine muted the differences between controls and the sarin groups. No significant values were obtained in aFS following the dobutamine injection.

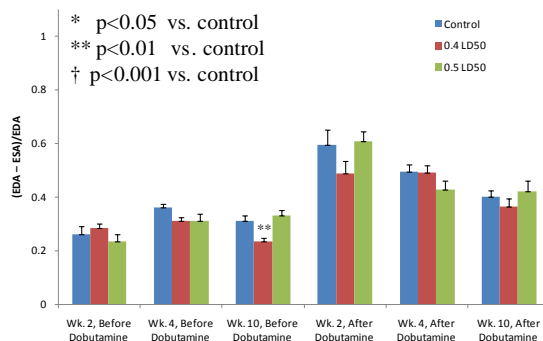


Figure 43 Results of Echocardiogram aFS.

Week 4 aFS was depressed in the sarin groups, but not significantly ($f = 3.039$, $p = 0.065$). Week 10 aFS was significantly decreased in the 0.4 LD₅₀ group before dobutamine. Two-way ANOVA (controls x 0.4 x 0.5 LD₅₀ groups) did not show a significant difference in the interaction.

Two-way ANOVA on week 10 aFS gave similar results as the ESA and EDA analysis.

Difference between groups was significant ($p = 0.02$), the dobutamine had a significant effect ($p < 0.0001$), and the interaction was not significant ($p = 0.69$).

Pulsed wave Doppler imaging showed significant results in week 10 for the ET interval after dobutamine in the 0.5 LD₅₀ group ($p = 0.0079$). Additionally, the ICT + IVRT interval was increased after dobutamine administration in both sarin groups ($p = 0.0097$). Two-way ANOVA expressed significant differences in between-group and pre/post dobutamine effects for ET and ICT + IVRT, but did not show any differences in the interaction for either parameter.

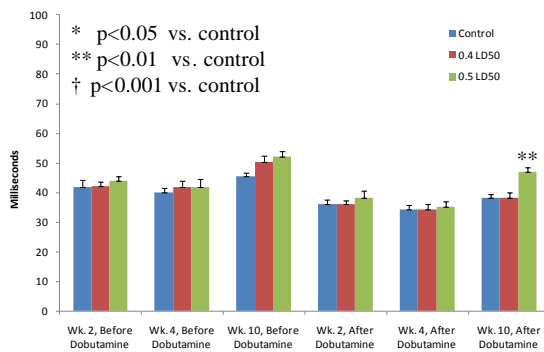


Figure 44 Results Doppler Derived ET.

In week 10 ET was increased in the 0.5 LD₅₀ group ($p = 0.0079$) following dobutamine. Two-way ANOVA (controls x 0.4 x 0.5 LD₅₀ groups) did not show a significant difference in the interaction.

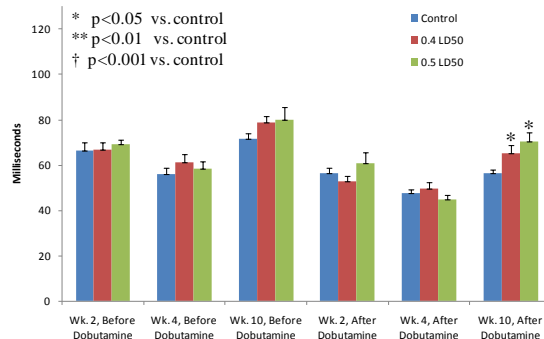


Figure 45 Results Doppler Derived ICT + IVRT.

Week 10 ICT + IVRT was increased in both sarin groups ($p = 0.0097$) following dobutamine. Two-way ANOVA (controls x 0.4 x 0.5 LD₅₀ groups) did not show a significant difference in the interaction.

Time matched one-way ANOVA on the derived parameters from the combined 2-D/ Doppler images gave significantly decreased indices in week 4 aFS/MPI before dobutamine in both sarin groups ($p = 0.026$), and the 0.4 LD₅₀ group also showed a significant decrease in week a10 FS/MPI ($p = 0.0023$) versus the controls. The Vcf index

was also decreased before the dobutamine administration in week 10 for the 0.4 LD₅₀ group (p = 0.0061).

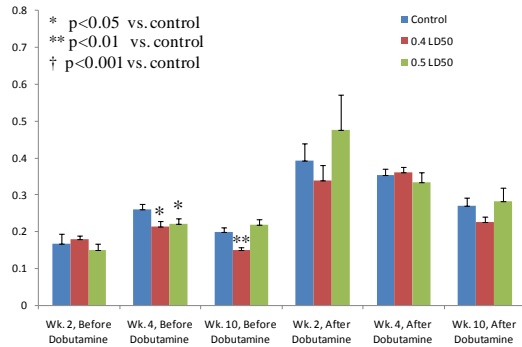


Figure 46 Results Echo/Doppler Derived aFS/MPI. Week 4 FS/MPI was significantly lower in the sarin groups before dobutamine. FS/MPI in the 0.4 LD₅₀ group was further decreased in week 10, and the 0.5 LD₅₀ group no longer showed a difference. Two-way ANOVA (Controls x 0.4 x 0.5 LD₅₀ Groups) did not show a significant difference for the interaction or group effect.

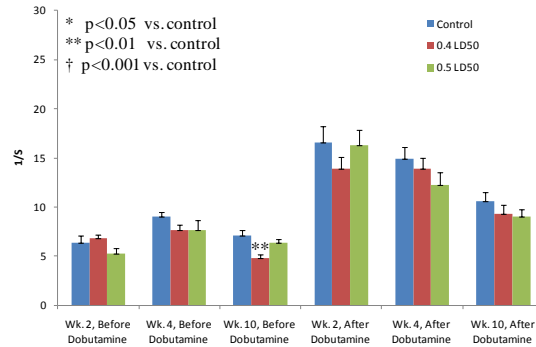


Figure 47 Results Echo/Doppler Derived Vcf. Week 10 Vcf was significantly decreased in the sarin groups before dobutamine, and the 0.5 LD₅₀ group was decreased but not significantly. Two-way ANOVA (controls x 0.4 x 0.5 LD₅₀ groups) did not show a significant difference for the interaction or group effect.

Two-way ANOVA expressed a significant difference pre/post dobutamine for both parameters (all weeks), but did not show any differences between groups or in the interaction for either parameter. Other 2-D, M-Mode, and Doppler derived parameters were not significant (to include the myocardial performance index (MPI)). Tabulated results of all the echocardiograms are listed in Appendix A: Tabulated Average Results of Controls, 0.4 LD₅₀, and 0.5 LD₅₀ Groups/Tabulated Results of Echocardiograms.

Results of the ECG Analysis

Results of quantifying the ECG tracings show ST_c depression following dobutamine stressing in the sarin mice. Visual qualification of the ECG tracings gave evidence of ST depression in three of the eleven control mice and in all but two of the sarin mice (combined groups). In the sarin groups, the J-point (upright t-wave with a broad inverted tail that is merged with the end of QRS as described by Mitchell *et al.*

(Mitchell, Jeron, & Koren, 1998)) was significantly depressed. In both sarin groups, the t-wave was shifted toward QRS and lengthened. Figure 48 – Figure 53 demonstrate the differences seen in the t-wave for the control mice versus the sarin mice.

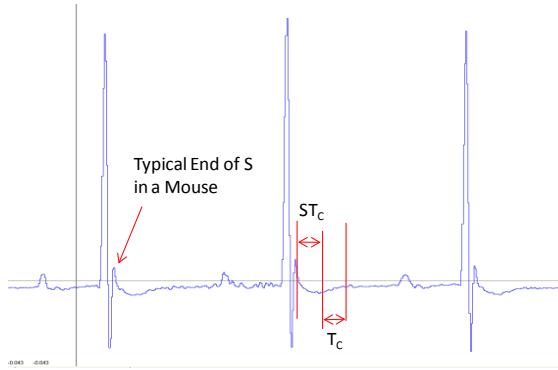


Figure 48 Control Mouse ECG Trace Before Dobutamine Injection.

The J-point rises above the iso-electric point and the T-wave tail falls below the iso-electric point before returning (marking the iso-electric relaxation time). Note: as depicted T_c is not corrected by the $(RR/100)^{1/2}$.

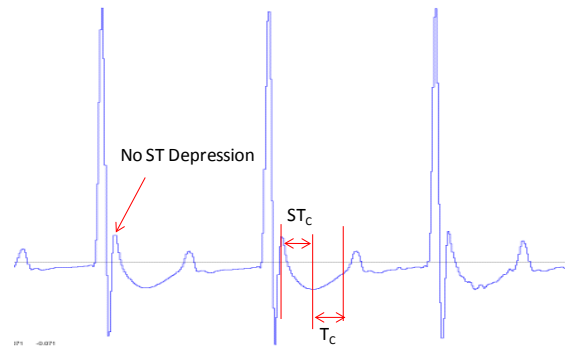


Figure 49 Control Mouse ECG Trace After Dobutamine Injection.

The J-point rises above the iso-electric point. The ST_c segment and T_c segments do not change markedly.

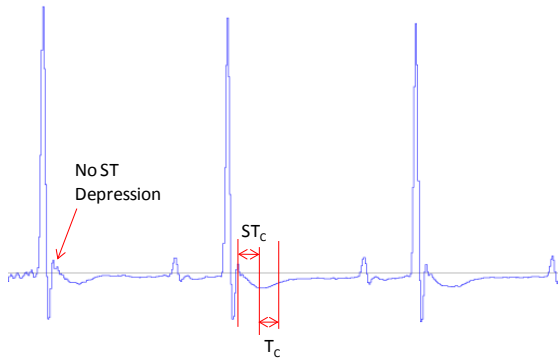


Figure 50 Sarin Mouse ECG Trace Before Dobutamine Injection.

The J-point rises above the iso-electric point slightly less than the controls (but not markedly).

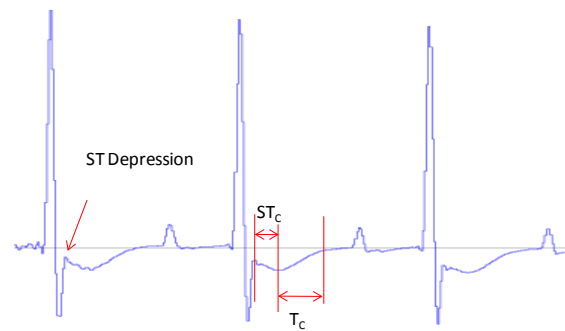


Figure 51 Sarin Mouse ECG Trace After Dobutamine Injection Showing ST Depression.

The J-point does not rise to the iso-electric point. The ST_c segment is slightly shortened when compared to the controls and T_c segment is significantly lengthened.

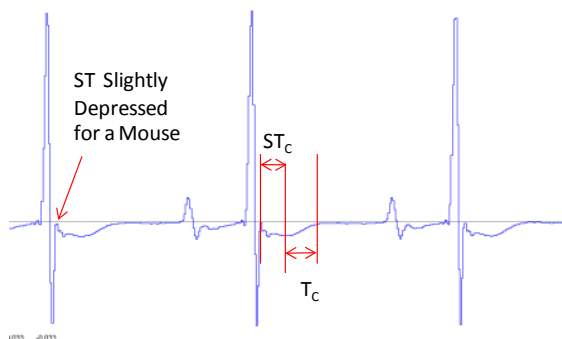


Figure 52 Sarin Mouse ECG Trace Before Dobutamine Injection.

The ST is slightly depressed. The T-wave tail falls below the iso-electric point before returning.

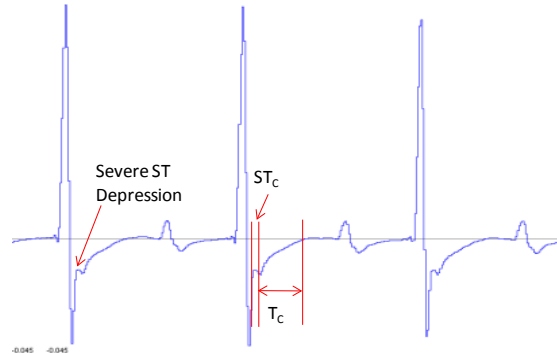


Figure 53 Sarin Mouse ECG Trace After Dobutamine Injection Showing Severe ST Depression.

The J-point does not rise to the iso-electric point. The ST_c segment is significantly shortened when compared to the controls and T_c segment is significantly lengthened.

One-way and two-ANOVA show significant shortening in the ST_c segment and a significant increase in T_c . (One control mouse was excluded from the ST_c and T_c analysis due to the presence of inverted t-waves; inclusion in the analysis skews results to show an even greater difference between the controls and sarin groups). Additionally, the PR interval showed a significant increase in the 0.5 LD_{50} sarin group after dobutamine in week 10 (see Figure 54, Figure 55, and Figure 56). Two-way ANOVA (control group x either sarin group) did not show a difference in dobutamine effect for any of the significant parameters. Two-way ANOVA (controls x 0.4 LD_{50} x 0.5 LD_{50}) was also performed on heart rate, and the results did not show a significant difference in the dobutamine interaction of the groups ($p = 0.33$) or any other parameter (between groups or pre/post dobutamine).

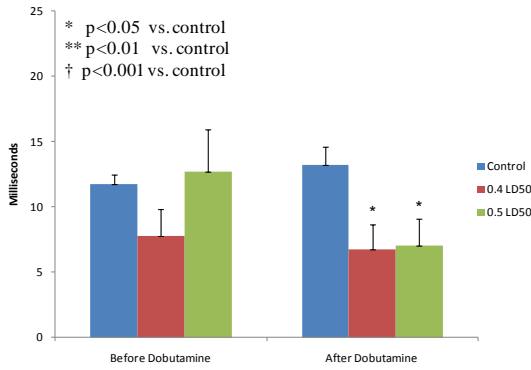


Figure 54 Results of ST Segment Measurements.

Results show a significant decrease in segment length in the sarin groups following the dobutamine injection. Two-way ANOVA shows significant results for sarin groups vs. controls ($p=0.0015$) and for dobutamine effect ($p < 0.0001$), but do not show that dobutamine had a different affect on controls vs. sarin groups ($p = 0.82$).

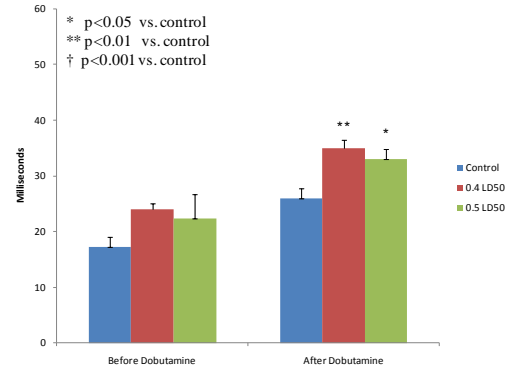


Figure 55 Results of T-Peak to T-End.

Results show a significant alteration of the T-Wave in both sarin groups following the dobutamine injection. Two-way ANOVA shows significant results for sarin groups vs. controls ($p=0.032$) but not for dobutamine effect ($p < 0.2$) or that dobutamine had a different affect on controls vs. sarin groups ($p = 0.16$).

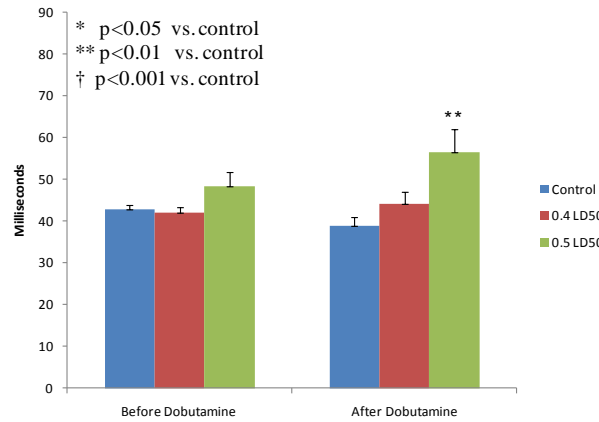


Figure 56 Results of PR Interval.

Measurements show a significant segment length increase in the 0.5 LD₅₀ group following the dobutamine injection ($p = 0.0056$). Two-way ANOVA did not show significant results. Sarin groups vs. controls ($p=0.11$); dobutamine effect ($p = 0.26$); dobutamine had a different affect on controls vs. the sarin groups ($p = 0.67$).

Other measured ECG parameters were not significant to include the QT_C interval.

Tabulated results of all measured ECG parameters are listed in Appendix A: Tabulated

Average Results of Controls, 0.4 LD₅₀, and 0.5 LD₅₀ Groups/Tabulated Results of ECG

Data Analysis.

Results of ANP/BNP Stain Quantification

Both ANP and BNP levels in the sarin mice were elevated in the LVs and RVs.

Figure 57 and Figure 58 show the differing levels of natriuretic peptides (BNP was similar to the ANP sections) in the control and sarin groups.

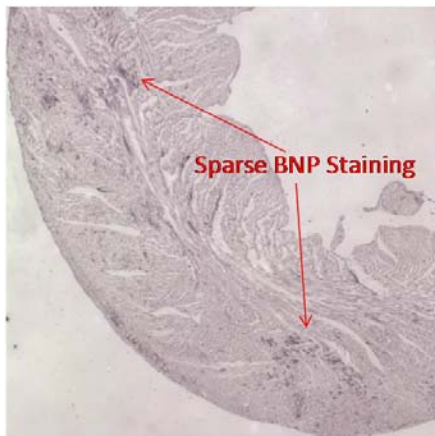


Figure 57 5X Magnification Images of BNP Staining in the Control Group Representative BNP (and ANP) Stain Pattern for the Control Mice

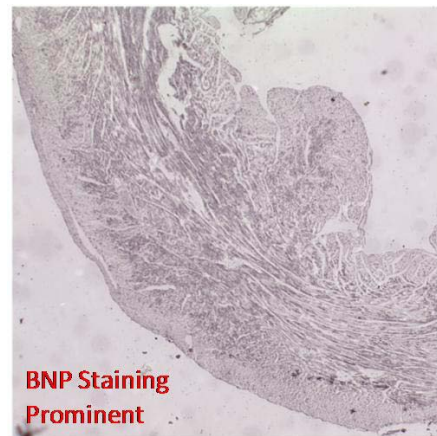


Figure 58 5X Magnification Images of BNP Staining in the 0.4 LD₅₀ Sarin Group and Representative of the BNP (and ANP) Stain Pattern for both Sarin Groups.
Sarin mice had a greater prominence of BNP (and ANP).

ANOVA results of the ANP staining show significant increases in ANP levels in the 0.4 LD₅₀ group. The LV wall, septum, and total ANP levels in the LV (LV wall and septum) were significantly higher (see Figure 59). While increased ANP levels were seen in the RV, the results were not significant. (Results shown exclude one heart section from the 0.4 LD₅₀ group; visual analysis of the section did not show any indication of stain in the section, and the quantification gave results up to 4X the standard error below the lowest quantified result of any other section, regardless of group). Because a similar trend was noticed between both sarin groups, a *Student's* t-test was performed; controls x combined average of the two sarin groups. Results of the t-test indicate that all sarin animals had a significant increase in ANP in LV wall (see Figure 60).

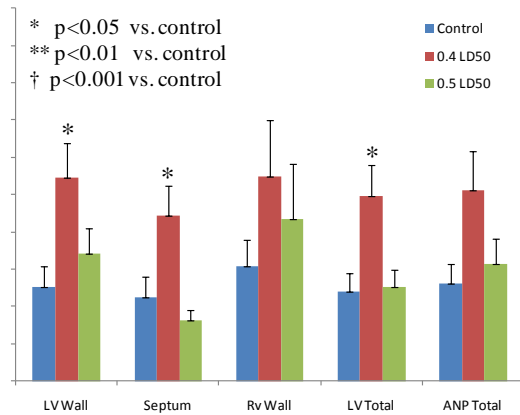


Figure 59 Unitless Representation of ANP Quantification.

Results show a significant increase in LV ANP levels in the 0.4 LD₅₀ group (LV wall, septum, LV total (LV wall + septum)). The 0.5 LD₅₀ group failed to show significant Results, but demonstrated an increased trend in both ANP and BNP quantification (Figure 61).

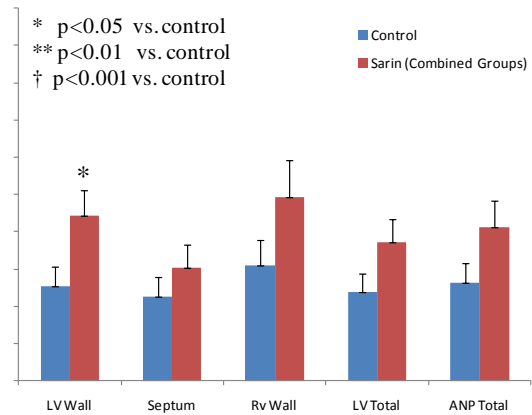


Figure 60 ANP Quantification With The Two Sarin Groups (0.4 LD₅₀ and 0.5 LD₅₀) Combined.

Results of the combined ANP analysis shows a significant difference ($p = 0.028$) in ANP levels in the LV wall for the sarin mice.

BNP levels follow the ANP levels in showing an increased trend in the LV wall, septum, and total BNP levels in the LV. However, BNP results were slightly less than significant ($p = 0.07$) when compared individually (see Figure 61). To increase statistical power and because a similar trend was noticed between both sarin groups, a Student's t-test was performed (controls by combined-average of the two sarin groups: Figure 62). As with the ANP levels, BNP levels were significantly ($p = 0.01$) higher in the LV wall. Additionally, total average BNP levels in the heart section (average LV wall, septum, and RV) were significantly higher in the sarin animals ($p = 0.04$). Tabulated results of the ANP and BNP quantification are listed in Appendix A: Tabulated Average Results of Controls, 0.4 LD₅₀, and 0.5 LD₅₀ Groups/Tabulated Results of Histology: ANP/BNP Quantification.

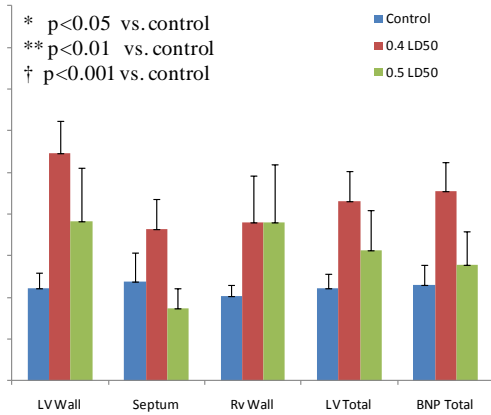


Figure 61 Unitless Representation of BNP Quantification.
 Groups lack statistical power to show a significant deviation ($p = 0.07$), but follow the ANP level trends.

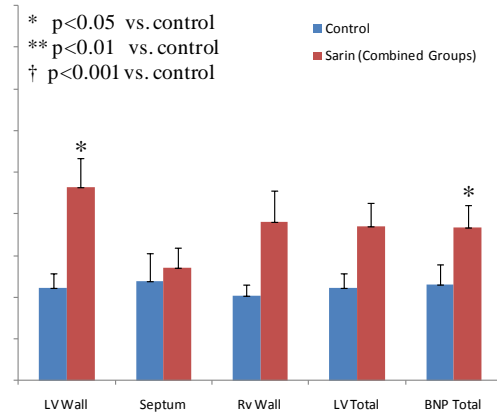


Figure 62 BNP Quantification With The Two Sarin Groups Combined (0.4 LD₅₀ and 0.5 LD₅₀).
 Results of the combined BNP analysis shows a significant difference ($p = 0.010$) in BNP levels in the LV wall and in the total BNP percentage ($p = 0.04$) for the sarin mice.

Results of Cardiomyocyte Size via H&E Analysis

Cardiomyocyte size in the sarin groups increased significantly when compared to the control mice. Figure 63 depicts the typical myocyte arrangement in a control mouse; Figure 64 shows increased size and density of the myocytes in a sarin mouse.

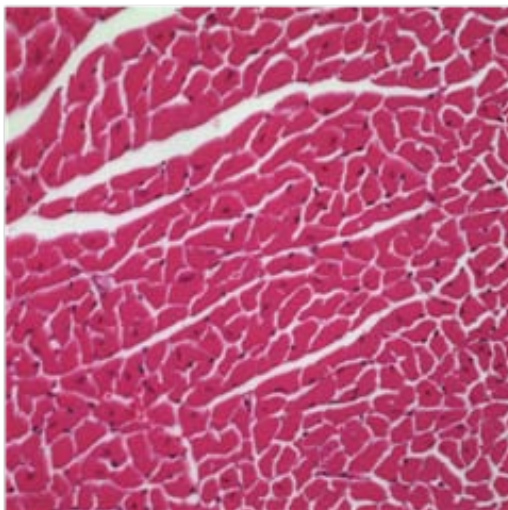


Figure 63 40X Magnification Image of the Cardiomyocytes in the LV Wall of an H&E Stained Control Mouse

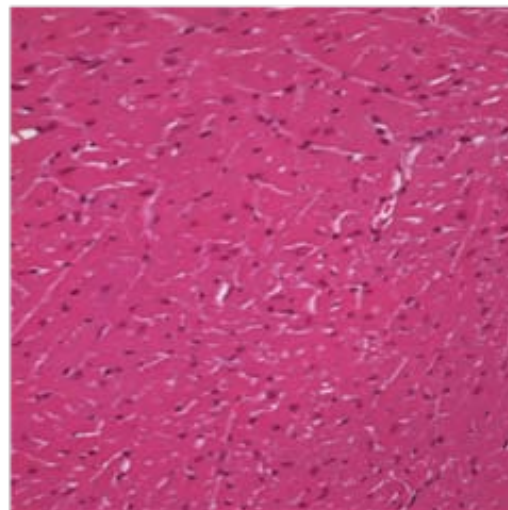


Figure 64 40X Magnification Image of the Cardiomyocytes in the LV Wall of an H&E Stained Sarin Mouse Showing Myocyte Enlargement and Expansion into the Intercellular Space

One-way ANOVA on the H&E did not show a significant difference between the two sarin groups and the controls (see Figure 65). However, the data did show a trend in both sarin groups (f-statistic = 3.2, $p = 0.06$) of increased average cardiomyocytes size in the LV (LV wall and septum). When the two sarin groups were combined and compared against the controls using Student's t-test, cell size was significantly increased ($p = 0.025$) in the LV wall of the sarin mice. Cell size was not shown to be different in the septum (see Figure 66).

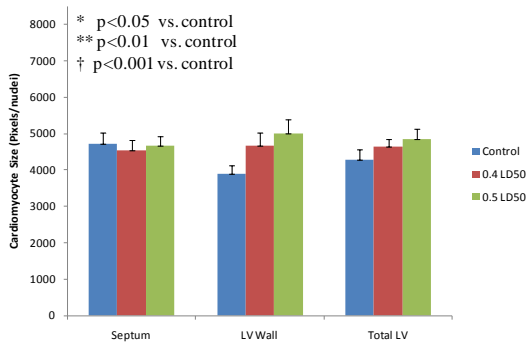


Figure 65 Results of H&E Analysis.

Results lacked statistical power to show a significant difference ($p = 0.07$ for LV wall). Analysis did show an increasing trend in cell size for both sarin groups.

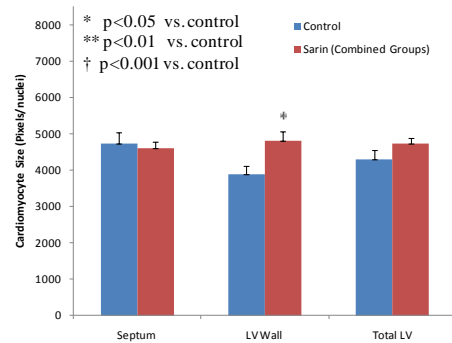


Figure 66 Results of Combined H&E Analysis.

Combining the two sarin groups (0.4 LD50 and 0.5 LD50), demonstrates increased cell size in the LV wall ($p = 0.025$) for the H&E analysis.

Tabulated results of the cell size quantification (\pm standard error) are listed in Appendix

A: Tabulated Average Results of Controls, 0.4 LD50, and 0.5 LD50 Groups/Tabulated

Results of Cell Size Quantification from H&E Staining, Collagen Quantification from

Picrosirius Red Staining.

Results of Collagen Quantification via Picrosirius Red Staining

Collagen quantification did not show significant differences between the sarin subjected mice and the controls. Results for the collagen quantification are listed in Appendix A: Tabulated Average Results of Controls, 0.4 LD₅₀, and 0.5 LD₅₀ Groups/ Tabulated Results of Cell Size Quantification from H&E Staining, Collagen Quantification from Picrosirius Red Staining.

V. Discussion

Body Weights, Tissue and Heart Sectioning Weights

Although body weight was suppressed in the sarin mice, percent weight gain did not show a significant difference after two weeks. Weight gain depression was seen in the sarin mice 24 hours after exposure; the 0.5 LD₅₀ group showed significant depression while for the 0.4 LD₅₀ group the depression was less severe. Weight losses leveled off by the fourth week (see Figure 35), and the pattern was consistent with the literature for nerve agent exposures in mice and other small mammals (Bide & Risk, 2004; Grauer, et al., 2008; Shih, Hulet, & McDonough, 2006). Nonetheless, by week four weight gains had leveled off, and no more significant results were noticed. As such, the heart had 10 weeks to normalize to the changes in weight, and weight gain/loss is not expected to be a significant factor in this experiment.

Signification of Histological Evidence

Figure 67 illustrates the histological evidence of sarin induced murine LV hypertrophy. Heart tissue weight ratios (corrected by body weight) were significantly larger in the sarin mice. In addition, there was significant reduction in LV lumen in both sarin groups as quantified from the three-millimeter heart section. Both measures are suggestive of hypertrophy, and the heart sectioning specifies LV hypertrophy.

Similarly, H&E staining reveals higher cross-sectional areas of the cardiomyocytes. The role of cardiomyocytes in hypertrophic cardiomyopathy has been previously established in the literature (Takeda, et al., 2010; Harada, et al., 1997), and

the results of the H&E stain myocyte size quantification of cardiomyocyte size coincides with heart weight and sectioning data.

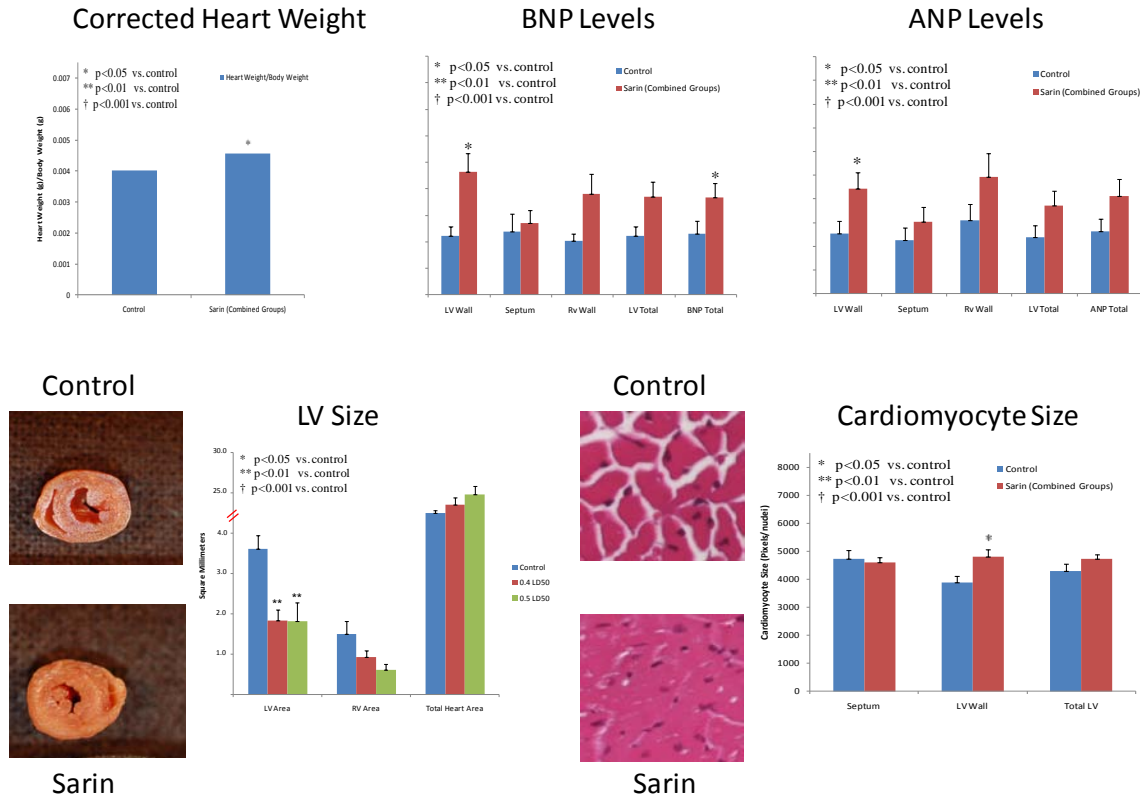


Figure 67 Histology Showing LV Hypertrophy in Sarin Mice.

The ratio of heart weight/body weight ratio (Hw/Bw) (mg/g) was evaluated and found significantly higher in the sarin mice. Paraffin-sectioned LVs were stained with H&E and the cross-sectional areas of cardiomyocytes were significantly larger in the sarin animals. ANP and BNP quantification found significantly higher in the LV of the sarin mice.

Additionally, ventricular expression of ANP/BNP is up-regulated in the LV in a host of cardiac pathological conditions leading to cardiac remodeling such as LV hypertrophy (Yasuno, et al., 2009), and Harada *et al.* have shown that significantly higher ANP/BNP production in cardiomyocytes (and non-cardiomyocytes) accompanies hypertrophic conditions (Harada, et al., 1997). Indeed, disruption of the ANP gene or knockout of the receptor, NPR1, in mice induces such remodeling (Lopez, et al., 1995;

Knowles, et al., 2001), and ANP when expressed in the ventricles serves a role as one of the most conservative markers of LV hypertrophy (Day, et al., 1987). In addition, BNP is released by the ventricles and serves as a superior diagnostic marker for heart failure (Mair, 2008). Therefore, the higher levels of ANP and BNP seen in the two sarin groups gives strong evidence of cardiac remodeling and LV hypertrophy. Such results of corrected heart weights, section sizing, cardiomyocyte size, and ANP/BNP level increases have been reported in the literature for mice with LV hypertrophy (Honsho, et al., 2009; Galindo, et al., 2009; Takeda, et al., 2010).

Collagen levels in the heart were not increased in either sarin group; increased collagen levels normally serve as an excellent indicator of decreased cardiac performance (Lutgens, Daemen, Muinck, Debets, Leenders, & Smits, 1999; Kerckhove, Kalkmana, Saxena, & Schoemaker, 2000). Nonetheless, the absence of increased collagen does not turn aside cardiac dysfunction; indeed remodeling and LV hypertrophy has been shown in mice without increased collagen formation (Holtwick, et al., 2003), and in gene knockout-mice (where the removal gene has been shown not to inhibit collagen levels) (Fedak, et al., 2010; Kassiri, et al., 2009).

Electrocardiographs: Inference of Ventricular Performance and Hypertrophy

Coinciding with the histology, the murine ECG data shows significant ST segment changes and ST depression in the dobutamine stress test; ST segment deviations are demonstrated in Figure 68. Similar to humans, the ST segment in a mouse corresponds to the leveling in action potentials when the heart is depolarized; the T-wave corresponds to ventricular re-polarization (London, 2001). As such, ST segment

deviations (depression, e.g.) are well-documented indicators of myocardial/sub-endocardial ischemia in mice and humans (Tomai, Crea, Chiariello, & Giofrè, 1999; Lambiase, Edwards, Cusack, Bucknall, Redwood, & Marber, 2003; Chu, Otero, Lopez, Morgan, Amende, & Hampton, 2001; Stoller, et al., 2007).

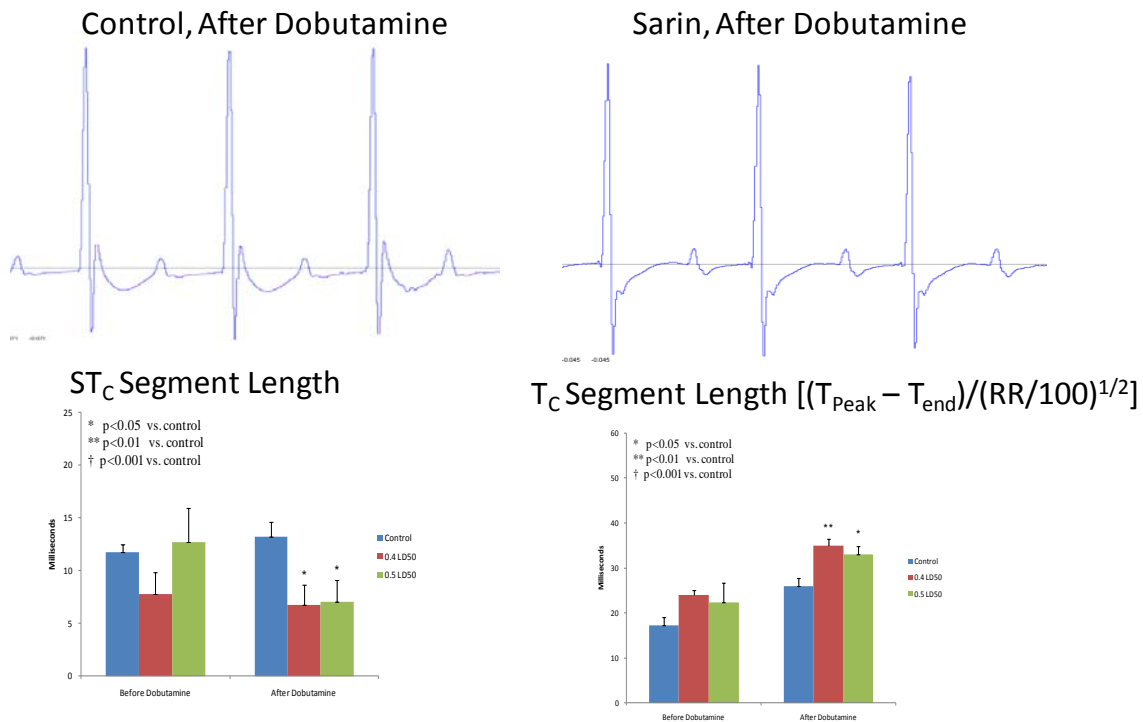


Figure 68 ECG Showing ST Changes in Sarin mice.

Results are indicative of myo/endocardial ischemia in sarin mice. The ST_c segment was depressed in the sarin mice following dobutamine; T-Peak was shifted left and the T_c interval lengthened.

Additionally, dobutamine stress testing is a well documented test for ischemia

(Shaheen, Luria, Klutstein, Rosenmann, & Tzivoni, 1998), and ischemia has been

associated with cardiac hypertrophy, because the coronary circulation system does not

experience concomitant growth with the hypertrophic cardiac muscle (Smits & Smits,

2004). Accordingly, ST and T-wave changes represent decreased cardiac performance

under stress and ventricular strain patterns that could be associated with LV hypertrophy (Hsieh, Pham, & Froelicher, 2005).

Prolongation of the QT_C interval has been reported in rat sarin studies (Abraham, Oz, Sahar, & Kadar, 2001) and organophosphate poisonings in humans (Roth, Zellinger, Arad, & Atsmon, 1993; Chuang, Jang, Lin, Chern, Chen, & Hsu, 1996), however, this study did not show changes in QT_C interval. It is unknown at this time why QT_C prolongation was not seen in this study. Allon *et al.* also report QT_C interval changes in rats exposed to sarin, but the QT_C interval change is only apparent in rats that received a high dose (convulsive) and only in the first two weeks post exposure. After two weeks time (within four weeks after exposure), most of the animals' QT_C intervals had returned to the control level (Allon, Rabinovitz, Manistersky, Weissman, & Grauer, 2005). Because this study only collected ECG tracing in week 10, it is impossible to ascertain if no QT_C prolongation or if QT_C prolongation may have occurred earlier in the study as described by Allon *et al.* Additionally, seven animals from the 0.5 LD₅₀ group died, and it is possible that these animals may have had an increased QT_C had they lived.

Echocardiograms and Implication to Left Ventricular Performance

2-D echocardiography showed a significant decrease in LV performance and function in the sarin animals. Sarin mice before dobutamine infusion showed significantly increased ventricular areas and decreased aFS in the later weeks of the study (weeks 4 and 10). This data parallels a previous, unpublished study by this lab in which mice injected with sarin (64µg/kg) showed significant increases in ESA, EDA four and eight weeks (no changes at 2) following the exposure (Morris, Shewalel, Lucot, &

Izu, 2007) (although, this previous study did not use Doppler imaging). In addition, in this study the combined 2-D and Doppler imaging parameters, aFS/MPI (weeks 4 and 10) and Vcf (week 10), were significantly decreased before dobutamine (see Figure 69).

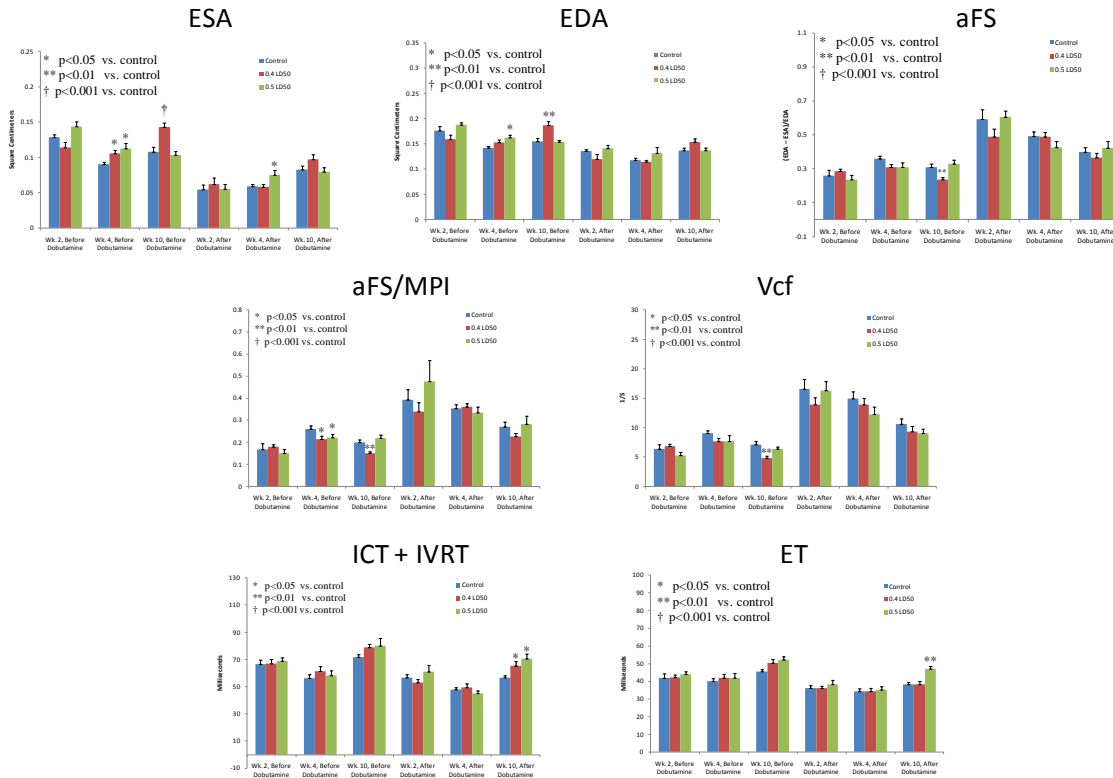


Figure 69 Echocardiography Data Showing Decreased LV Performance in Sarin Mice.

ESA was significantly increased in the sarin mice in week 4 and in the 0.4 LD50 group in week 10, and EDA was increased in the 0.5 and the 0.4 LD50 groups in weeks 4 and 10, respectively. Performance parameters, aFS, aFS/MPI, and Vcf were also decreased significantly in weeks 4 and 10.

aFS/MPI and Vcf serve as superior indicators of overall LV function since these values take into account both geometric and temporal measures of LV function (Broberg, et al., 2003; Syed, Diwan, & Hahn, 2005), and these values compare to the traditional 2-D echocardiography parameter aFS. Additionally, the ICT + IVRT and ET (0.5 after dobutamine) parameters were significantly lengthened after dobutamine. Tei *et al.* have shown both parameters to correlate with LV function and dysfunction (Tei,

Nishimura, Seward, & Tajik, 1997), and both parameters have been shown as effective measures after dobutamine infusion (Norager, Husic, Moller, & Egstrup, 2004; Duncan, Francis, Henein, & Gibson, 2003). While ICT + IVRT usually lengthens during LV dysfunction, longer ET intervals are usually associated with a healthy heart; nevertheless, ET lengthening has been shown to increase when hypertrophic cardiomyopathy is present (Hamada, et al., 2003; Nahrendorf, et al., 2006).

ESA and EDA increases can serve as early indicators of cardiac pathology; whereas, decreased aFS is indicative of diminished cardiac performance (Syed, Diwan, & Hahn, 2005). Increases in ESA and EDA seen in week 4 in the 0.5 LD₅₀ group with reversion in week 10 could be an early onset of the pathology. By week 4, the disease had progressed further in the 0.5 LD₅₀ group as evident by the larger changes in the EDA and ESA than the 0.4 LD₅₀ group in week 4. The pathology causing the increased ESA/EDA induced the onset of remodeling (hypertrophy) earlier in the 0.5 LD₅₀ group, and by week 10 the concentric hypertrophy (thus thickening of the LV walls) was more advanced in the 0.5 LD₅₀ group. Therefore, the week 10 echocardiograms of the 0.5 LD₅₀ group show correction as the remodeling thickened the muscle and reduced the ESAs and EDAs (often seen in later stages of concentric hypertrophy (Shub, 2008)). There is some evidence for this in the histology as well. The 0.5 LD₅₀ group showed a higher trend in corrected heart weight (Figure 36), decreased ventricular area and increased whole heart muscle area (Figure 40), and increased cell size (Figure 65) when compared to the 0.4 LD₅₀ group; indicating an increased level of hypertrophy in the 0.5

LD₅₀ group. Additionally, the 0.4 LD₅₀ group tended to have increased ANP (Figure 59) and BNP (Figure 61) levels when compared to the 0.5 LD₅₀ group; indicating an increased level of ongoing remodeling in the 0.4 LD₅₀ group. Nevertheless, this study cannot prove this (additional weeks would be needed to observe whether or not the 0.4 LD₅₀ group eventually corrected to the control levels in echocardiography and ANP/BNP levels) and additional study is needed to provide further insight.

Finally, the results of the M-mode echocardiography did not correlate with the 2-D results. In addition, M-mode failed to show increased thickness of the SWT or PWT, and LV hypertrophy could not be confirmed by M-mode echocardiography. In general, 2-D echocardiography is a more robust technique of measuring the LV than M-mode (Prasad, Atherton, Smith, McKenna, Frenneaux, & Nihoyannopoulos, 1999; Shub, 2008). In M-mode only a plane of the LV is measured with a single ultrasound beam; whereas, 2-D analysis allows for a more complete geometric description and spacial distribution of the LV. Therefore, one possible explanation is that the remodeling (or hypertrophy) cannot be readily diagnosed in M-mode (but easily seen in the 2-D) due the location of the cardiomyopathy in the LV (Maron, Gottdiener, Bonow, & Epstein, 2010).

Additionally, short comings with M-mode echocardiography have been cited in the literature (to include image quality or delineation of the edges, angularity, and ensuring that the plane of measurement passes through the largest dimension of the LV chamber), which may have added to the overall error seen in this study and served to reduce the overall significance of the M-mode measurements (Schiller & Foster, 1996; Sahn, DeMaria, Kisslo, & Weyman, 1978). Nevertheless, the decrease seen in the

indexes in the derived 2-D echocardiograms combined with histological data gives strong evidence of hypertrophic cardiomyopathy.

Additional Observations of Sarin's Effects on the Heart

Dobutamine Stress Testing

In order to test stimulated heart function in mice, a low dose (1 mg/kg) of dobutamine was injected. Dobutamine, a short acting nonselective β_1 adrenergic agonist (Anderson, Moore, & Larson, 2008), increases heart rate, contractility, and cardiac output (Wiesmann, et al., 2001). Measurements were made by echocardiography and ECG before and after the drug and two-way ANOVA did not demonstrate a significant difference in the interaction between dobutamine x sarin group x controls (for any parameter). Therefore, dobutamine produced similar increases in heart rate and cardiac output in both sarin and controls, indicating that the β_1 adrenoreceptor cascade was intact and that the sarin mice had adequate cardiac reserve to respond to the dobutamine stimulus.

The ECG PR Interval

The PR interval in the 0.5 LD₅₀ group was significantly increased after dobutamine infusion. On the ECG, the PR interval is an indicator of AV conduction time. Lengthening of the PR interval can represent a host of cardiac problems (including ischemia) and can be attributed to ischemia, conduction and/or neurological dysfunction (Mirvis & Goldberger, 2008). Because PR segment lengthening only occurred in 0.5 LD₅₀ group, it is not known if this is related to an early onset of another delayed sarin effect or if it is an artifact of the small sample size (n = 5). Moreover, this

study did not evaluate the conduction system, autonomic nervous system, or atriums; further study is needed to evaluate the conduction system and atria/ventricle timings before the implications of this finding are known.

Limitations of this Study

Seven of the 12 mice from the 0.5 LD₅₀ group died following the second sarin injection. This severely limited statistical power in the ANOVA where the 0.5 LD₅₀ group was included. More importantly, it is possible that the mice that were able to survive the second injection were more resistant to sarin, and this group was selectively biased; additionally, the stress from the convulsions may have created secondary pathologies in this group.

The increased ESA and EDA, and the differences between the week 4 and 10 results in 0.5 LD₅₀ groups remain unclear. Moreover, in the absence of histology (esp. in weeks two and four), it is not possible to ascertain whether the differences seen in the ventricular areas are causative, resultant, or extrinsic of the aforementioned pathology. Similarly, the death of half the mice in the 0.5 LD₅₀ after the second injection may have selectively created a group of mice resistant to sarin's effect, or pathologies in this group not seen in the 0.4 LD₅₀ group.

Finally, the current data does not give indication as to the cause of the remodeling or pathology (whether a direct response to a cardiac insult or an indirect response to performance degradation of the autonomic or conduction system). The current literature has expressed pathology in the brain and autonomic nervous system degradation following sarin exposure. Autonomic changes in humans following the

Tokyo subway attack have shown by Yokoyama *et al.*, and in rats following a single whole body dose of sarin (Yokoyama, et al., 1998, pp. 317 - 323; Yokoyama, et al., 1998, pp. 249 - 256; Grauer, et al., 2008). Likewise, Morris *et al.* have demonstrated significant deviations in heart rate variability (HRV) in mice exposed to sarin that suggest these changes in the brain and autonomic nervous system affect the heart (Morris, Key, & Farah, 2007). Nevertheless, it is possible that the cardiomyopathy is a direct effect of a change to the heart rather than the central nervous system (conduction system, e.g.). Therefore, further study is needed to determine the cause/origin of the cardiac dysfunction; perhaps using more robust methods such as polymerase chain reaction (PCR) and implanted ECG probes that allow for continuous recording.

Future Work

As described above, the mechanism of sarin's action on the cardiac system is unknown. Understanding the mechanism of action can help develop effective treatment regimes following a known or expected exposure (i.e. accident, split-MOPP decision, munitions demolition, etc). Similarly, drugs such as propranolol are known to protect the heart in some instances (such as hypertension). Thus, there is a need for further study that is focused on determining mechanisms of action and treatment techniques.

Furthermore, the effects of treatment (atropine and palidoxime chloride or 2-PAM) have not been studied and the pathology of sarin (or lack of pathology) following treatment has not been investigated. Additional study is needed to determine if

atropine and 2-PAM are an effective long-term treatment, or if supplementary medical care is needed to treat the long-term effects demonstrated in this study.

Conclusion

The preponderance of evidence in this study indicates delayed onset of morphology and reduced cardiac function of mice exposed to the nerve agent, sarin. Histology gives strong evidence of left ventricular cardiomyopathy and remodeling (possibly hypertrophy) by means of increased heart weight, cell size, natriuretic peptides production, and a reduction of ventricular area. ECGs under dobutamine stress give evidence of ischemia and decreased cardiac performance as a result of the sarin exposures. Similarly, in the later weeks of the experiment (weeks 4 and 10), the sarin mice demonstrated reductions the echocardiograph performance parameters (aFS, Vcf, and aFS/MPI) in the left ventricle; these mice showed signs of increased stress (volume overload, pressure, etc) as the ventricle areas (ESA and EDA) were enlarged.

The ECG results present as nearly normal before dobutamine stressing; after dobutamine stressing the ECG shows significant detriment to cardiac performance. This insidious nature of the sarin pathology has far reaching military implications. A military member who had been exposed to an asymptomatic dose of sarin (possibly without knowledge) could show near normal cardiac parameters on a routine check-up yet could have a severe cardiac reaction to physiological stress. Moreover, symptoms may not present until well after the post deployment health assessment that is currently required for all military personnel upon returning from a deployment.

Finally, these observations coincide with other observations of pathology seen in literature of sarin and organophosphate toxicology. Additionally, the cardiomyopathy described here is in line with studies performed by Haley *et al.* in Gulf war veterans. The studies gave evidence of altered diurnal patterns of heart rate and HRV correlated to reduced parasympathetic drive to the heart, possibly resulting from damage to the CNS (Haley, et al., 2004; Haley, Fleckenstein, Marshall, McDonald, Kramer, & Petty, 2000). Although it is unlikely that Gulf War Illness can ever be directly linked to sarin, this study along with similar studies in the literature present compelling need for continued investigation of the low dose toxicological effects of sarin.

Appendix A: Tabulated Average Results of Controls, 0.4 LD₅₀, and 0.5 LD₅₀ Groups

Tabulated Results of Weights and Heart Section Measurements

Table 1 Tabulated Results of Average Percent Changes in Body Weight

	Control	0.4 LD ₅₀	0.5 LD ₅₀
Baseline Body Wt. (g)	30.8 ± 0.6	29.6 ± 0.4	29.4 ± 0.5
% Change at 24 Hr	-0.027 ± 0.3	-2.50 ± 0.54	-5.5 ± 1.6*
% Change 4 WK	10.2 ± 1.5	6.8 ± 1.4	9.5 ± 1.3
% Change 7 Wk	6.4 ± 0.7	3.1 ± 2.8	5.0 ± 1.7
% Change 10 WK	8.6 ± 0.8	10.7 ± 4.0	9.6 ± 1.3

All values are expressed as the Mean ± SE

* p < 0.05 when compared to controls, ** p < 0.01 when compared to controls, † p < 0.001 when compared to controls

Table 2 Tabulated Results of Average Body Weight

	Control	0.4 LD ₅₀	0.5 LD ₅₀
Baseline Body Wt. (g)	30.8 ± 0.6	29.6 ± 0.4	29.4 ± 0.5
24 Hr After Sarin (g)	30.8 ± 0.6	28.9 ± 0.4**	27.8 ± 0.3†
4 WK Body Wt. (g)	34.0 ± 0.9	30.8 ± 0.4**	30.4 ± 0.2**
7 Wk Body Wt. (g)	36.2 ± 0.9	31.8 ± 0.9**	31.9 ± 0.8*
10 WK Body Wt. (g)	39.3 ± 1.2	35.2 ± 0.8	35.0 ± 1.2

All values are expressed as the Mean ± SE

* p < 0.05 when compared to controls, ** p < 0.01 when compared to controls, † p < 0.001 when compared to controls

Table 3 Tabulated Results of Week 10 Average Body Weights, Heart Weights, and Corrected Heart Weights (Heart Weight/Body Weight)

	Control	0.4 LD ₅₀	0.5 LD ₅₀
Body Weight (grams)	38.2 ± 1.2	34.9 ± 1.2	36.0 ± 1.5
Heart Weight (grams)	0.152 ± 0.004	0.156 ± 0.003	0.166 ± 0.007
Corrected Heart Weights	(4.02 ± 0.2) X 10 ⁻³	(4.49 ± 0.1) X 10 ⁻³	(4.64 ± 0.2) X 10 ⁻³
Corrected Heart Weights (Combined Data)	(4.02 ± 0.21) X 10 ⁻³	(4.55 ± 0.11) X 10 ^{-3*}	

All values are expressed as the Mean ± SE

* p < 0.05 when compared to controls, ** p < 0.01 when compared to controls, † p < 0.001 when compared to controls

Table 4 Tabulated Results of the Heart Areas in Square Millimeters

	Control	0.4 LD ₅₀	0.5 LD ₅₀
LV Area (cm ²)	3.60 ± 0.3	1.83 ± 0.3**	1.82 ± 0.5**
RV Area (cm ²)	1.51 ± 0.3	0.92 ± 0.2	0.62 ± 0.1
Total Heart Area (cm ²)	24.5 ± 1.0	23.6 ± 0.8	24.8 ± 1.0

All values are expressed as the Mean ± SE

* p < 0.05 when compared to controls, ** p < 0.01 when compared to controls, † p < 0.001 when compared to controls

Tabulated Results of Echocardiograms

Table 5 Tabulated Results of 2-Dimensional Echocardiograph Data

	Control		0.4 LD ₅₀		0.5 LD ₅₀	
	Before Dobutamine	After Dobutamine	Before Dobutamine	After Dobutamine	Before Dobutamine	After Dobutamine
Week 2 Results						
EDA (cm)	0.176 ± 0.008	0.136 ± 0.003	0.159 ± 0.009	0.120 ± 0.009	0.187 ± 0.004	0.141 ± 0.006
ESA (cm)	0.128 ± 0.004	0.054 ± 0.007	0.114 ± 0.007	0.062 ± 0.009	0.143 ± 0.007	0.055 ± 0.006
Area FS	0.260 ± 0.031	0.593 ± 0.056	0.286 ± 0.014	0.488 ± 0.047	0.234 ± 0.028	0.606 ± 0.036
Week 4 Results						
EDA (cm)	0.142 ± 0.003	0.118 ± 0.005	0.152 ± 0.006	0.115 ± 0.003	0.162 ± 0.006	0.132 ± 0.011
ESA (cm)	0.091 ± 0.003	0.060 ± 0.004	0.105 ± 0.005*	0.058 ± 0.003	0.112 ± 0.008*	0.075 ± 0.007
Area FS	0.359 ± 0.015	0.494 ± 0.026	0.309 ± 0.016	0.490 ± 0.026	0.310 ± 0.027	0.426 ± 0.036
Week 10 Results						
EDA (cm)	0.155 ± 0.006	0.137 ± 0.005	0.187 ± 0.007**	0.154 ± 0.007	0.154 ± 0.003	0.137 ± 0.004
ESA (cm)	0.108 ± 0.007	0.082 ± 0.005	0.143 ± 0.006†	0.097 ± 0.006	0.103 ± 0.005	0.079 ± 0.006
Area FS	0.310 ± 0.021	0.399 ± 0.026	0.235 ± 0.013**	0.365 ± 0.028	0.331 ± 0.021	0.421 ± 0.041

All values are expressed as the Mean ± SE

* p < 0.05 when compared to controls, ** p < 0.01 when compared to controls, † p < 0.001 when compared to controls

Table 6 Tabulated Results of M-Mode Echocardiograph Data

	Control		0.4 LD ₅₀		0.5 LD ₅₀	
	Before Dobutamine	After Dobutamine	Before Dobutamine	After Dobutamine	Before Dobutamine	After Dobutamine
Week 2 Results						
Heart Rate (bpm)	472 ± 24	523 ± 14	498 ± 16	555 ± 11	481 ± 23	531 ± 29
PWT (cm)	0.083 ± 0.007	0.101 ± 0.004	0.093 ± 0.004	0.114 ± 0.007	0.105 ± 0.008	0.108 ± 0.006
SWT (cm)	0.089 ± 0.005	0.102 ± 0.004	0.090 ± 0.003	0.114 ± 0.005	0.090 ± 0.006	0.110 ± 0.008
EDD (cm)	0.371 ± 0.018	0.303 ± 0.010	0.377 ± 0.017	0.285 ± 0.007	0.374 ± 0.012	0.305 ± 0.015
ESD (cm)	0.238 ± 0.015	0.141 ± 0.010	0.266 ± 0.016	0.134 ± 0.007	0.250 ± 0.009	0.130 ± 0.007
FS	0.309 ± 0.014	0.537 ± 0.024	0.299 ± 0.017	0.529 ± 0.020	0.331 ± 0.027	0.602 ± 0.030
RWT	0.477 ± 0.044	0.675 ± 0.031	0.498 ± 0.031	0.809 ± 0.055	0.522 ± 0.046	0.726 ± 0.054
Week 4 Results						
Heart Rate (bpm)	508 ± 19	630 ± 20	510 ± 17	630 ± 33	552 ± 27	656 ± 29
PWT (cm)	0.106 ± 0.003	0.114 ± 0.003	0.096 ± 0.003	0.110 ± 0.002	0.097 ± 0.003	0.109 ± 0.004
SWT (cm)	0.104 ± 0.003	0.120 ± 0.002	0.099 ± 0.001	0.120 ± 0.003	0.109 ± 0.004	0.120 ± 0.001
EDD (cm)	0.371 ± 0.005	0.322 ± 0.014	0.374 ± 0.008	0.309 ± 0.009	0.375 ± 0.013	0.318 ± 0.013
ESD (cm)	0.233 ± 0.011	0.163 ± 0.014	0.233 ± 0.005	0.149 ± 0.013	0.236 ± 0.004	0.160 ± 0.019
FS	0.373 ± 0.022	0.493 ± 0.030	0.375 ± 0.015	0.521 ± 0.034	0.369 ± 0.017	0.500 ± 0.041
RWT	0.568 ± 0.020	0.742 ± 0.037	0.526 ± 0.021	0.751 ± 0.024	0.558 ± 0.027	0.727 ± 0.033
Week 10 Results						
Heart Rate (bpm)	435 ± 14	525 ± 16	394 ± 12	491 ± 13	407 ± 23	457 ± 18
PWT (cm)	0.097 ± 0.004	0.108 ± 0.003	0.098 ± 0.003	0.110 ± 0.003	0.100 ± 0.003	0.116 ± 0.003
SWT (cm)	0.103 ± 0.003	0.110 ± 0.002	0.098 ± 0.005	0.105 ± 0.003	0.106 ± 0.003	0.113 ± 0.003
EDD (cm)	0.379 ± 0.008	0.341 ± 0.008	0.387 ± 0.006	0.326 ± 0.011	0.390 ± 0.012	.0339 ± 0.013
ESD (cm)	0.229 ± 0.014	0.154 ± 0.007	0.256 ± 0.008	0.160 ± 0.011	0.229 ± 0.010	0.163 ± 0.012
FS	0.400 ± 0.026	0.550 ± 0.014	0.340 ± 0.015	0.513 ± 0.022	0.413 ± 0.014	0.522 ± 0.021
RWT	0.530 ± 0.022	0.645 ± 0.024	0.453 ± 0.037	0.668 ± 0.025	0.530 ± 0.026	0.682 ± 0.030

All values are expressed as the Mean ± SE

* p < 0.05 when compared to controls, ** p < 0.01 when compared to controls, † p < 0.001 when compared to controls

Table 7 Tabulated Results of Pulsed-Wave Doppler Data & Derived Parameters

	Control		0.4 LD ₅₀		0.5 LD ₅₀	
	Before Dobutamine	After Dobutamine	Before Dobutamine	After Dobutamine	Before Dobutamine	After Dobutamine
Week 2 Results						
Ao VTI	0.004 ± 0.000	0.004 ± 0.000	0.004 ± 0.000	0.005 ± 0.000	0.004 ± 0.000	0.004 ± 0.000
ET (ms)	41.9 ± 2.3	36.2 ± 1.4	42.1 ± 1.6	35.2 ± 1.2	44 ± 1.3	38.1 ± 2.4
ICT+IVRT (ms)	66.6 ± 3.3	56.4 ± 2.5	67.0 ± 3.1	52.8 ± 2.5	69.1 ± 2.1	60.9 ± 5.0
Ao V _{Max}	0.151 ± 0.014	0.169 ± 0.009	0.148 ± 0.011	0.182 ± 0.009	0.122 ± 0.002	0.160 ± 0.016
FS/MPI	0.168 ± 0.026	0.394 ± 0.045	0.180 ± 0.008	0.339 ± 0.041	0.150 ± 0.017	0.475 ± 0.096
Vcf (1/s)	6.33 ± 0.78	16.54 ± 1.69	6.83 ± 0.0344	13.91 ± 1.21	5.31 ± 0.51	16.29 ± 1.59
Week 4 Results						
Ao VTI	0.003 ± 0.000	0.004 ± 0.000	0.004 ± 0.000	0.004 ± 0.000	0.003 ± 0.000	0.004 ± 0.000
ET (ms)	40.2 ± 1.5	34.2 ± 1.4	41.9 ± 2.2	36.6 ± 1.8	41.7 ± 2.8	35.2 ± 1.8
ICT+IVRT (ms)	56.2 ± 2.8	47.6 ± 1.8	61.3 ± 3.7	49.6 ± 2.8	58.3 ± 3.4	44.9 ± 1.9
Ao V _{Max}	0.108 ± 0.005	0.142 ± 0.015	0.123 ± 0.009	0.174 ± 0.021	0.108 ± 0.006	0.166 ± 0.018
FS/MPI	0.261 ± 0.014	0.354 ± 0.017	0.215 ± 0.014*	0.360 ± 0.015	0.22 ± 0.014*	0.334 ± 0.026
Vcf (1/s)	9.06 ± 0.47	14.92 ± 1.15	7.65 ± 0.58	13.91 ± 1.14	7.64 ± 1.06	12.28 ± 1.24
Week 10 Results						
Ao VTI	0.004 ± .000	0.004 ± 0.000	0.005 ± 0.000	0.005 ± 0.001	0.004 ± 0.000	0.005 ± 0.000
ET (ms)	45.4 ± 1.3	38.1 ± 1.2	50.3 ± 2.1	40.4 ± 1.9	52.1 ± 1.9	46.9 ± 1.7**
ICT+IVRT (ms)	71.6 ± 2.3	56.5 ± 1.8	79.0 ± 2.5	65.3 ± 3.4*	80.1 ± 5.7	70.6 ± 3.7*
Ao V _{Max}	0.113 ± 0.013	0.146 ± 0.009	0.129 ± 0.010	0.158 ± 0.013	0.122 ± 0.007	0.136 ± 0.008
FS/MPI	0.200 ± 0.012	0.271 ± 0.022	0.150 ± .008**	0.225 ± 0.015	0.218 ± 0.016	0.283 ± 0.036
Vcf (1/s)	7.08 ± 0.56	10.58 ± 0.90	4.77 ± 0.40**	9.32 ± 0.92	6.36 ± 0.43	9.01 ± 0.79

All values are expressed as the Mean ± SE

* p < 0.05 when compared to controls, ** p < 0.01 when compared to controls, † p < 0.001 when compared to controls

Tabulated Results of ECG Data Analysis

Table 8 Tabulated Results of ECG Telemetry

	Control		0.4 LD ₅₀		0.5 LD ₅₀	
	Before Dobutamine	After Dobutamine	Before Dobutamine	After Dobutamine	Before Dobutamine	After Dobutamine
RR Interval (ms)	152.8 ± 4.3	112.7 ± 9.5	153.4 ± 4.8	115.5 ± 2.6	158.4 ± 12.1	128.0 ± 7.2
Heart Rate (bpm)	395.2 ± 11.2	553.6 ± 36.5	394.6 ± 13.0	521.8 ± 11.9	387.6 ± 29.0	474.5 ± 26.4
QRS (ms)	16.5 ± 0.8	17.3 ± 0.9	18.2 ± 1.0	19.5 ± 1.1	17.0 ± 1.4	19.2 ± 1.4
PR Interval (ms)	42.9 ± 1.4	39.0 ± 2.7	42.0 ± 1.1	44.2 ± 2.3	48.3 ± 3.3	56.5 ± 5.6**
P Width (ms)	12.6 ± 0.7	11.8 ± 0.6	14.2 ± 1.2	14.6 ± 0.9	13.2 ± 0.6	14.7 ± 0.4
QT Interval (ms)	54.6 ± 7.0	59.4 ± 7.2	57.5 ± 1.3	64.3 ± 2.4	61.3 ± 4.4	64.8 ± 4.5
QT _C	44.2 ± 1.8	56.5 ± 1.6	46.5 ± 1.0	59.8 ± 1.8	48.7 ± 2.6	57.1 ± 3.0
T _C Interval (ms)	17.3 ± 1.1	25.9 ± 1.5	24.0 ± 1.7	35.0 ± 1.8**	22.4 ± 4.2	33.1 ± 1.7*
ST _C Length (ms)	7.8 ± 2.0	6.7 ± 1.9	11.7 ± 0.8	13.2 ± 1.4*	12.7 ± 3.2	7.0 ± 2.1*

All values are expressed as the Mean ± SE

* p < 0.05 when compared to controls, ** p < 0.01 when compared to controls, † p < 0.001 when compared to controls

Tabulated Results of Histology: ANP/BNP Quantification

Table 9 Tabulated Results of the Average ANP Expressed as the Natural Log of the Average Percent in Each Area

	Control	0.4 LD ₅₀	0.5 LD ₅₀
LV Wall	12.6 ± 2.7	27.2 ± 4.7*	17.1 ± 3.4
Septum	11.2 ± 2.7	22.2 ± 4.0*	8.1 ± 1.4
RV Wall	15.4 ± 3.4	27.4 ± 7.5	21.7 ± 7.5
LV Total (Wall +Septum)	11.9 ± 2.5	24.7 ± 4.2*	12.6 ± 2.4
ANP Total	13.1 ± 2.6	25.6 ± 5.1	15.6 ± 3.4
Sarin Groups Combined ANP Combined Data			
LV Wall	12.6 ± 2.7	23.0 ± 3.3*	
Septum	11.2 ± 2.7	15.1 ± 3.1	
RV Wall	15.4 ± 3.4	24.6 ± 5.0	
LV Total (Wall +Septum)	11.9 ± 2.5	18.3 ± 3.1	
ANP Total	13.1 ± 2.6	20.6 ± 3.5	

All values are expressed as the Mean ± SE

* p < 0.05 when compared to controls, ** p < 0.01 when compared to controls, † p < 0.001 when compared to controls

Table 10 Tabulated Results of the Average BNP Expressed as the Average Percent of BNP in Each Area

	Control	0.4 LD ₅₀	0.5 LD ₅₀
LV Wall	11.1 ± 1.8	27.3 ± 3.9	19.1 ± 6.5
Septum	11.8 ± 3.4	18.2 ± 3.6	8.7 ± 2.4
RV Wall	10.1 ± 1.4	19.0 ± 5.5	19.0 ± 7.0
LV Total (Wall +Septum)	11.5 ± 2.4	22.7 ± 3.5*	13.9 ± 4.0
BNP Total	11.0 ± 1.7	21.5 ± 3.6	15.6 ± 4.8
Sarin Groups Combined BNP Combined Data			
LV Wall	11.1 ± 1.8	23.2 ± 3.5*	
Septum	11.8 ± 3.4	13.5 ± 2.5	
RV Wall	10.1 ± 1.4	19.0 ± 3.8	
LV Total (Wall +Septum)	11.5 ± 2.4	18.3 2.3	
BNP Total	11.0 ± 1.7	18.5 ± 3.8*	

All values are expressed as the Mean ± SE

* p < 0.05 when compared to controls, ** p < 0.01 when compared to controls, † p < 0.001 when compared to controls

Tabulated Results of Cell Size Quantification from H&E Staining, Collagen Quantification from Picrosirius Red Staining

Table 11 Tabulated Results of Cell Size in the Left Ventricle Expressed as Pixels/Nuclei

	Control	0.4 LD ₅₀	0.5 LD ₅₀
LV Wall	4544 ± 274	4726 ± 308	4664 ± 254
Septum	3890 ± 232	4678 ± 356	5011 ± 371
LV Total (Wall +Septum)	4291 ± 272	4643 ± 216	4837 ± 287
Sarin Groups Combined Cell Size Data			
LV Wall	4544 ± 274	4817 ± 252*	
Septum	3890 ± 232	4599 ± 180	
LV Total (Wall +Septum)	4291 ± 272	4724 ± 168	

All values are expressed as the Mean ± SE

* p < 0.05 when compared to controls, ** p < 0.01 when compared to controls, † p < 0.001 when compared to controls

Table 12 Tabulated Results of Collagen in the Heart Expressed as a Ratio of Pixels Stained with Sirius Red to Total Heart Area (Pixels)

	Control	0.4 LD ₅₀	0.5 LD ₅₀
Total	0.00103 ± (8 X 10 ⁻⁵)	0.00102 ± (2.7 X 10 ⁻⁴)	0.000952 ± (9.6 X 10 ⁻⁵)

All values are expressed as the Mean ± SE

* p < 0.05 when compared to controls, ** p < 0.01 when compared to controls, † p < 0.001 when compared to controls

Appendix B: Unpublished Heart Weight Data

Heart Weight Data (Unpublished Study)

20 male C57BL/6J mice were housed individually at 22°C with a 12:12-hour dark-light cycle. Mice had free access to a standard diet and tap water. Mice were injected with sarin: 64µg/kg 0.4 LD₅₀ or saline (control group) on two consecutive days. Each group (controls, 0.4 LD₅₀) consisted of ten mice. Mice body weights, heart weights, and kidney weights were collected 8 weeks following the sarin injections. Heart weights normalized to kidney weights are a superior indicator of abnormal heart growth because kidneys weights do not fluctuate with diet or as much as body weights. In the study presented in this thesis, kidney weights were not collected so this data is only available from this separate unpublished study.

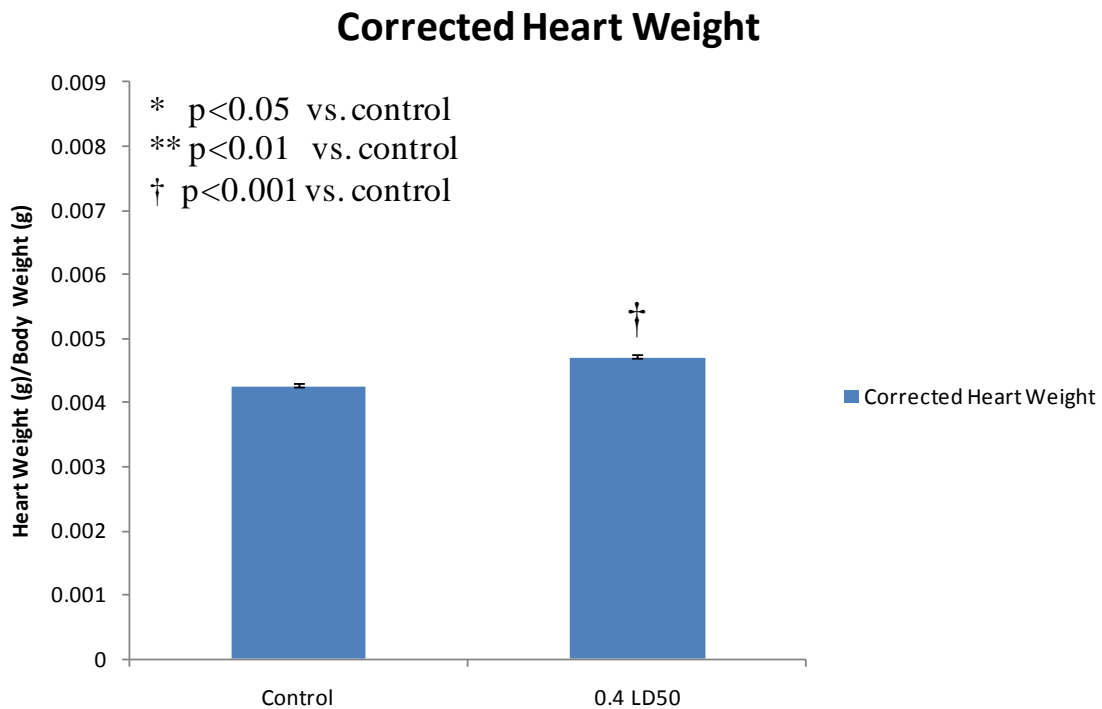


Figure 70 Unpublished Heart Weight to Body Weight Data

Normalized Heart Weight

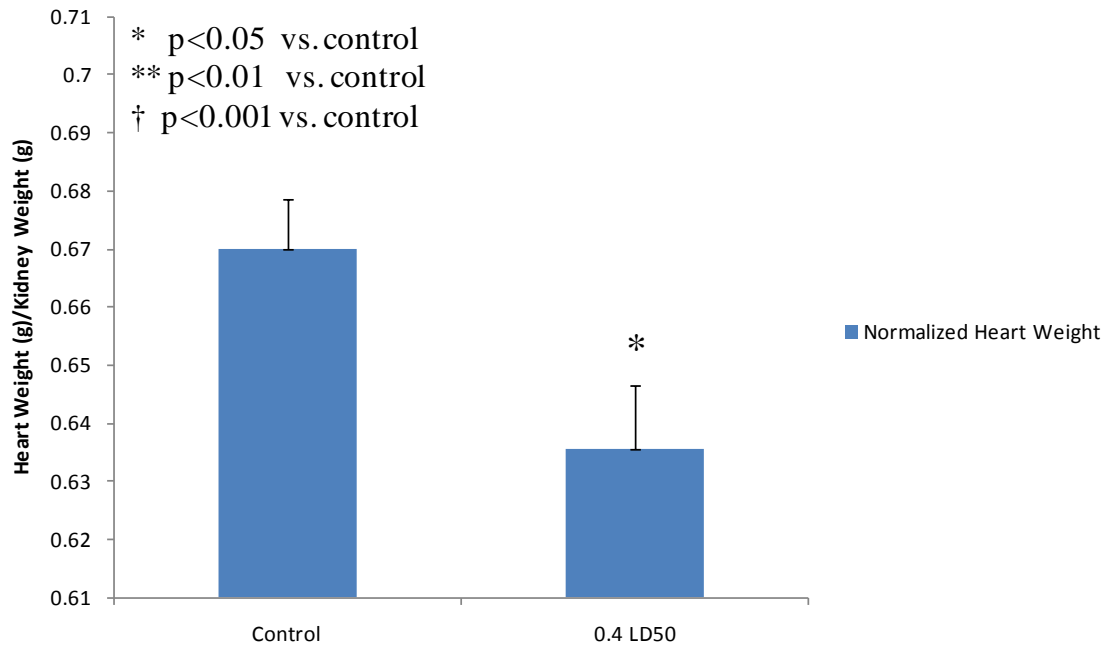


Figure 71 Unpublished Heart Weight to Kidney Weight Data

Bibliography

- Abraham, S., Oz, N., Sahar, R., & Kadar, T. (2001). QTc Prolongation and Cardiac Lesions Following Acute Organophosphate Poisoning in Rats. *Proc. West Pharmacol. Soc.* , 185 - 186.
- Alaoui, M. Y., Mossadeq, A., Faroudy, M., & Sbihi, A. (2009). Cardiac Complications Associated with Organophosphate Poisoning. *Ann. Cardiol. Angeiol. (Paris)* .
- Ali, J. (2001). Chemical Weapons and the Iran-Iraq War: A Case Study in Noncompliance. *Nonproliferation Review* , 43 - 58.
- Allon, N., Rabinovitz, I., Manistersky, E., Weissman, B. A., & Grauer, E. (2005). Acute and Long-Lasting Cardiac Changes Following a Single Whole-Body Exposure to Sarin Vapor in Rats. *Toxicological Sciences* , 385 - 390.
- Anderson, M., Moore, D., & Larson, D. F. (2008). Comparison of Isoproterenol and Dobutamine in the Induction of Cardiac Hypertrophy and Fibrosis. *Perfusion* , 231- 235.
- Atkielski, A. (2007, January 13). *Wikimedia Commons*. Retrieved 01 12, 2010, from Wikipedia: <http://en.wikipedia.org/wiki/File:SinusRhythmLabels.svg>
- Bar-Meir, E., Schein, O., Eisenkraft, A., Rubinshtein, R., Grubstein, A., Militianu, A., et al. (2007). Guidelines for Treating Cardiac Manifestations of Organophosphates Poisoning with Special Emphasis on Long QT and Torsades De Pointes. *Crit Rev. Toxicol.* , 279 - 285.
- Bazett, H. (1920). An Analysis of the Time-Relations of Electrocardiograms. *Heart* (7), 353-370.
- Bide, R. W., & Risk, D. J. (2004). Inhalation Toxicity in Mice Exposed to Sarin (GB) for 20 - 720 Min. *J. Appl. Toxicol.* , 459 - 467.
- Broberg, C. S., G. A., Barber, B. J., Mack, G. K., Lee, K., Thigpen, T., et al. (2003). Validation of the Myocardial Performance Index by Echocardiography in Mice: A Noninvasive Measure of Left Ventricular Function. *Journal of the American Society of Echocardiography* , 814 - 823.
- CDC. (1999). *Background Document on Gulf War-Related Research for the Health Impact of Chemical Exposures During the Gulf War: A Research Planning Conference*. Atlanta GA: CDC (Center for Disease Control and Prevention).
- Central Intelligence Agency; Department of Defense. (1997, 09 4). *Modeling the Chemical Warfare Agent Release at the Khamisiyah Pit*. Retrieved 02 09, 2010, from CIA Home: <https://www.cia.gov/library/reports/general-reports-1/gulfwar/555/425055597.html>

- Chavesa, A. A., Dech, S. J., Nakayama, T., Hamlin, R. L., Bauera, J. A., & Carnes, C. A. (2003). Age and Anesthetic Effects on Murine Electrocardiography. *Life Sciences* , 2401 - 2412.
- Chu, V., Otero, J. M., Lopez, O., Morgan, J. P., Amende, I., & Hampton, T. G. (2001). Method for non-invasively recording electrocardiograms in conscious mice. *BMC Physiology* .
- Chuang, F. R., Jang, S. W., Lin, J. L., Chern, M. S., Chen, J. B., & Hsu, K. T. (1996). QTc Prolongation Indicates a Poor Prognosis in Patients with Organophosphate Poisoning. *American Journal of Emergency Medicine* , 451 - 453.
- Committee on Gulf War and Health: Updated Literature Review of Sarin. (2004). Gulf War and Health: Updated Literature Review of Sarin. In *Gulf War and Health: Updated Literature Review of Sarin* (pp. 14 - 17). Washington DC: National Academy of Sciences.
- Conover, M. B. (2003). *Understanding Electrocardiography*, p. 34-40. St. Louis: Mosby, Inc.
- Couzin, J. (2004, October 1). VA Advisers Link Gulf War Illnesses to Neurotoxins. *Science Magazine* , pp. 26 - 27.
- Daly, A. L., Linares, O. A., Smith, M. J., Starling, M. R., & Supiano, M. A. (1997). Dobutamine Pharmacokinetics During Dobutamine Stress Echocardiography. *The American Journal of Cardiology* , 1381 - 1386.
- Damodaran, T. V., Jones, K. H., Patel, A. G., & Abou-Donia, M. B. (2003). Sarin (Nerve Agent GB)-Induced Differential Expression of mRNA Coding for the Acetylcholinesterase Gene in the Rat Central Nervous System . *Biochemical Pharmacology* , 2041- 2047 .
- Day, M. L., Schwartz, D., Wiegand, R. C., Stockman, P. T., Brunnert, S. R., Tolunay, H. E., et al. (1987). Ventricular Atriopeptin. Unmasking of Messenger RNA and Peptide Synthesis by Hypertrophy or Dexamethasone. *Hypertension* , 485 - 491.
- Diez, J., Lopez, B., Gonzadlez, A., & Querejeta, R. (2001). Clinical Aspects of Hypertensive Myocardial Fibrosis. *Current Opinion in Cardiology* , 328 - 335.
- Duncan, A. M., Francis, P. D., Henein, Y. M., & Gibson, D. G. (2003). Limitation of Cardiac Output by Total Isovolumic Time During Pharmacologic Stress in Patients with Dilated Cardiomyopathy. *J Am Coll Cardiol* , 121 - 128.
- Ellman, G., Courtney, K., Andres, V., & Feather-Stone, R. (1961). A New and Rapid Colorimetric Determination of Acetylcholinesterase Activity. *Biochem. Pharmacol.* (7), 88-95.

- Eroschenko, V. P. (2008). *diFiore's Atlas of Histology with Functional Correlations (11th ed.)*. Baltimore MD: Lippincott Williams & Wilkins.
- Fedak, P. W., Smookler, D. S., Kassiri, Z., Ohno, N., Leco, K. J., Verma, S., et al. (2010). TIMP-3 Deficiency Leads to Dilated Cardiomyopathy. *Circulation* , 2401 - 2409.
- Galindo, C. L., Skinner, M. A., Errami, M., Olson, L. D., David A. Watson, J. L., McCormick, J. F., et al. (2009). Transcriptional profile of isoproterenol-induced cardiomyopathy and comparison to exercise-induced cardiac hypertrophy and human cardiac failure. *BMC Physiology* , 9 - 23.
- Goetze, J. P., Georg, B., Jorgensen, H. L., & Fahrenkrug, J. (2009). Chamber-Dependent Circadian Expression of Cardiac Natriuretic Peptides. *Regulatory Peptides (Uncorrected Proof)* , 1 - 6.
- Gohel, D. R., Oza, J. J., Panjwani, S. J., & Gajjar, P. P. (1996). Organophosphate Compound Poisoning and Cardiac Toxicity. *Assoc Physicians India* , 287.
- Grauer, E., Chapman, S., Rabinovitz, I., Raveh, L., Weissmana, B.-A., Kadara, T., et al. (2008). Single Whole-Body Exposure to Sarin Vapor in Rats: Long-term Neuronal and Behavioral Deficits. *Toxicology and Applied Pharmacology* , 265 - 275.
- Haley, R. W., Fleckenstein, J. L., Marshall, W. W., McDonald, G. G., Kramer, G. L., & Petty, F. (2000). Effect of Basal Ganglia Injury on Central Dopamine Activity in Gulf War Syndrome: Correlation of Proton Magnetic Resonance Spectroscopy and Plasma Homovanillic Acid Levels. *Arch. Neurol.* , 1280 - 1285.
- Haley, R. W., Kurt, L. T., & Hom, J. (1997). Is there a Gulf War Syndrome? *JAMA* 277 , 215-222.
- Haley, R. W., Vongpatanasin, W., Wolfe, G. I., Bryan, W. W., Armitage, R., Hoffmann, R. F., et al. (2004). Blunted Circadian Variation in Autonomic Regulation of Sinus Node Function in Veterans with Gulf War syndrome. *Am. J. Med.* , 469 - 478.
- Hamada, M., Shigematsu, Y., Ohshima, K., Suzuki, J., Ogimoto, A., Ohtsuka, T., et al. (2003). Diagnostic Usefulness of Carotid Pulse Tracing in Patients With Hypertrophic Obstructive Cardiomyopathy Due to Midventricular Obstruction. *Chest* , 1275 - 1283.
- Harada, M., Itoh, H., Nakagawa, O., Ogawa, Y., Miyamoto, Y., Kuwahara, K., et al. (1997). Significance of Ventricular Myocytes and Nonmyocytes Interaction During Cardiocyte Hypertrophy. *Circulation* , 3737 - 3744.
- Hartley, C. J., Michael, L. H., & Entman, M. L. (1995). Noninvasive Measurement of Ascending Aortic Blood Velocity in Mice. *Am J Physiol Heart Circ Physiol* , H499 - H505.

- Hartley, C. J., Taffet, G. E., Reddy, A. K., Entman, M. L., & Michael, L. H. (2002). Noninvasive Cardiovascular Phenotyping in Mice. *ILAR Journal* , 147 - 158.
- Holtwick, R., Eickels, M. v., Skryabin, B. V., Baba, H. A., Bubikat, A., Begrow, F., et al. (2003). Pressure-Independent Cardiac Hypertrophy in Mice with Cardiomyocyte-Restricted Inactivation of the Atrial Natriuretic Peptide Receptor Guanylyl Cyclase-A. *The Journal of Clinical Investigation* , 1399 - 1407.
- Honsho, S., Nishikawa, S., Amano, K., Zen, K., Adachi, Y., Kishita, E., et al. (2009). Pressure-Mediated Hypertrophy and Mechanical Stretch Induces IL-1 Release and Subsequent IGF-1 Generation to Maintain Compensative Hypertrophy by Affecting Akt and JNK Pathways. *Circulation Research* , 1149 - 1158.
- Hsieh, B. P., Pham, M. X., & Froelicher, V. F. (2005). Prognostic Value of Electrocardiographic Criteria for Left Ventricular Hypertrophy. *American Heart Journal* , 161 - 167.
- Jamal, G. A. (1998). Gulf War Syndrome - A Model for the Complexity of Biological and Environmental Interaction with Human Health. *Adverse Drug React Toxicol Rev* , 1 - 17.
- Jamal, G. A., Hansen, S., Apartopoulos, F., & Peden, A. (1996). The "Gulf War syndrome". Is there evidence of dysfunction in the nervous system? *J Neurol Neurosurg Psychiatry* , 449 - 451.
- Joaquim, L. F., Farah, V. M., Bernatova, I., Rubens Jr., F., Grubbs, R., & Morris, M. (2004). Enhanced Heart Rate Variability and Baroreflex Index after Stress and Cholinesterase Inhibition in Mice. *Am J Physiol Heart Circ Physiol* , 251 - 257.
- Jokanovic, M., Kosanovic, M., & Maksimovic, M. (1996). Interaction of Organophosphorus Compounds with Carboxylesterases in the Rat. *Archives of Toxicology* , 444 - 450.
- Jones, K. H., Dechkovskaia, A. M., Herrick, E. A., Abdel-Rahman, A. A., Khan, W. A., & Abou-Donia, M. B. (2000). Subchronic Effect Following a Single Sarin Exposure on Blood-Brain and Blood-Testes Barrier Permeability, Acetylcholinesterase, and Acetylcholine Receptors in the Central Nervous System of Rat: A Dose-Response Study . *Journal of Toxicology and Environmental Health, Part A* , 695 - 707.
- Junqueira, L. C., Bignolas, G., & Brentani, R. R. (1979). Picrosirius Staining Plus Polarization Microscopy, a Specific Method for Collagen Detection in Tissue Sections. *Histochem J* , 447 - 455.

- Kassa, J., Krejcová, G., Skopec, F., Herink, J., Bajgar, J., Sevelová, L., et al. (2004). The Influence of Sarin on Various Physiological Functions in Rats Following Single or Repeated Low-Level Inhalation Exposure. *Inhalation Toxicology* , 517 - 530.
- Kassiri, Z., Oudit, G. Y., Kandalam, V., Awad, A., Wang, X., Ziou, X., et al. (2009). Loss of TIMP3 Enhances Interstitial Nephritis and Fibrosis. *J Am Soc Nephrol* , 1223 - 1235.
- Kawakami, R., Saito, Y., Kishimoto, I., Harada, M., Kuwahara, K., Takahashi, N., et al. (2010). Overexpression of Brain Natriuretic Peptide Facilitates Neutrophil Infiltration and Cardiac Matrix Metalloproteinase-9 Expression After Acute Myocardial Infarction. *Circulation* , 3306 - 3312.
- Kerckhove, R. V., Kalkmana, E. A., Saxena, P. R., & Schoemaker, R. G. (2000). Altered Cardiac Collagen and Associated Changes in Diastolic Function of Infarcted Rat Hearts. *Cardiovascular Research* , 316 - 323.
- Kiss, Z., & Fazekas, T. (1979). Arrhythmias in Organophosphate Poisonings. *Acta Cardiol.* , 323 - 330.
- Knowles, J. W., Esposito, G., Mao, L., Hagaman, J. R., Fox, J. E., Smithies, O., et al. (2001). Pressure-Independent Enhancement of Cardiac Hypertrophy in Natriuretic Peptide Receptor A-Deficient Mice. *The Journal of Clinical Investigation* , 975 - 984.
- Kramer, K., Kinter, L., Brockway, B. P., Voss, H.-P., Remie, R., & Van Zutphen, B. L. (2001). The Use of Radiotelemetry in Small Laboratory Animals: Recent Advances. *Contemporary Topic by American Association for Laboratory Animal Science* , 40 (1).
- Kramer, K., van Acker, S. A., Voss, H. P., Grimbergen, J. A., van der Vijgh, W. J., & Blast, A. (1993). Use of Telemetry to Record Electrocardiogram and Heart Rate in Freely Moving Mice. *J. Pharmacol. Toxicol. Methods* , 209-213.
- Lambiase, P. D., Edwards, R. J., Cusack, M. R., Bucknall, C. A., Redwood, S. R., & Marber, M. S. (2003). Exercise-Induced Ischemia Initiates the Second Window of Protection in Humans Independent of Collateral Recruitment. *J Am Coll Cardiol* , 1174 - 1182.
- Li, B., Sedlacek, M., Manoharan, I., Boopathy, R., Duysen, E. G., Masson, P., et al. (2005). Butyrylcholinesterase, Paraoxonase, and Albumin Esterase, but not Carboxylesterase, are Present in Human Plasma . *Biochemical Pharmacology* , 1673 - 1684.
- London, B. (2001). Cardiac Arrhythmias: From (Transgenic) Mice to Men. *Journal of Cardiovascular Electrophysiology* , 1089 - 1091.

Long, C. S., & Brown, R. D. (2002). The Cardiac Fibroblast, Another Therapeutic Target for Mending the Broken Heart? *J Mol Cell Cardiol* , 1273 - 1278.

Lopez, M. J., Wong, S. K., Kishimoto, I., Dubois, S. M., Friesen, J., Garbers, D. L., et al. (1995). Salt-Resistant Hypertension in Mice Lacking the Guanylyl Cyclase-A Receptor for Strial Natriuretic Peptide. *Nature* , 65 -68.

Lutgens, E., Daemen, M. J., Muinck, E. D., Debets, J., Leenders, P., & Smits, J. F. (1999). Chronic Myocardial Infarction in the Mouse: Cardiac Structural and Functional Changes. *Cardiovascular Research* , 556 - 563.

Mair, J. (2008). Biochemistry of B-type Natriuretic Peptide – Where Are We Now? *Clin Chem Lab Med* , 1507 – 1514.

Maron, B. J., Gottdiener, J. S., Bonow, R. O., & Epstein, S. E. (2010). Hypertrophic cardiomyopathy with unusual locations of left ventricular hypertrophy undetectable by M-mode echocardiography. Identification by wide-angle two-dimensional echocardiography. *Circulation* , 409 - 418.

Marosi, G., Ivan, J., Vass, K., Gajdacs, A., & Ugocsai, G. (1989). ECG Repolarization Disorder (QT Lengthening) in Organophosphate Poisoning. *Orv. Hetil.* , 111 - 115.

Marrs, T. C. (2007). Toxicology of Organophosphate Nerve Agents. In T. C. Marrs, R. L. Maynard, & F. R. Sidell, *Chemical Warfare Agents Toxicology and Treatment* (pp. 191 - 223). West Sussex, England: John Wiley & Sons Ltd.

Menon, P. M., Nasrallah, H. A., Reeves, R. R., & Ali, J. A. (2004). Hippocampal Dysfunction in Gulf War Syndrome. A Proton MR Spectroscopy Study. *Brain Res.* , 189 - 194.

Mertes, H., Sawada, S. G., Ryan, T., Segar, D. S., Kovacs, R., Foltz, J., et al. (1993). Symptoms, Adverse Effects, and Complications Associated With Dobutamine Stress Echocardiography: Experience in 1118 Patients. *Circulation* , 15 - 19.

Mirvis, D. M., & Goldberger, A. L. (2008). CHAPTER 12 – Electrocardiography. In P. Libby, R. O. Bonow, D. L. Mann, & D. P. Zipes, *BRAUNWALD'S Heart Disease A Textbook of Cardiovascular Medicine* (pp. 149 - 195). Philadelphia PA: Saunders, an imprint of Elsevier Inc.

Mitchell, G. F., Jeron, A., & Koren, G. (1998). Measurement of Heart Rate and Q-T Interval in the Conscious Mouse. *Am J Physiol Heart Circ Physiol* , 747-751.

Morgan, E. E., Faulx, M. D., McElfresh, T. A., Kung, T. A., Zawaneh, M. S., Stanley, W. C., et al. (2004). Validation of Echocardiographic Methods for Assessing Left Ventricular Dysfunction in Rats with myocardial Infarction. *Am J Physiol Heart Circ Physiol* , 2049-2053.

Morris, M., Key, M. P., & Farah, V. (2007). Sarin Produces Delayed Cardiac and Central Autonomic Changes. *Experimental Neurology* , 110 - 115.

Morris, M., Lucot, J., & Shewale, S. (2009). Dayton, OH: Wright State University, Boonshoft School of Medicine.

Morris, M., Shewale, S., Lucot, J., & Izu, B. (2007). Delayed Effects of Low Dose Sarin on Cardiac Morphology and Function in Mice. *Unpublished* . Dayton, OH: Wright State University, Boonshoft School of Medicine.

Murata, K., Araki, S., Yokoyama, K., Okumura, T., Ishimatsu, S., Takasu, N., et al. (1997). Asymptomatic Sequelae to Acute Sarin Poisoning in the Central and Autonomic Nervous System 6 Months After the Tokyo Subway Attack. *J. Neurol.* , 601 – 606.

Nahrendorf, M., Streif, J. U., Hiller, K.-H., Hu, K., Nordbeck, P., Ritter, O., et al. (2006). Multimodal Functional Cardiac MRI in Creatine Kinase-Deficient Mice Reveals Subtle Abnormalities in Myocardial Perfusion and Mechanics. *Am J Physiol Heart Circ Physiol* , 2516 - 2521.

Norager, B., Husic, M., Moller, J. E., & Egstrup, K. (2004). The Myocardial Performance Index During Low Dose Dobutamine Echocardiography in Control Subjects and Patients with Recent Myocardial Infarction: a New Index of Left Ventricular Functional Reserve? *J Am Soc Echocardiog* , 732-738.

Nossuli, T. O., Lakshminarayanan, V., Baumgarten, G., G. E. Taffet, C. M., Michael, L. H., & Entman, M. L. (2000). A Chronic Mouse Model of Myocardial Ischemia-Reperfusion: Essential in Cytokine Studies. *Am J Physiol Heart Circ Physiol* , 1049-1055.

Persian Gulf War Illnesses Task Force. (1997, 04 02). *Khamisiyah: A Historical Perspective on Related Intelligence*. Retrieved 02 09, 2010, from GulfLINK: http://www.gulflink.osd.mil/cia_wp/

Plante, E., Lachance, D., Drolet, M.-C., Roussel, É., Couet, J., & Arsenault, M. (2005). Dobutamine stress echocardiography in healthy adult male rats. *Cardiovasc Ultrasound* , 3 - 34.

Powell, D. W., Mifflin, R. C., Valentich, J. D., Crowe, S. E., Saada, J. I., & West, A. B. (1999). Myofibroblasts. I. Paracrine Cells Important in Health and Disease. *Am J Physiol Cell Physiol* , 1 - 19.

- Prasad, K., Atherton, J., Smith, G. C., McKenna, W. J., Frenneaux, M. P., & Nihoyannopoulos, P. (1999). Echocardiographic Pitfalls in the Diagnosis of Hypertrophic Cardiomyopathy. *Heart* , (supplement III):III8–III15.
- Puchtler, H., Waldrop, F. S., & Valentine, L. S. (1973). Polarization Microscopic Studies of Connective Tissue Stained with Picro-Sirius Red FBA. *Beitr Path* , 174 - 187.
- Robertson, N. (2002). *Disturbing Scenes of Death Show Capability with Chemical Gas*. Atlanta GA: CNN.
- Roden, D. M. (2001). Antiarrhythmic Drugs. In J. G. Hardman, L. Limbird, & A. G. Gilman, *Goodman & Gilman's The Pharmacological Basis of Therapeutics (10th ed.)* (pp. 935 - 970). New York NY: McGraw - Hill.
- Roth, A., Zellinger, I., Arad, M., & Atsmon, J. (1993). Organophosphates and the heart. *Chest* , 576 - 582.
- Roth, D. M., Swaney, J. S., Dalton, N. D., Gilpin, E. A., & Ross Jr, J. (2002). Impact of Anesthesia on Cardiac Function During Echocardiography in Mice. *Am J Physiol Heart Circ Physiol* , 2134 - 2140.
- Sahn, D., DeMaria, A., Kisslo, J., & Weyman, A. (1978). Recommendations Regarding Quantitation in M-Mode Echocardiography: Results of a Survey of Echocardiographic Measurements. *Circulation* , 1072-1083.
- Schiller, N. B., & Foster, E. (1996). Analysis of left ventricular systolic function. *Heart* , 17 - 26.
- Scott, N. J., Ellmers, L. J., Lainchbury, J. G., Maeda, N., Smithies, O., Richards, A. M., et al. (2009). Influence of Natriuretic Peptide Receptor-1 on Survival and Cardiac Hypertrophy During Development. *Biochimica et Biophysica Acta* , 1175 - 1184 .
- Shaheen, J., Luria, D., Klutstein, M. W., Rosenmann, D., & Tzivoni, D. (1998). Diagnostic Value of 12-lead Electrocardiogram During Dobutamine Echocardiographic Studies. *American Heart Journal* , 1061 - 1064.
- Shih, T.-M., Hulet, S. W., & McDonough, J. H. (2006). The Effects of Repeated Low-Dose Sarin Exposure. *Toxicology and Applied Pharmacology* , 119 - 134.
- Shub, C. (2008). Cardiac Imaging. In J. L. Izzo, H. R. Black, & D. A. Sica, *Hypertension Primer (4th ed.)* (p. 363). Philadelphia: American Heart Association.
- Sidell, F. R., & Borak, J. (1992). Chemical warfare agents: II. Nerve agents. *Annals of Emergency Medicine* , 865 – 871.

- Smits, A. M., & Smits, J. F. (2004). Ischemic Heart Disease: Models of Myocardial Hypertrophy and Infarction. *Drug Discovery Today: Disease Models* , 273 - 274.
- Stein, A. B., Tiwari, S., Thomas, P., Hunt, G., Levent, C., Stoddard, M. F., et al. (2005). Effects of Anesthesia on Echocardiographic Assessment of Left Ventricular Structure and Function in Rats. *Basic Res Cardiol* , 28 - 41.
- Stoller, D., Kakkar, R., Smelley, M., Chalupsky, K., Earley, J. U., Shi, N.-Q., et al. (2007). Mice Lacking Sulfonylurea Receptor 2 (SUR2) ATP-Sensitive Potassium Channels are Resistant to Scute Cardiovascular Stress. *Journal of Molecular and Cellular Cardiology* , 445 - 454.
- Swaney, J. S., Roth, D. M., Olson, E. R., Naugle, J. E., Meszaros, J. G., & Insel, P. A. (2005). Inhibition of Cardiac Myofibroblast Formation and Collagen Synthesis by Activation and Overexpression of Adenylyl Cyclase. *PNAS* , 437 - 442.
- Swoap, S. J., Overton, J. M., & Garber, G. (2004). Effect of Ambient Temperature on Cardiovascular Parameters in Rats and Mice: a Comparative Approach. *Am J Physiol Regulatory Integrative Comp Physiol* , 391 - 396.
- Syed, F., Diwan, A., & Hahn, H. S. (2005). Murine Echocardiography: A Practical Approach for Phenotyping Genetically Manipulated and Surgically Modeled Mice. *Journal of the American Society of Echocardiography* , 982-990.
- Takeda, N., Manabe, I., Uchino, Y., Eguchi, K., Matsumoto, S., Nishimura, S., et al. (2010). Cardiac Fibroblasts are Essential for the Adaptive Response of the Murine Heart to Pressure Overload. *The Journal of Clinical Investigation* , 254 - 265.
- Tamura, N., Ogawa, Y., Chusho, H., Nakamura, K., Nakao, K., Suda, M., et al. (2000). Cardiac Fibrosis in Mice Lacking Brain Natriuretic Peptide. *PNAS* , 4239 - 4244.
- Tan, T. P., Gao, X.-M., Krawczynszyn, M., Feng, X., Kiriazis, H., Dart, A. M., et al. (2003). Assessment of Cardiac Function by Echocardiography in Conscious and Anesthetized Mice: Importance of the Autonomic Nervous System and Disease State. *J Cardiovasc Pharmacol* , 182 - 190.
- Taylor, P. (2001). Anticholinesterase Agents. In J. G. Hardman, L. E. Limbird, & A. G. Gilman, *Goodman & Gilman's: The Pharmacological Basis of Therapeutics* (pp. 175-191). New York NY: McGraw Hill Companies, Inc.
- Tei, C., Nishimura, R. A., Seward, J. B., & Tajik, A. J. (1997). Noninvasive Doppler-Derived Myocardial Performance Index: Correlation with Simultaneous Measurements of Cardiac Catheterization Measurements. *Journal of the American Society of Echocardiography* , 169-178.

Tomai, F., Crea, F., Chiariello, L., & Gioffrè, P. A. (1999). Ischemic Preconditioning in Humans : Models, Mediators, and Clinical Relevance. *Circulation* , 559 - 563.

United States Air Force. (2007, January 26). Counter-Chemical, Biological, Radiological, and Nuclear Operations. *Air Force Doctrine Document 2-1.8* . Headquarters Air Force Doctrine Center.

van Acker, S. A., Kramer, K., Grimbergen, J. A., van der Vijgh, W. J., & Blast, A. (1996). Doxorubicin-Induced Chronic Cardiotoxicity Measured in Freely Moving Mice. *Cancer Chemother Pharmacol* , 95-101.

Wehrens, X. H., Kirchhoff, S., & Doevendans, P. A. (2000). Mouse Electrocardiography: An Interval of Thirty Years. *Cardiovascular Research* , 231 - 237.

Weissman, N. J., Levangie, M. W., Guerrero, J. L., Weyman, A. E., & Picard, M. H. (1996). Effect of B-blockade on Dobutamine Stress Echocardiography. *American Heart Journal* , 698 - 703.

Wiesmann, F., Ruff, J., Engelhardt, S., Hein, L., Dienesch, C., Leupold, A., et al. (2001). Dobutamine-Stress Magnetic Resonance Microimaging in Mice : Acute Changes of Cardiac Geometry and Function in Normal and Failing Murine Hearts. *Circulation Research* , 563 - 569.

Yasuno, S., Usami, S., Kuwahara, K., Nakanishi, M., Arai, Y., Kinoshita, H., et al. (2009). Endogenous Cardiac Natriuretic Peptides Protect the Heart in a Mouse Model of Dilated Cardiomyopathy and Sudden Death. *Am J Physiol Heart Circ Physiol* , 1804 - 1810.

Yokoyama, K., Araki, S., Murata, K., Nishikitani, M., Okumura, T., Ishimatsu, S., et al. (1998). Chronic Neurobehavioral and Central and Autonomic Nervous System Effects of Tokyo Subway Sarin Poisoning. *J Physiol Paris* . , 317 - 323.

Yokoyama, K., Araki, S., Murata, K., Nishikitani, M., Okumura, T., Ishimatsu, S., et al. (1998). Chronic Neurobehavioral Effects of Tokyo Subway Sarin Poisoning in Relation to Posttraumatic Stress Disorder. *Arch. Environ. Health* , 249 - 256.

REPORT DOCUMENTATION PAGE				Form Approved OMB No. 074-0188	
The public reporting burden for this collection of information is estimated to average 1 hour per response, including the time for reviewing instructions, searching existing data sources, gathering and maintaining the data needed, and completing and reviewing the collection of information. Send comments regarding this burden estimate or any other aspect of the collection of information, including suggestions for reducing this burden to Department of Defense, Washington Headquarters Services, Directorate for Information Operations and Reports (0704-0188), 1215 Jefferson Davis Highway, Suite 1204, Arlington, VA 22202-4302. Respondents should be aware that notwithstanding any other provision of law, no person shall be subject to a penalty for failing to comply with a collection of information if it does not display a currently valid OMB control number. PLEASE DO NOT RETURN YOUR FORM TO THE ABOVE ADDRESS.					
1. REPORT DATE (DD-MM-YYYY) 03-25-2010		2. REPORT TYPE Master's Thesis		3. DATES COVERED (From - To) Aug. 2008 - March 2010	
4. TITLE AND SUBTITLE Low Dose Sarin Leads To Murine Cardiac Dysfunction				5a. CONTRACT NUMBER	
				5b. GRANT NUMBER GW060050	
				5c. PROGRAM ELEMENT NUMBER	
6. AUTHOR(S) Horezniak, Michael W. Capt, USAF, BSC				5d. PROJECT NUMBER NA	
				5e. TASK NUMBER	
				5f. WORK UNIT NUMBER	
7. PERFORMING ORGANIZATION NAMES(S) AND ADDRESS(S) Air Force Institute of Technology Graduate School of Engineering and Management (AFIT/EN) 2950 Hobson Way, Building 640 WPAFB OH 45433-7765				8. PERFORMING ORGANIZATION REPORT NUMBER AFIT/GIH/ENV/10 - M03	
9. SPONSORING/MONITORING AGENCY NAME(S) AND ADDRESS(ES) Wright State University, Boonshoft School of Medicine ATTN: Doctor Mariana Morris 3640 Colonel Glenn Hwy., Dayton, OH 45435-0001 Telephone # (937) 775-2463				10. SPONSOR/MONITOR'S ACRONYM(S) NA	
				11. SPONSOR/MONITOR'S REPORT NUMBER(S)	
12. DISTRIBUTION/AVAILABILITY STATEMENT APPROVED FOR PUBLIC RELEASE; DISTRIBUTION UNLIMITED					
13. SUPPLEMENTARY NOTES This material is declared a work of the U.S. Government and is not subject to copyright protection in the United States.					
14. ABSTRACT It has been reported that low dose sarin is associated with long-term pathology in the brain and heart; however, the effects of sarin on the heart have yet to be determined. In addition, sarin has been implicated as an etiological agent in <i>Gulf War Illness</i> . Thus, the role of sarin in producing illness has important military implications. This study used echocardiography, electrocardiography, and histology to determine sarin's effect on the murine cardiovascular system. C57BL/6J mice were injected with sarin at 0.4 LD ₅₀ , 0.5 LD ₅₀ , or saline on two consecutive days and studied for 10 weeks post exposure. The sarin animals had marked increases in heart weight to body weight ratios ($p = 0.026$) and the left ventricular lumen size was significantly decreased ($p = 0.0014$). In addition, cardiomyocytes were significantly larger in the sarin mice ($p = 0.025$), and atrial/brain natriuretic peptide levels were increased ($p = 0.028$ and 0.010 , respectively). Results of the electrocardiograms show significant ST/T-wave changes in the sarin groups ($p = 0.0015$ and 0.032 , respectively). Similarly, echocardiograms showed significantly decreased performance of the left ventricle in the sarin animals. This study indicates that sarin plays a role in cardiac remodeling and reducing cardiac performance.					
15. SUBJECT TERMS <i>Sarin, organophosphate, mice, heart, hypertrophy, toxicology, histology, cardiac, murine, pathology, electrocardiogram, echocardiogram</i>					
16. SECURITY CLASSIFICATION OF: Unclassified			17. LIMITATION OF ABSTRACT	18. NUMBER OF PAGES	19a. NAME OF RESPONSIBLE PERSON David A. Smith, Director, GES, (AFIT/ENV)
a. REPORT	b. ABSTRACT	c. THIS PAGE			19b. TELEPHONE NUMBER (Include area code) (937) 255-3636, ext 4711 David.A.Smith@afit.edu
U	U	U	UU	110	